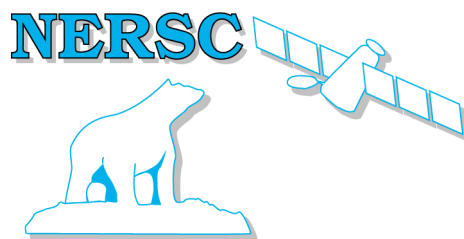


Nansen Environmental and Remote Sensing Center

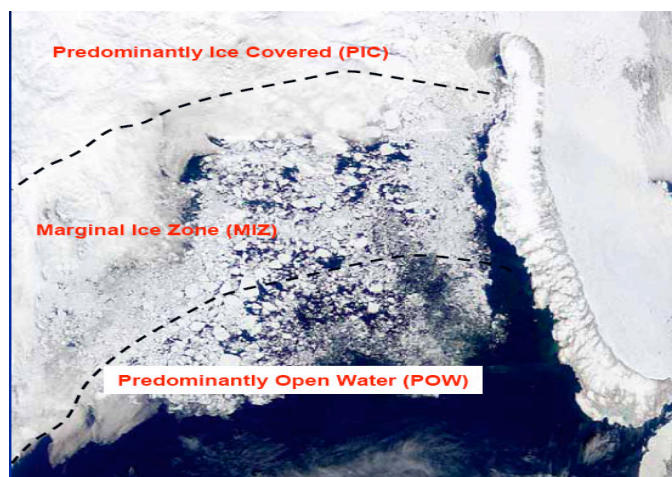
A non-profit
Research institute affiliated
With the University of
Bergen



Thormøhlensgate 47
N-5006 Bergen,
Norway
<http://www.nersc.no>

NERSC Technical Report no. 279

Review of air-ice-ocean processes in the Margial Ice Zone of importance for offshore activities in the Barents Sea region



Satellite image from AQUA MODIS with Marginal Ice Zone definition by K. Maiti


Project for Total E&P Norge AS

Contract no. 4100P06.073

Authors:

Stein Sandven, Laurent Bertino, Knut Arild Lisæter, Hanne Sagen,
Kjetil Lygre and Mohamed Babiker

March 2007

 <p>NERSC</p>	<p>Nansen Environmental and Remote Sensing Center (NERSC)</p> <p>Thormøhlensgate 47 N-5006 Bergen, Norway Phone: + 47 55 20 58 00 Fax: + 47 55 20 58 01 E-Mail: Stein.Sandven@nersc.no http://www.nersc.no</p>
---	--

<p>TITLE:</p> <p>Review of air-ice-ocean processes in the Marginal Ice Zone of importance for offshore activities in the Barents Sea region</p>	<p>REPORT IDENTIFICATION</p> <p>NERSC Technical report no. 279</p>
<p>CLIENT</p> <p>Total E&P Norge</p>	<p>CONTRACT</p> <p>Contract no. 4100P06.073</p>
<p>CLIENT REFERENCE</p> <p>Laurence Pinturier and Ulf Einar Moltu</p>	<p>AVAILABILITY</p> <p>Customer report</p>
<p>INVESTIGATORS</p> <p>Stein Sandven, Laurent Bertino, Knut Arild Lisæter, Hanne Sagen, Kjetil Lygre and Mohamed Babiker</p>	<p>AUTHORISATION</p> <p>Bergen, 12 March 2007</p> <p>Stein Sandven</p>

Contents

EXECUTIVE SUMMARY	3
1. INTRODUCTION TO THE MARINE ENVIRONMENT OF THE ARCTIC	4
1.1 THE ROLE OF THE ARCTIC SHELF SEAS	4
1.2 OCEAN DYNAMICS OF THE SHELF SEAS	5
1.3 CHANGES IN CROSS-SHELF TRANSPORT OF WATER MASSES	6
1.4 ECOSYSTEM CHANGE AND IMPACT ON ENVIRONMENT	8
1.5 TIMING OF SEA ICE EVENTS, SPRING BLOOM, RIVER BREAK-UP AND PEAK IN HYDROLOGICAL DISCHARGE.....	9
1.6 ARCTIC POLYNYAS	10
1.7 TOPICS REVIEWED IN THIS REPORT	12
2. ATMOSPHERIC PROCESSES	13
2.1 AIR PRESSURE IN THE ARCTIC	13
2.2 THE ARCTIC ENERGY BUDGET AND NORTH-SOUTH FLOWS.....	14
2.3 THE ARCTIC OSCILLATION AND THE NORTH ATLANTIC OSCILLATION	18
2.4 SURFACE AIR TEMPERATURE.....	20
2.5 POLAR LOWS.....	23
2.6 CLOUDS	24
2.7 PRECIPITATION.....	26
2.8 FEEDBACK LOOPS: INTERACTIONS THAT INFLUENCE ARCTIC CLIMATE	29
2.8.1 <i>Temperature—Albedo Feedback</i>	29
2.8.2 <i>Temperature—Cloud Cover—Radiation Feedbacks</i>	30
2.9 METEOROLOGICAL CONDITIONS OF IMPORTANCE FOR OPERATIONS AND NAVIGATION	31
2.9.1 <i>Visibility</i>	31
2.9.2 <i>Wind regime</i>	32
2.9.3 <i>Icing on vessels</i>	33
3. SEA ICE PROCESSES	37
3.1 TREND AND VARIABILITY IN SEA ICE EXTENT IN THE ARCTIC	37
3.2 SEA ICE CONDITIONS OF IMPORTANCE FOR OPERATION, NAVIGATION AND OIL SPILL EVENTS	44
3.2.1 <i>Sea ice types and properties</i>	44
3.2.2 <i>Sea processes in the MIZ</i>	51
3.3 ICEBERGS.....	56
4. SEA ICE MODELING OF THE MARGINAL ICE ZONE	60
4.1 INTRODUCTION TO SEA ICE MODELING	60
4.2 MODEL TOOLS AND SEA ICE RHEOLOGIES.....	61
<i>Sea ice dynamics models</i>	61
<i>Lagrangian approach</i>	65
4.3 OCEAN-ICE INTERACTION	66
<i>Ocean waves</i>	67
4.4 CONCLUSION OF SEA ICE MODELLING IN THE MIZ.....	68
5. OCEAN PROCESSES.....	68
5.1 WATER MASSES AND CURRENTS	68
5.2 SEA LEVEL.....	70
5.3 WAVES IN THE OPEN OCEAN	72
5.4 WAVE IN SEA ICE	74
5.4.1 <i>Swell observation techniques</i>	75
5.4.2 <i>Wave modelling in the MIZ</i>	77
5.4.3 <i>Concluding remarks on waves in ice</i>	78
5.5 FRESHWATER FROM RIVERS AND GLACIERS	78
6. OIL SPILL IN ICE-COVERED SEAS	83

6.1 BEHAVIOUR OF OIL SPILLS IN ICE CONDITIONS	83
6.2 PREDICTING THE FATE OF OIL IN ICE	88
6.3 OIL SPILL RECOVERY IN ICE CONDITIONS	90
7. MODELLING OF PRIMARY PRODUCTION AND SPREADING OF PASSIVE TRACERS	93
7.1 BACKGROUND AND STATUS OF KNOWLEDGE	93
7.1.1 <i>Regional scale and climate related processes</i>	93
7.1.2 <i>Variability along the ice edge</i>	94
7.1.3 <i>Mesoscale eddies</i>	94
7.1.4 <i>Links between climate and processes on shorter time scales</i>	96
7.1.5 <i>Coupling of atmosphere and ocean</i>	96
7.2 MODELLING	96
7.3 RESEARCH NEEDS	97
8. CONCLUSIONS AND RECOMMENDATIONS.....	97
ACKNOWLEDGEMENT	100
REFERENCES	101

Executive Summary

In this report we have reviewed air-ice-ocean processes in the Marginal Ice Zone (MIZ) of importance for offshore operations and related environmental issues. The MIZ is an important region that determines meteorological conditions, sea ice conditions and oceanographical conditions including primary production and marine living resources. A large part of future oil and gas exploration and tanker transportation will take place in the MIZ. If oil spills and other sea pollutants are captured in ice, it will be difficult to clean-up the pollutants and the impact on the environment will be severe. It is therefore of high importance to improve the monitoring and forecasting systems for air-ice-ocean physical processes, ecosystems studies and systems for pollution monitoring and mitigation. Characteristic processes have been described based on observations and modelling studies in newer literature. The current modelling and forecasting capabilities for the process have been assessed, and recommendations for further work are proposed.

The MIZ is a characteristic feature of the circumpolar Arctic and sub-Arctic seas. The review has therefore included literature from the different Arctic sectors: the European, Russian, US and Canadian parts of the Arctic. The focus, however, has been on the Barents Sea and adjacent regions where offshore exploration plans are quite extensive. The Barents Sea is partly ice-covered in the winter season in the northern and eastern regions. The sea ice in combination with wind, waves and currents provide harsh environmental conditions, especially in the winter. The MIZ can be defined as the zone extending from typical 100 km outside the ice edge to 100 km inside the ice edge, where certain air-ice-ocean processes dominate and have significant impact in the environment. The physical environment is determined by an integrated system of atmospheric, oceanic and sea ice processes, including wind, waves, ocean eddies, jets and current features, convergence/divergences, sea ice processes and their variability. Many of the processes are not well understood, because observations and modeling capability is not yet well developed. The uncertainty in description of many physical processes is a major reason for the large discrepancy between different climate model simulations in the Arctic.

The report describes first the general environmental and climate processes of the Arctic Ocean, providing an overview of scientific issues to be considered by offshore operators. The main atmospheric processes are reviewed regarding climate as well as meteorological conditions for operations in Arctic and sub-Arctic seas. The sea ice conditions are of major importance because the MIZ is defined by the extent and variability of the ice edge region. Sea ice is also the main constraint for offshore operations and transportation in the Arctic, and improved monitoring and forecasting of sea ice is therefore a major task to ensure safe and cost-efficient operations. The sea ice extent, drift and thickness are determined by dynamic and thermodynamic forcing from the atmosphere and the ocean. A warming of the ocean in the Arctic regions has been observed in recent years, contributing to reduced extent and thickness of sea ice observed in the last two – three decades. In the last few years, the Barents Sea has had less ice in the winter than the average, and this can be attributed to higher ocean temperature as well as to warmer air masses in the region. Sea level change in combination with storm surges and waves will have impact on coastal constructions, vessels and offshore operations. More storms and extreme sea level height and wave height can be expected in the future. In the Barents Sea area, icebergs originating from calving glaciers in Svalbard, Franz Josef Land and Novaya Zemlya represent one of the main hazard factors for offshore operations. The amount of icebergs drifting into the drilling areas varies considerable from year to year. An extreme event of many icebergs drifting into the Shtokman area was observed in May 2003. Prediction of iceberg occurrence in regions of offshore operations is not feasible. It is therefore important to develop good monitoring and forecasting systems for icebergs. The report describes the main elements of the oil spill problem in the MIZ, including observation and modeling of oil spills as well as recovery solutions. Finally, some elements of primary production in the MIZ is described. The report concludes with recommendations for further work to support the development of oil and gas exploration in the Arctic and sub-Arctic seas.

1. Introduction to the marine environment of the Arctic

1.1 The role of the Arctic shelf seas

The large potential oil and gas fields in the Arctic are located on the continental shelf surrounding the deep Arctic Ocean. These areas, also called the Arctic shelf seas, represent about half of the Arctic Ocean and 25% of the entire Ocean shelves. They are vitally important for Arctic communities, all living on or near the seashores, since shelf seas provide most of the necessary living resources. The Barents Sea and the Bering Sea are among the most productive oceanic areas on Earth. Considering the importance of the Arctic and sub-Arctic seas for global fisheries and harvesting of a wide range of marine resources, projected Arctic climate changes are likely to have substantial repercussions at the ecosystem level, further extending to different economic and societal sectors.

The Arctic shelf seas are to a large extent covered by the seasonal sea-ice zone, defined as the areas that are covered by sea ice in winter and are ice-free the summertime. The marginal ice zone (MIZ)¹ is defined to be a zone extending from typical 100 km outside the ice edge to 100 km inside the ice edge, where certain air-ice-ocean processes dominate and have significant impact in the environment. The MIZ is therefore a subset of the seasonal sea ice zone, moving northwards in the summer and southwards in the winter. The seasonal sea-ice zone are expected in the near future to offer important waterways for major world transportation of goods and natural resources as well as for oil and gas development (Figure 1.1). Arctic shelf seas receive 10% of the global freshwater discharge, including all the freshwater from Siberian and Canadian rivers, and transport it to the deep Arctic basin.

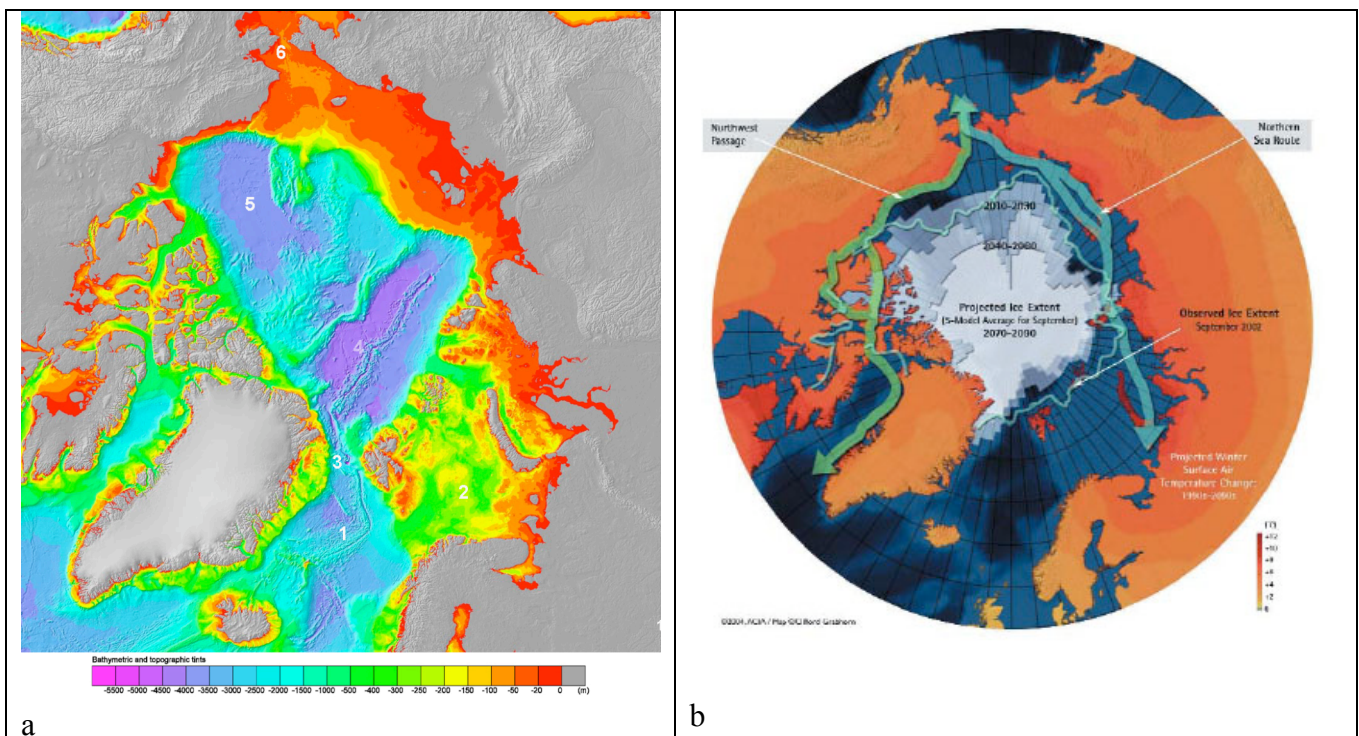


Figure 1.1 (a). Bathymetric chart of the Arctic Ocean and shallow shelf seas; (b) map of the main sailing routes in the Arctic shelf sea areas which will be opened up for sea traffic in the future with less sea ice areas. The sailing routes coincides with the main offshore operation areas and the marginal ice zones.

¹ There are several definitions of the Marginal Ice Zone, see for example the image on the front page

The resulting layer of 100–200 m thick low-saline water covers the entire Arctic Ocean and serves a primary role in sea-ice formation during freezing periods. Arctic shelf seas are very active in sea-ice and brine formation, as evidenced by the presence of frequent latent heat and coastal polynyas. Over the past decade, evidence has accumulated that the Arctic is undergoing several significant changes, and many of them occur in the Arctic shelf seas. The most severe changes include:

- increased air temperature and enhanced wind mixing over most of the Arctic shelf seas,
- reduced sea-ice cover and destabilization of the landfast ice with more frequent break-out events,
- significant changes in the sea ice-cloud-albedo feedback mechanisms,
- marked changes in amplitude and seasonality of river discharge,
- enhanced coastal erosion due to degradation of permafrost, increases in wave action and sediment transport by sea ice,
- changing pathways of suspended particulate matter, nutrients, and contaminants from land across the shelves and continental slopes to the deep Arctic Ocean,
- significant changes in the marine ecosystems and food web structures of the shelf seas, and
- changes to the transfer of mass and gas across the ocean-sea ice-atmosphere interface.

These changes have already started to affect the shelf environments in particular and, if it continues as predicted by climate models, would have major implications for the ecology and for human activities in the circum-Arctic. However, the mechanisms amplifying or damping these potential changes are not well understood but are essential for understanding and modelling the entire system across disciplines over the next five decades and to project their influence over the global climate. With respect to increasing levels of shipping and resource exploitation in Arctic shelf seas a number of scientific problems need to be further explored, as described in the following sections

1.2 Ocean dynamics of the shelf seas

In the context of a highly stratified upper Arctic, shelves and shelf breaks are of considerable importance from the perspective of vertical mixing, deep ocean ventilation and transfer of dissolved and particulate matter (Figure 1.2). Mixing is also of critical importance to areas of high biological production over the Bering, Chukchi and Barents shelves.

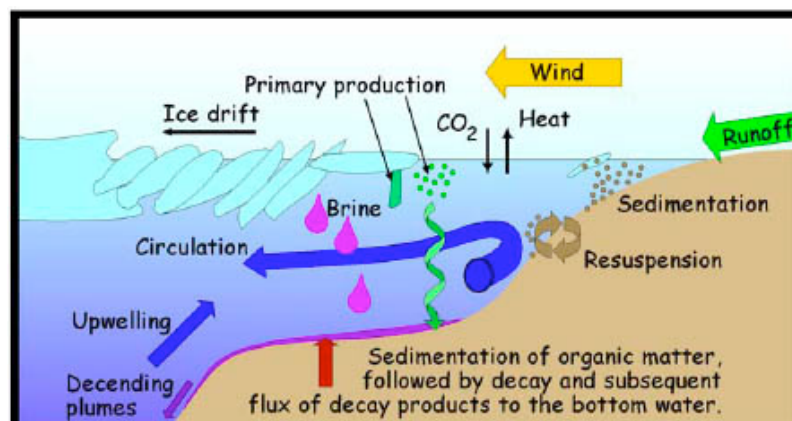


Figure 1.2: A simplified schematic diagram showing processes on Arctic shelf seas and their land-shelf-ocean interactions (ICARP-2, 2005)

Currently, strong stratification over much of the circum-Arctic shelf seas confines brine production to coastal and flaw polynyas along the landfast ice bordering the coastlines in the Chukchi/Beaufort and Siberian Seas. However, even in these regions, the substantial supply of freshwater from the large rivers greatly limits deep mixing. Hence, only polynyas close to the shelf break in the Beaufort, Chukchi, Laptev, eastern Kara Seas and the northern and eastern Barents Sea are likely to contribute in a major fashion to brine transfer into the deep basins.

With lowering of sealevel pressure over the Siberian shelf and increasing pressure gradients, penetration of storm systems into the shelf and associated wind mixing of shelf seas is likely to increase. This effect is likely to be amplified by the reductions in ice cover and increase in wind fetch. Storage of summer heat in this mixed surface layer appears to be retarding ice grow in the fall thus forming a „feedback“ which is amplifying the observed reduction of the aerial extent of sea ice (particularly in the Chukchi Sea and Amundsen Gulf). During winter, the westward trend of predominant winds over the shelf break combined with an increase of the Atlantic water layer temperature will favor warmer water upwelling and its expansion into the outer shelf. This may dramatically affect bottom water hydrography, sedimentation as well as outer shelf biodiversity. It may also feedback into the sea-ice layer providing a ready heat source to either retard growth in the fall or to increase melt in the spring. Due to changes in wind patterns the Transpolar Drift of ice and freshwater discharge from the Siberian shelf seas is expected to be weaker and turned eastward during winter, while during summer along-shore transport of riverine water will dominate the shelf hydrography. The combination of these anticipated changes may actually result in an increase in surface salinity in the central Kara and Laptev Seas, despite potential increases in river discharge. Weaker density stratification will enhance vertical mixing, affecting the downward fluxes of dissolved oxygen and nutrients that are critical for biological productivity.

The observed thinning and shrinking of the Arctic sea-ice cover and its predicted further decline are of central importance to shelf processes. The changes are particularly pronounced in the East Siberian, Chukchi and Beaufort Seas, where thick multiyear ice that occupied much of the shelf during the entire year has now been replaced with thin seasonal ice (Figure 1.1). During the summer months much of the shelves are now ice-free. Referring to these changes we should focus upon:

- Linkages between landfast ice, coastal polynyas/leads and brine production;
- Impact of increased freshwater flux and reduced ice cover;
- Effect of changing ice regime on transfer of gas, mass and energy across the ocean-sea ice-atmosphere interface;
- Processes coupling atmospheric forcing to oceanic upwelling at shelf/slope breaks;
- Mechanisms sustaining flaw lead and polynya systems and thus their brine production;
- Integrated impact of climate change on marine transportation and exploitation of natural resources.

1.3 Changes in cross-shelf transport of water masses

An increased mean annual river discharge of about 20% for the rivers that flow into the Arctic and a shift in the timing of peak flows to earlier in the spring is expected by the later decades of this century. Greater winter and spring runoff will increase flows of sediments, nutrients, and contaminants across the shelves to the Arctic Ocean. Moreover increasing air and water temperatures over most of the Arctic shelves are likely to accelerate the thawing of coastal and submarine permafrost along the Siberian shelf seas in particular. A considerable amount of organic carbon is stored in the upper layer of permafrost and gas hydrates are expected within and beneath the submarine permafrost. Thawing of permafrost could release large quantities of greenhouse gases into the atmosphere, further increasing global warming. Even though the submarine permafrost is of importance for the global climate system, our knowledge on its distribution and recent dynamics is inadequate and nonexistent for most of the Arctic shelf seas.

Due to the delay of freeze-up the shelf seas are ice-free for a longer period and the impact of autumn storms will be stronger. The autumn storms cause vertical mixing of the entire water column as well as the resuspension of bottom material and the enhanced removal of surface reactive contaminants. Thus, increased sediment and contaminant export from the shelves to the deep Arctic Ocean can be expected. The distribution and dynamics of suspended matter influence the primary production in terms of the availability of nutrients and of the absorption of light. Many contaminants are hydrophobic and consequently tend to be absorbed to and transported by organic and inorganic matter. As a result, the fate and transport of these pollutants may be controlled largely by the distribution, composition, and concentration of suspended matter. Arctic shelf seas receive their suspended matter load mainly via riverine discharge (Figure 1.3). Other sediment sources are coastal and seafloor erosion. Dissolved matter (e.g. nutrients and dissolved inorganic carbon) is also converted through biological processes into particular matter. Some of the particulate matter, of both terrestrial and marine origin, remain on the shelf and gets buried in the sediment where it, and notably the carbon, can be sequestered for long periods of time. Part of the particulate and dissolved matter might be transported by bottom currents into the deep Arctic Ocean or incorporated into sea ice. Biological processes also contribute to the transport. For instance, sea-ice flora and fauna are conveyors of contaminants.



Figure 1.3. Dirty ice north off the Lena Delta after the break-up of River Lena in spring. Ice is an efficient vehicle for the transport of particulate and dissolved matter in the Arctic (ICARP-2, 2005).

A detailed knowledge of the “environmental” pathways of sediments, nutrients and contaminants and their possible response to climate change is of critical importance to understand and to forecast the impact of environmental changes on land-shelf-ocean interactions. However, this depth of understanding is currently lacking. Therefore time series and process studies on the following issues are needed:

- Estimating stability factors and biogeochemical cycles in submarine permafrost. In particular methane formation and/or oxidation;
- Quantifying the dynamics of sediments, nutrients and contaminants in the context of climate variability and change;
- Effects of changes in the sea-ice regime, enhanced hydrological cycle, increased coastal

- erosion and changes in ocean circulation on cross-shelf to basin transport;
- Role of productivity and ecosystem changes in enhanced transport;
 - Role of shelves for carbon sequestration;
 - Process of carbon exchange across the ocean-sea ice-atmosphere interface and the biochemical processes which drive this exchange.

1.4 Ecosystem change and impact on environment

Global warming has resulted in a continuous increase in seawater temperature and a reduction in ice cover in the Arctic. This long-term development is complicated by the extensive inter-annual variation that characterizes Arctic shelves. Ecological changes nevertheless follow global warming (Figure 1.4); for example, the first Atlantic-invasion species, such as the blue mussel and blue whiting, have recently been observed in the Barents Sea and near Svalbard as has the presence of Capelin in Hudson Bay. In addition the reduction in ice cover and increased run-off delivered by rivers creates a scenario where surface water stratification increases on the important internal shelves but will decrease over time on inflow shelves such the Barents and Chukchi Seas. Shifts in stratification lead to significant changes in the physical forcing of productivity (light, vertical mixing, length of growing season, availability of nutrients, harvestable production, etc.). Currently there are about ten select pan-arctic shelf regions where some basic knowledge regarding the food webs and their physical forcing exists, knowledge that will be available just ahead of the IPY period. However, further work in these regions is necessary to investigate inter-annual variability and change.



Figure 1.4: Polar bears are unlikely to survive as a species if there is an almost complete loss of summer sea-ice cover before the end of this century (ICARP-2, 2005).

For the majority of pan-arctic shelves where no information is available, the need to acquire knowledge is compelling. Also, as many of the pan-arctic shelves are difficult to access, modelling investigations, based in particular on physical-biological coupled 3D models, need to be developed, verified and applied to estuarine circulation and marginal ice zone scenarios on the inner and open shelves, respectively. Polynyas are particularly sensitive to current changes in

oceanic and atmospheric forcing. Some polynyas appear to be increasing in size while other are beginning to disappear all together. The effect of warming on polynyas affect all element of the marine ecosystem including benthic and pelagic processes as well as biochemical cycling and rate processes. Given this preamble the key science questions should focus around:

- Northward shift of high-production zones;
- Longer and changing periodicity of open-water periods and increased meteorological forcing on nutrient dynamics and plankton succession;
- Invasion of species from lower latitudes and changes in food-web structure, with higher trophic-level species as sentinels of this change;
- Overall and regional changes in productivity as affected by changes in meteorological; oceanographic, hydrological, and biogeochemical boundary conditions;
- Distribution of marine resources as related in changing fronts, hot spots and polynyas.

1.5 Timing of sea ice events, spring bloom, river break-up and peak in hydrological discharge.

Climate models predict marked changes in amplitude and seasonality of Arctic rivers due to melting of permafrost, regional increases in net precipitation, decreased snowfall, earlier spring-melt, and a delay in the onset of sea-ice cover.

The entry, distribution and fate of particulate and dissolved elements (especially carbon and nutrients) in the Arctic Ocean, and thus the development and sustenance of Arctic ecosystems, are strongly a function of the timing of physical events. The arrival of sufficient irradiation to drive photosynthesis in the ice and the ocean below is determined certainly by solar-planetary positioning but also by a complex function of cloud cover, and the thermodynamic state of the snow/sea ice system. Precipitation plays a pivotal role in that a small temperature change (less than 1°C) can have a profound impact when precipitation arrives in the form of rain rather than snow. As ice break-up proceeds, cloud cover becomes a notable differentiator between open water (more and different types of clouds) and the remaining ice-covered ocean. Along with riverine input of organic matter, albeit of lesser quality, the spring blooms of sea-ice algae and marine phytoplankton (themselves disjunct in time) provide that year's supply of resources for the existing ecosystem. To the degree that shifts in key physical events alter these carbon (and riverine nutrient) inputs, an ecosystem can be jump-started by intense ice-algal blooms and extended open-water bloom seasons or stunted in its development by late ice break-up (Figure 1.5) and early freeze-up. The timing of these various elements within the marine ecosystem are not well understood and can have length scales ranging from days to interannual effects (e.g. survival of one cohort impacting that of another in the next season). A trend towards an earlier bloom season in the Arctic may initially support a richer overall ecosystem, including commercially viable fisheries, but over the long term the supply of key plant nutrients (nitrate and silicate) will determine ecosystem complexity and the number of trophic levels that can be supported. As the hydrological cycle, complete with its nutrient components, is altered by climate change, so will ecosystems change. Enhanced silicate input to a given region will ensure competitive diatom blooms (nitrate also being in sufficient supply), which in turn support larger organisms up the trophic ladder; reductions in the silicate supply will favor smaller-celled phytoplankton, prey items for different and smaller predators. Changes in the timing of physical events and delivery of key nutrients can thus shift keystone species, leaving an altered ecosystem that may no longer favor the higher trophic levels of today or traditional use activities by native peoples. Such species shifts can also lead to an altered biological pump with less carbon delivered to the seafloor for the support of benthic resources or eventual burial. Thus, we should focus upon:

- Impacts on ecosystems, marine resources, depositional environments and polynya dynamics;

- Changes in the significance of the biological and dissolution pump;
- Links between primary changes (atmospheric pressure, air temperature, ice cover, riverine input, etc.) and complex changes in shelf-ocean interaction, ecological structure and function (including higher trophic levels), and the hydrological cycle;
- the key links between radiative exchange, clouds and snow on sea ice requires significant development so that the links between the hydrological cycle and the geocosystem can eventually be modelled.



Figure 1.5: Break-up of River Lena in June. The most changeable time of the year is during spring river break-up, when the interaction between river Lena and the Laptev Sea is most dynamic. The sudden influx of the relatively warm riverine freshwater and high amounts of dissolved and particulate matter into the cold marine ice covered Laptev Sea results in drastic environmental changes (ICARP-2, 2005).

1.6 Arctic polynyas

The environmental, socio-economic and geopolitical consequences of an eventual sustained reduction of Arctic sea ice will be significant. For example the continuing reduction of sea ice is very likely to lengthen the navigation season and increase marine access to the Arctic's natural resources. Here, polynyas play a central role as they are thought to be model systems for how the Arctic will respond to regional and circumarctic oceanic and atmospheric forcing.

Polynyas, currently small components of the Arctic System, are expected to expand in size and duration in the near future especially on the Arctic shelves until the entire shelf region is open virtually year-round. The responses on the scale of a polynya, evident for example in increased local cloud formation, generate feedbacks to climatic conditions that may reach a larger scale. The evidence that the physical boundaries of polynyas have changed over the course of satellite history or are poised for potentially rapid change is building.

For example, the Cape Bathurst polynya that forms on the Mackenzie Shelf is intimately connected to the degree of reduction in average areal sea-ice concentration in the southern Beaufort Sea, in turn driven by scale-dependent atmospheric and oceanic forcing throughout the annual cycle. Atmospheric forcing is believed to drive oceanic upwelling at the shelf-slope break and contribute to early reduction in sea-ice concentration. Fall formation of sea ice is then delayed

by surface mixing of a summer warming of the surface layer. These climatic responses and feedbacks have resulted in a polynya that has begun to change in geographic location (to migrate eastward) with a tendency towards increased negative sea-ice anomalies over the past 25 years. This migration eastwards along the shelf and overall reduction in sea ice has potentially important implications to higher trophic levels, since this region provides critical feeding grounds for marine mammals, especially whale populations, and the native peoples that derive sustenance from them in traditional ways. Meanwhile, the atmospheric and oceanic forcings at work in the annual formation and closure of the North Water in northern Baffin Bay have yielded a geographically stable polynya over satellite history, with a highly productive ecosystem that rivals the Barents and Bering Seas. Longer-term history recorded in the sediments and in anthropological data suggests that polynya productivity and carbon export have been reliably high over hundreds to perhaps thousands of years. Yet, recent climatic and oceanic changes (their relative importance requires further study) appear to have reduced the duration of the major ice bridge that connects Ellesmere Island and Greenland and, along with winds and currents, enables annual polynya formation. The demise of this ice bridge is expected to bring more ice into the polynya region, potentially reducing primary productivity and the current richness and robustness of the larger ecosystem. The recent demise of an ice bridge with similar physical function on the northeast Greenland shelf has resulted in the conversion of the previously well-defined Northeast Water polynya to an open-water shelf system of unknown altered ecosystem performance.

Hardly anything, however, is known on the impact of climate changes on the Eurasian continental shelf polynyas although these are major sources of dense water (Kara, Barents and Chukchi Polynyas) and sites of high net-ice production rates in the Arctic Ocean (mainly Laptev-Sea Polynya; Figure 1.6). In addition they are of vital importance for navigation along the Northern Sea Route. These polynyas are understudied as ecosystems but well-studied as dynamic interfaces between hydrological input from the major Siberian river systems, with their particulate and dissolved loads, and the broad depositional shelf areas dropping to the deep sea. Since polynyas are focal points for intense biological production and the sustenance of higher trophic levels, changes in the timing of key events associated with their formation, areal extent, and closure can be closely linked to ecosystem structure and bounty.



Figure 1.6: The Laptev Sea flaw polynya north off the Lena Delta (roughly 1 km wide) in the Siberian Arctic (ICARP-2, 2005).

In order to assess the dynamics and relevance of polynyas for the arctic climate system, it will be essential to investigate both, their long-term history and their highly variable annual and interannual dynamics by integrated multidisciplinary studies. Only then will it be possible to model the near future of this unique polar oasis. Focus should be upon:

- Interannual, decadal and longer-term variability in oceanic, sea-ice and atmospheric forcing;
- Dramatic impacts on higher-trophic levels by changes in polynya formation and size;
- Role of scale in atmospheric and oceanic forcing of circumarctic polynya systems;
- Feedbacks between polynyas the more regional scales of marginal ice zones and shelf/basin systems;
- Predictions from observation-based models;
- Long-term history and paleo proxies of Arctic polynyas;
- Feedbacks to the Arctic System.

Many of these topics will be further investigated during the International Polar Year (IPY) from 2007 to 2009. More information about IPY projects can be found on <http://www.ipy.org/>.

1.7 Topics reviewed in this report

A selection of topics from the Arctic marine environment has been reviewed in this report, including regional and local processes associated with the MIZ as well as large scale processes affecting the whole Arctic Ocean and adjacent seas. The atmosphere of the Arctic is characterized by large scale pressure systems and flow of air masses that determine air temperature, cloud and radiation conditions, sea ice and meteorological conditions of importance for offshore operation and navigation. A particular phenomenon in the MIZ is the polar lows that can create extreme wind speeds that are difficult to predict by the standard weather forecasting services. The sea ice has different roles in the Arctic, both as a key factor in the climate system and as a barrier for marine operations and transportation. The location of the MIZ is determined by the extent of sea ice which has a strong seasonal variability and retreats further north as the sea ice area shrinks. The trend and variability in the ice extent and ice thickness over the last decades are discussed, and the local sea ice processes with direct impact on construction and vessels are described. Modelling of sea ice using different physical description of the sea ice is reviewed, and the specific challenges of modeling the sea ice in the MIZ are described. One of the characteristics of sea ice in the MIZ is the surface wave propagation in to the ice pack, causing the ice pack to be broken into smaller floes. Another property of the MIZ is the freezing and melting of sea ice as well as eddies and ice tongues transporting ice in different directions. The ocean plays an essential role because the freezing and melting of sea ice is strongly dependent on ocean temperature and salinity. The water masses and ocean currents are key factors in the Arctic climate including the physical and biological components of the marine environment. The sea level variability due to tides, storm surges and long-term sea level rise has important implications on coastal and offshore construction. The discharge of freshwater from rivers and melting glaciers has impact on the ocean water masses, where increased freshwater discharge tend to increase the surface layer of low-salinity water. Problems related to oil spills in ice-covered waters are reviewed, based to a large extent on reports from studies in US, Canada and in the Sakhalin area. The last topic is about modeling of primary production in the MIZ and the coupling to physical processes in atmosphere and ocean. In the concluding chapter, the major issues for offshore operations in the MIZ are summarized and recommendations for further work are proposed.

2. Atmospheric processes

2.1 Air Pressure in the Arctic

Several fronts and semi-permanent high and low pressure systems characterize the Arctic. The "polar front" marks the boundary between cold polar air masses and warm tropical air masses. The polar front is intermittent rather than continuous around the globe. The strength of the polar front depends on the magnitude of the horizontal temperature gradient across the front. Where the temperature gradient is steep, the front is strong and is a potential site for cyclone or low pressure system development. Where temperature contrast is small, the polar front is weak. Like the polar front, the "arctic front" is discontinuous and depends on the temperature contrast between two air masses. The arctic front is the boundary between polar and arctic air masses and lies to the north of the polar front. The arctic front can be as strong as the polar front. It is particularly prominent during summer in northern Eurasia.

Semi-permanent high and low pressure systems ("highs" and "lows") are identified with particular regions and have seasonal characteristics. In winter, the Icelandic Low extends from near Iceland north into the Barents Sea, and is associated with frequent cyclone activity. The Aleutian Low is present in the Gulf of Alaska. An example of winter pressure situation is shown in Fig. 2.1, where Low-pressure storm tracks (blue) dominate the picture. Here Atlantic cyclonic systems, spawned as far upwind as the northern Pacific, reach from middle latitudes northward, high into the Arctic. The guiding upper tropospheric standing wave pattern is plotted with contours.

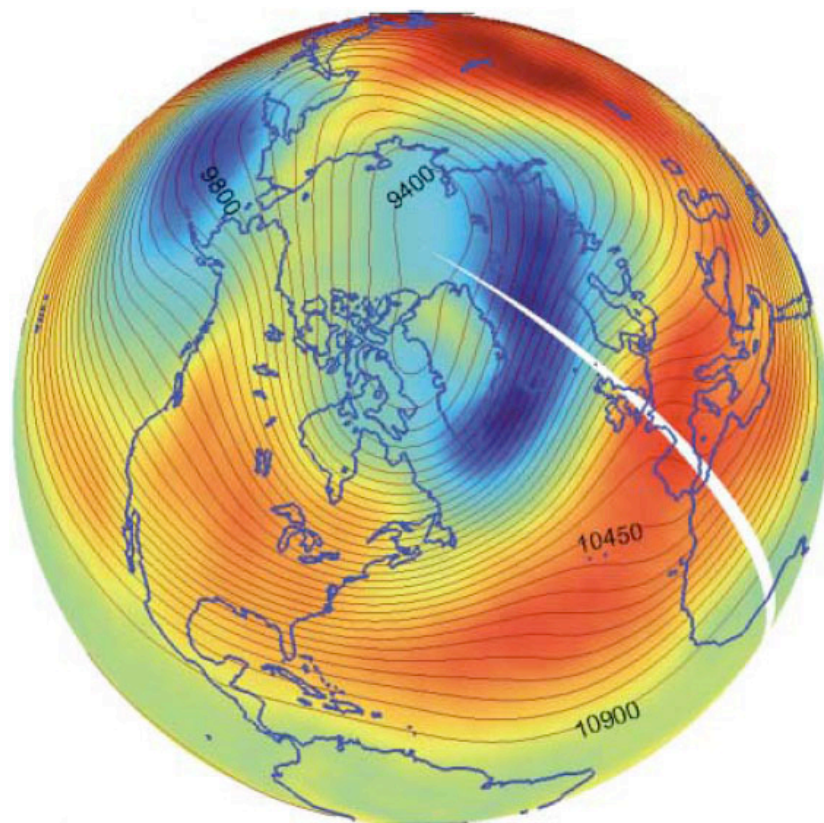


Figure 2.1. Mean sea-level pressure (colours) and 250mbar dynamic height (contours) are plotted for January to March 1993. Blue is low pressure reaching 993 mbar south-east of Greenland, red is high pressure, reaching 1023 mbar in the subtropical Atlantic. The 250 mbar dynamic height (m) is labelled along contours. Greenwich meridian is shown in white. (Rhines, 2006).

The Beaufort-Chukchi Sea region is dominated by a ridge of high pressure linking the Siberian High and high pressure over the Yukon of Canada. In April and May arctic pressure gradients decrease. The Icelandic and Aleutian lows weaken. The Siberian High disappears, and is replaced by a wide but shallow low. The Arctic High is centered over the Canadian Arctic Archipelago. In summer, pressure gradients are generally weak. Intermittently, however, cyclones enter the Arctic from northern Eurasia and the north Atlantic, and tend to persist over the Canadian Basin. By October the pattern has almost returned to the winter configuration. The Icelandic and Aleutian lows strengthen, as does the Siberian High.

The Polar vortex: The polar vortex is a persistent large-scale cyclonic circulation pattern in the middle and upper troposphere and the stratosphere, centered generally in the polar regions of each hemisphere. In the Arctic, the vortex is asymmetric and typically features a trough (an elongated area of low pressure) over eastern North America. It is important to note that the polar vortex is not a surface pattern. It tends to be well expressed at upper levels of the atmosphere (that is, above about five kilometers).

Aleutian Low: This semi-permanent low pressure center is located near the Aleutian Islands. Most intense in winter, the Aleutian Low is characterized by many strong cyclones. Traveling cyclones formed in the sub-polar latitudes in the North Pacific usually slow down and reach maximum intensity in the area of the Aleutian Low.

Icelandic Low: This low pressure center is located near Iceland, usually between Iceland and southern Greenland. Most intense during winter, in summer, it weakens and splits into two centers, one near Davis Strait and the other west of Iceland. Like its counterpart the Aleutian Low, it reflects the high frequency of cyclones and the tendency for these systems to be strong. In general, migratory lows slow down and intensify in the vicinity of the Icelandic Low.

Siberian High: The Siberian High is an intense, cold anticyclone that forms over eastern Siberia in winter. Prevailing from late November to early March, it is associated with frequent cold air outbreaks over east Asia.

Beaufort High: The Beaufort High is a high pressure center or ridge over the Beaufort Sea present mainly in winter.

North American High: The North American High is a relatively weak area of high pressure that covers most of North America during winter. This pressure system tends to be centered over the Yukon, but is not as well-defined as its continental counterpart, the Siberian High.

2.2 The Arctic Energy Budget and north-south flows

The energy that drives the circulating atmosphere and ocean comes largely from the sun, which strikes the low latitudes most directly. Thermal radiation is trapped by the atmosphere, absorbed by the ocean and redistributed by the combined atmosphere/ ocean circulation. Figure 2.2 schematically represents the mean annual energy budget of the Arctic ocean and atmosphere. The arrow T, q represent the advection of heat and moisture into the arctic atmosphere from lower latitudes. Solar and thermal (shortwave and longwave) radiation fluxes are represented by "S" and "L". "O" represents the flux of heat from the ocean to the atmosphere through openings in the ice (leads and polynyas). This flux is significant in winter, when the ocean is much warmer than the air. "P" represents precipitation, "M" represents the melting of snow and ice, and "R" represents the input of freshwater runoff. The "Ice" arrow symbolizes net ice production and export (export of ice from the Arctic occurs primarily through the Fram Strait along the east coast of Greenland), while the "Water" arrow symbolizes the influx of relatively warm Atlantic water into the Arctic Ocean. All of the elements in the figure represent processes that release or consume energy (such as precipitation and melting), or fluxes of energy. Over the course of a year, the net radiation

balance at the top of the atmosphere (a net loss of heat energy) roughly balances the advection of heat northward into the Arctic².

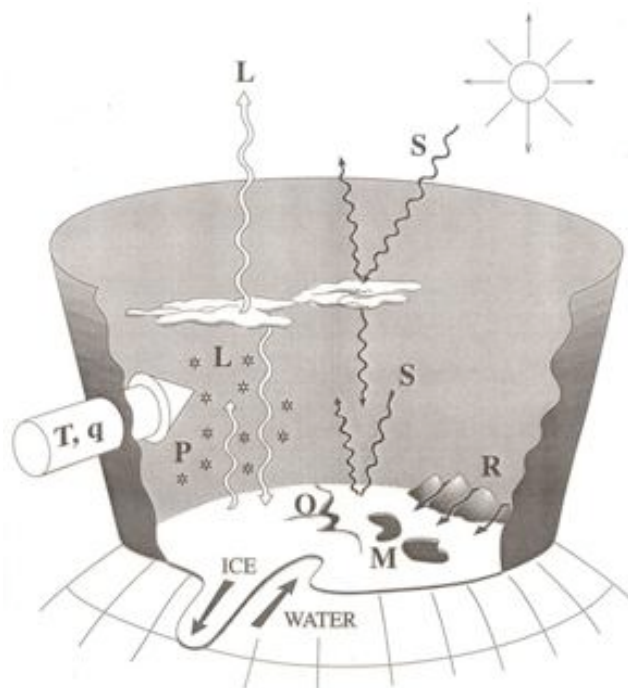


Figure 2.2. Arctic energy budget components: R = Runoff (freshwater); L = Longwave radiation; S = Shortwave radiation; O = Ocean heat; M = Melt (snow and ice); P = Precipitation; T = Temperature (heat transfer); q = moisture. (From "SHEBA, a research program on the Surface Heat Budget of the Arctic Ocean", NSF Arctic System Science Report No. 3, August 1993, by N. Untersteiner.)

Analyses of atmospheric observations by the major weather centres and oceanic observations from ships, satellites and autonomous undersea vehicles continue to home in on values for the net north-south flow of thermal energy, mass and salt. An intriguing aspect of this energy flow is that the air's 'sensible heat', the warmth we measure with a thermometer, carries only about one-third of the total. From the excess solar heating in low latitudes, just over two petawatts (2×10^{15} watts) of thermal energy is carried as sensible heat by the oceanic meridional overturning circulation (MOC). Of this total energy flow, about 1.2 petawatts occurs in the North Atlantic, peaking at about 20°N latitude. The atmosphere moves a peak value of about five petawatts northward and it is often pointed out that the oceanic contribution is the smaller of the two (these numbers vary with latitude of course, and are reported here as peak values). However, a more balanced view is that there are three forms of north-south energy transport rather than just the two oceanic and atmospheric contributions (from Rhines, 2006).

First is the basic 'warm south wind, cold north wind', or dry static energy transport in the atmosphere; second is the corresponding 'warm Gulf Stream, cold deep western boundary current', or thermal energy transport of the ocean. The third form of heat transport is shared jointly by atmosphere and ocean. Water vapour enters the atmosphere through evaporation from the warm sub-tropical ocean (thus increasing the salinity there). This vapour represents latent heat and moves poleward in the atmosphere finally releasing sensible heat as it precipitates out. The amplitude of each of the three forms of thermal energy transport is comparable, with peak values of roughly two petawatts (Bryden et al. 2001).

² http://bipolar.colorado.edu/arcticmet/factors/heat_budget.html

Delivery of heat from the sub-tropical oceans to the sub-polar atmosphere through water vapour transport has a crucial secondary effect in delivering water to form snow, ice and a buoyant, floating layer of low salinity on top of the sub-polar oceans. The return circuit for poleward-flowing atmospheric moisture is the equatorward flow of the ocean. There is a growing awareness of the importance of the hydrologic cycle, which encompasses many facets of fresh water movement on Earth. The acceleration of fresh water movement is one of the keystone predictions related to global warming (IPCC 2001).

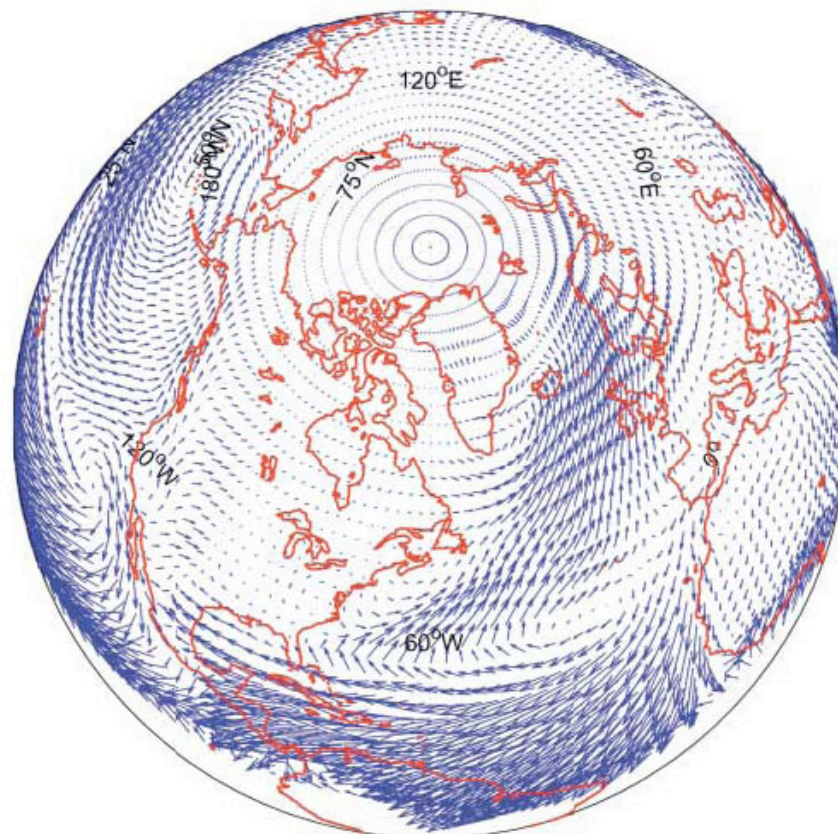


Fig. 2.3 The transport of fresh water by the atmosphere, averaged over the same period in winter 1993 as in Fig. 2.1. The total transport across latitude 60°N ranges between 0.12 and 0.18 Sverdrups. The eastern flank of the two oceanic low-pressure centres dominates this transport which involves synoptic cyclonic systems along these storm tracks. The Pacific moisture conduit rains out on the slopes of Alaskan mountains, freshening the waters of the North Pacific Ocean, while the Atlantic moisture track continues well into the Arctic basin (Rhines, 2006).

The co-operative flow of heat and moisture emphasises how tightly bound these two physical properties are. Condensation of water vapour into droplets or freezing of liquid water, involves great heat release. The winds and currents themselves can be compared quantitatively. Oceanographers measure water flow in Sverdrups, or megatonnes of mass per second³. The Amazon river (the world's largest river) flows with about 0.1 Sverdrup, while the Gulf Stream ranges from 30 to 150 Sverdrups at different locations. The ocean's global MOC has an amplitude of roughly 20 Sverdrups. The atmospheric circulation can also be expressed in these same terms;

³ 1 Sverdrup = $10^6 \text{ m}^3 \text{ s}^{-3}$

the wintertime westerly winds carry about 500 Sverdrups, while the average northerly and southerly winds carry about 100 Sverdrups in the tropics, 30 Sverdrups in the middle latitudes and 5 Sverdrups in the subpolar regions.

This meridional overturning, involving just over two petawatts of latent-heat transport, corresponds to about one Sverdrup of fresh water transport. While there is much recycling of moisture in the global hydrologic system, one Sverdrup is a good amplitude estimate for fresh water movement in the global atmospheric MOC. Where does this flow of energy actually occur? Can it be seen? Summing up the transports around circles of latitude is the traditional way to describe these cogs in the solar-driven climate heat-engine. As one moves further north, we find that the system becomes dominated by the Atlantic sector. The shape and strength of these flows is strongly influenced by the standing waves in the westerly winds (Fig. 2.1) and the veins and arteries of ocean circulation.

The atmospheric circulation pattern in the Northern Hemisphere owes its origin to the topography of the Rocky Mountains, to Greenland and to the Himalayan Plateau. In addition, forcing by contrasting thermal properties of continents and oceans contributes to the standing wave pattern (this is seen, for example in the contrast between winter and summer in the Northern Hemisphere, with sub-tropical high-pressure cells dominating over oceans in summer, while sub-polar low pressure dominates above the oceans in winter). In the Atlantic sector, the mean winds lie south-west/north-east, and as the air moves over the ocean, energy builds up in transient cyclonic systems. The Atlantic storm track, defined in this way, describes both ocean storms and climate processes. The transport of moisture (Fig. 2.3) shows concentrated conduits on the eastern sides of the oceanic low-pressure centres. In the North Pacific this moisture precipitates out before reaching the Arctic. The air collides with the Alaska Coast Range, causing enormous precipitation that contributes to the low salinity of the North Pacific Ocean (though some of this fresh water circulates through Bering Strait to freshen the waters of the Arctic). North of 60°N latitude, the Atlantic sector is left to dominate the net moisture transport. The rainfall of Scotland and coastal Norway produces both hydropower and the low salinity of the Baltic Sea. Condensation releases latent heat, warming these latitudes greatly. Perhaps the greatest monument to this moisture flux is Greenland itself. With its crest reaching greater than 3 km above sea-level, and its base depressed below sea-level by sheer weight, this ice mountain, if melted, would raise the world's ocean surface by more than 7 m. A consequence of the strong northward tracking of storms and the warmth they transport is that the Labrador Sea, Greenland Sea, Norwegian Sea and Barents Sea all remain nearly ice-free through the entire year. It is the co-operation between the mutually warmed ocean and atmosphere along this track, engaging in a game of heat- and moisture leap-frog, that warms the sub-polar zone and Arctic, which neither air nor sea alone could do.

The Arctic plays a key role in the earth's heat balance by acting as a "heat sink." The global earth-atmosphere system gains heat from incoming solar radiation, and returns heat to space by thermal radiation. Most of the heat gain occurs in low latitudes, and this gain is balanced (on average) by heat loss that takes place at latitudes north and south of about 40 degrees. Therefore the Arctic is said to act as a "heat sink" for energy that is transported from lower latitudes by ocean currents and by atmospheric circulation systems.

Heat is transported to the Arctic primarily in the following ways:

- Sensible heat is transported poleward during the exchange of air masses from the tropics to the middle and high latitudes. This transfer of heat is largely accomplished by cyclones.
- As storms travel poleward, some of the water vapor condenses as clouds, thereby releasing latent heat.

- Ocean currents bring heat from the tropics to the northern part of the Atlantic Ocean and into the Arctic.

2.3 The Arctic Oscillation and the North Atlantic Oscillation

The Arctic Oscillation (AO), shown in Figs. 2.4 and 2.5, is an important Arctic climate index with positive and negative phases, which represents the state of atmospheric circulation over the Arctic (Thompson and Wallace, 1998). The positive phase (red) brings lower-than-normal pressure over the polar region, steering ocean storms northward, bringing wetter weather to Scotland and Scandinavia, and drier conditions to areas such as Spain and the Middle East. While the value of the AO index was strongly positive in the early 1990's compared to the previous forty years, the value of the AO has been low and variable for the last nine years. The year to year persistence of positive or negative values and the rapid transition from one to the other is often referred to as "regime-like".

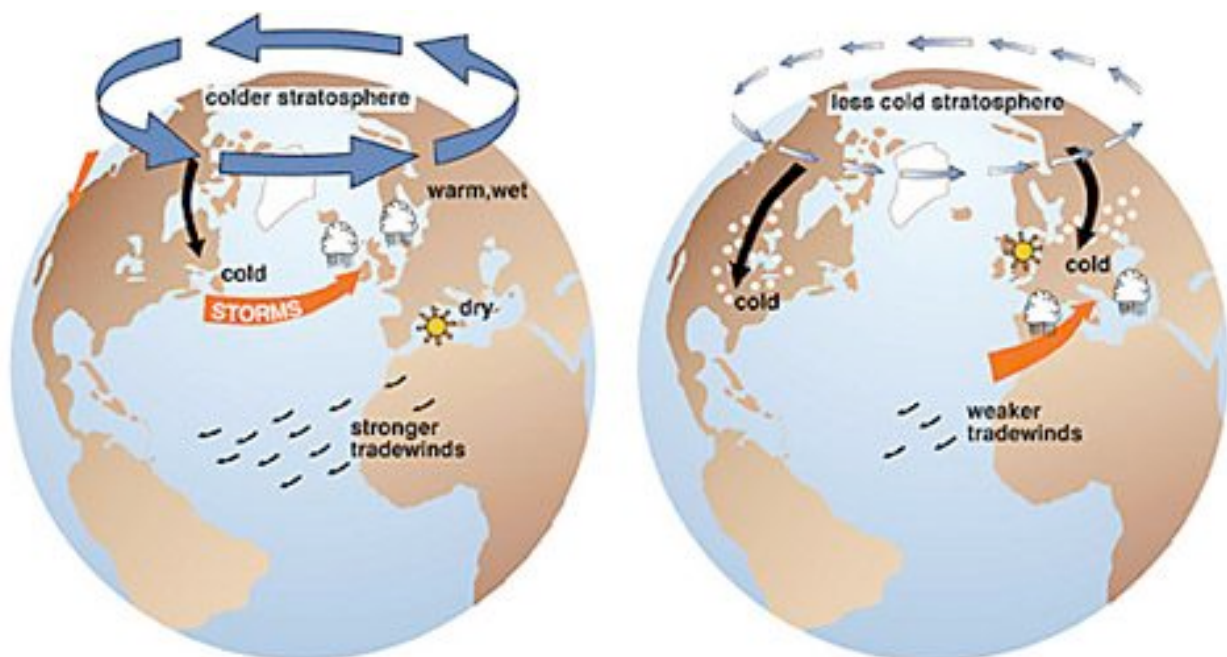


Figure 2.4 Effects of the Positive Phase (Left) and the Negative Phase (right) of the Arctic Oscillation (Courtesy J. Wallace, University of Washington)

The Arctic Oscillation (AO) appears to be the cause for much of the recent changes that have occurred in the Arctic. Its effects are not restricted just to the Arctic; it also represents an important source of variability for the Northern Hemisphere as a whole. The AO has been described as "a seesaw pattern in which atmospheric pressure at polar and middle latitudes fluctuates between positive and negative phases. The negative phase brings higher-than-normal pressure over the polar region and lower-than-normal pressure at about 45 degrees north latitude. The positive phase brings the opposite conditions, steering ocean storms farther north and bringing wetter weather to Alaska, Scotland and Scandinavia and drier conditions to areas such as California, Spain and the Middle East."

The AO appears related to a well-known mode of variability for the North Atlantic called the North Atlantic Oscillation (NAO). NAO is defined as the surface pressure difference between two stations in Portugal and Iceland. The NAO has been recognized for decades and has been considered

"the dominant mode of winter climate variability in the North Atlantic region ranging from central North America to Europe and much into Northern Asia. The NAO is a large scale see-saw in atmospheric mass between the subtropical high and the polar low. The corresponding index varies from year to year, but also exhibits a tendency to remain in one phase for intervals lasting several years." The positive phase of the NAO is associated with more frequent and intense storms in the North Atlantic Ocean, warmer and wetter winters in Europe, and cooler, drier winters in Greenland and northern Canada (Fig. 2.6).

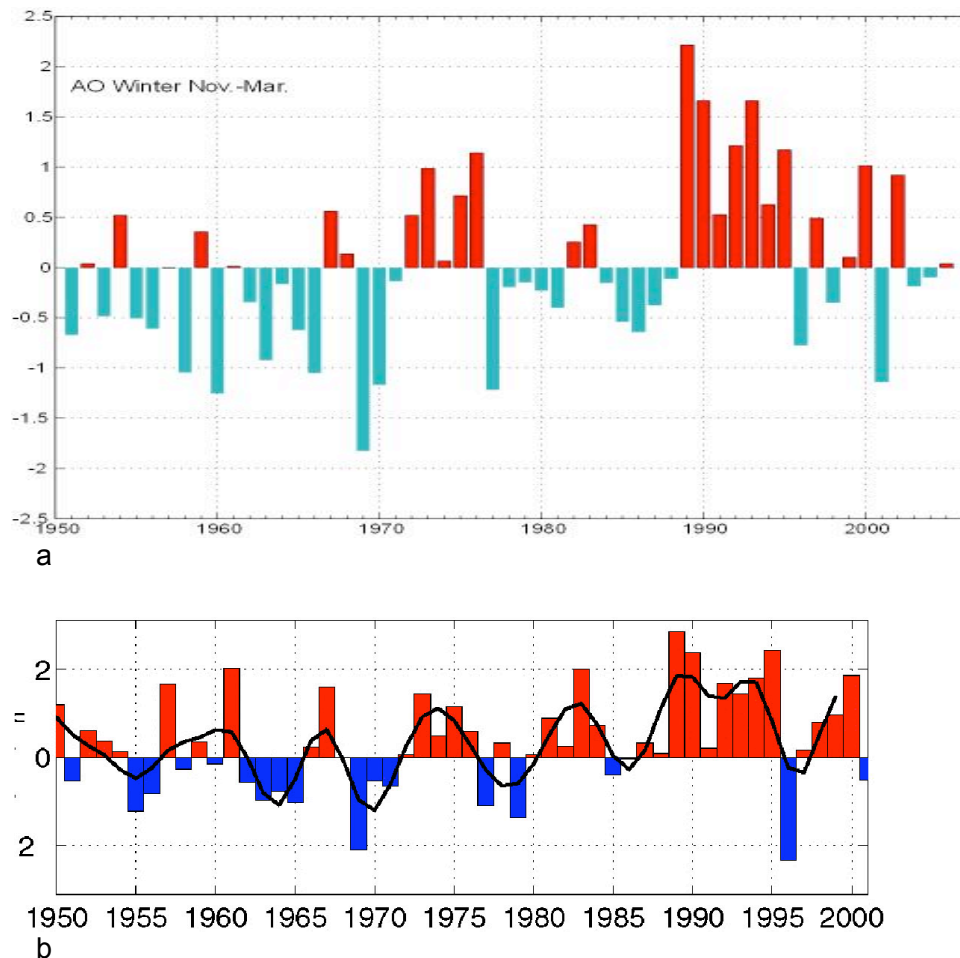


Figure 2.5. (a) Annual Arctic Oscillation (AO) index in Winter (November to March). Data from National Center for Environmental Prediction (<http://www.ncep.noaa.gov/>); (b) annual NAO index from 1950.

During the winter, the Arctic Oscillation extends up through the stratosphere, 6 to 30 miles above the Earth's surface. "The stratosphere's effect on the Arctic Oscillation's behavior appears particularly intriguing because it is opposite of what happens in other major climate systems," Baldwin said. When the oscillation changes phases, the strengthening or weakening of the circulation around the pole tends to begin in the stratosphere and work its way down through lower levels of the atmosphere. In phenomena such as El Niño in the equatorial Pacific Ocean, the changes begin in the ocean and work their way up through the atmosphere.

Stratosphere cooling in the last few decades has caused the counterclockwise circulation around the North Pole to strengthen in winter. In turn, the belt of westerly winds at the surface along 45 degrees north latitude has shifted farther north, the scientists said, sweeping larger quantities of mild ocean air across Scandinavia and Russia and bringing balmy winters over most of the United States as well.

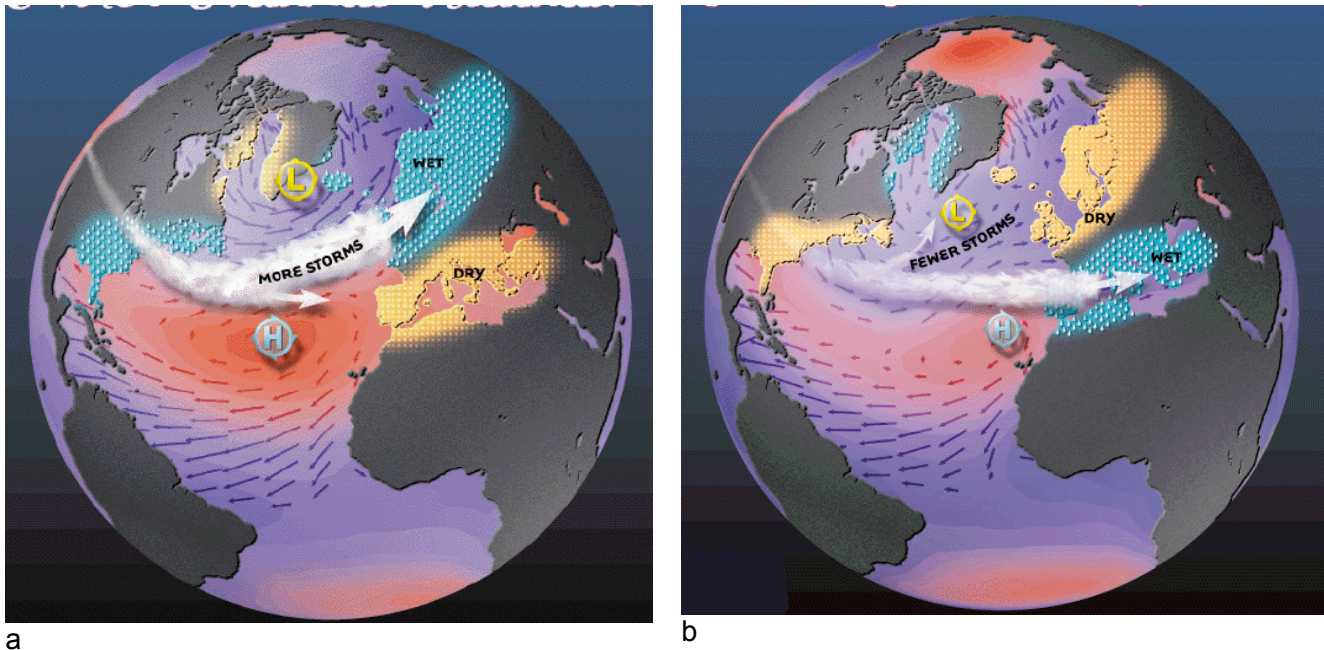


Figure 2.6 Characteristic weather patterns during positive (a) and negative (b) NAO index (courtesy: M. Visbeck at <http://www.ldeo.columbia.edu/NAO/>)

The Arctic Oscillation is an alternate view of what many scientists call the North Atlantic Oscillation, the researchers said. Year-to-year fluctuations in the North Atlantic Oscillation are thought to be prompted primarily by changes in the ocean, as with El Niño. However, it can be argued that the North Atlantic Oscillation is in fact part of the Arctic Oscillation, which involves atmospheric circulation in the entire hemisphere. There is a trend toward a stronger, tighter circulation around the North Pole could be triggered just as well by processes in the stratosphere as by those in the ocean. The trend in the Arctic Oscillation has been reproduced in climate models with increasing concentrations of greenhouse gases (Thompson et al., 2000).

2.4 Surface air temperature

The huge warming of the Arctic that started in the early 1920s and lasted for almost two decades is one of the most spectacular climate events of the twentieth century (Johannessen et al., 2004). During the peak period 1930–40, the annually averaged temperature anomaly for the area 60°–90°N amounted to some 1.7°C (Fig. 2.7). The warming in recent years, which is stronger and extends further south than in 1930–40, is illustrated in Fig. 2.8. The surface temperature has been observed around the Arctic Ocean in a network of stations (Fig. 2.9.a), some of them have data records back to the 1850s. The temperature anomalies for December-January and April are presented in Fig. 2.9 b and c.

Johannessen et al., (2004) suggest that natural variability is a likely cause, with reduced sea ice cover being crucial for the warming. A robust sea ice–air temperature relationship was

demonstrated by a set of four simulations with the atmospheric ECHAM⁴ model forced with observed SST and sea ice concentrations. An analysis of the spatial characteristics of the observed early twentieth-century surface air temperature anomaly revealed that it was associated with similar sea ice variations. Further investigation of the variability of Arctic surface temperature and sea ice cover was performed by analyzing data from a coupled ocean–atmosphere model.

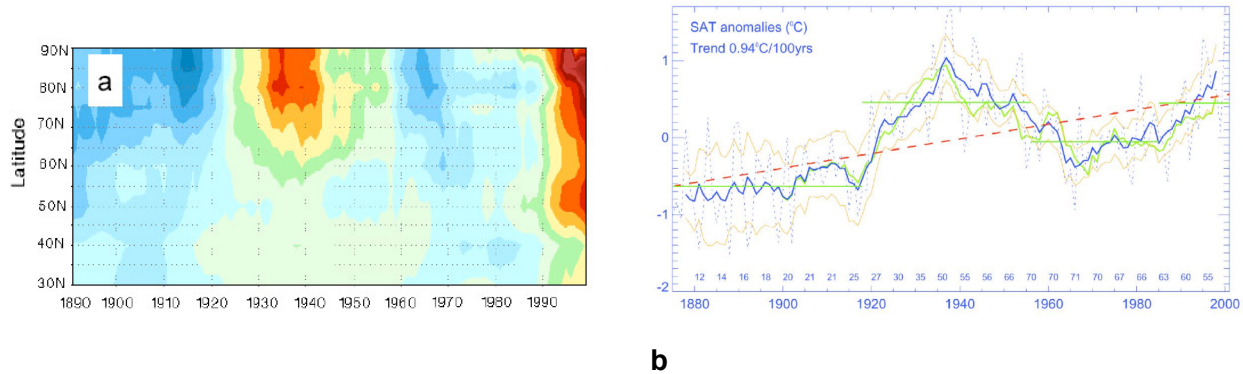


Figure 2.7 Surface air temperature changes during the twentieth century. (a) from Johannessen et al, 2004; (b) from Polyakov et al., 2005.

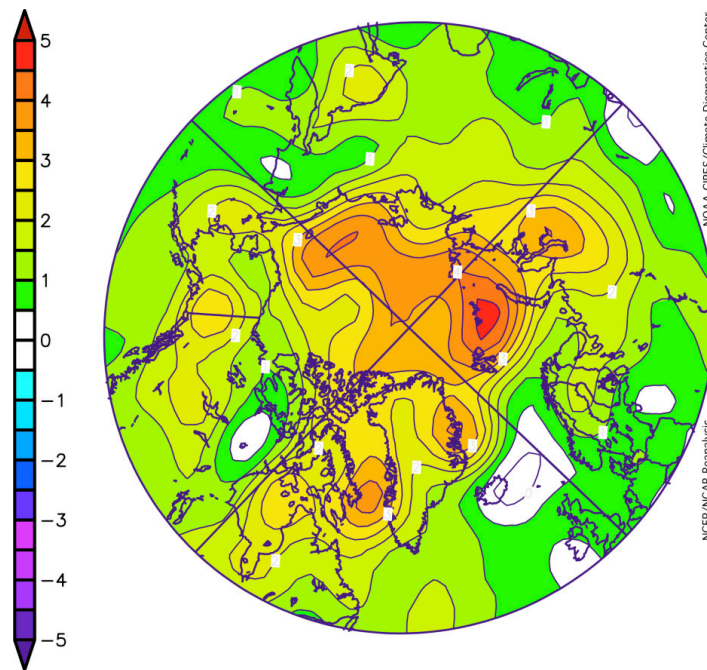
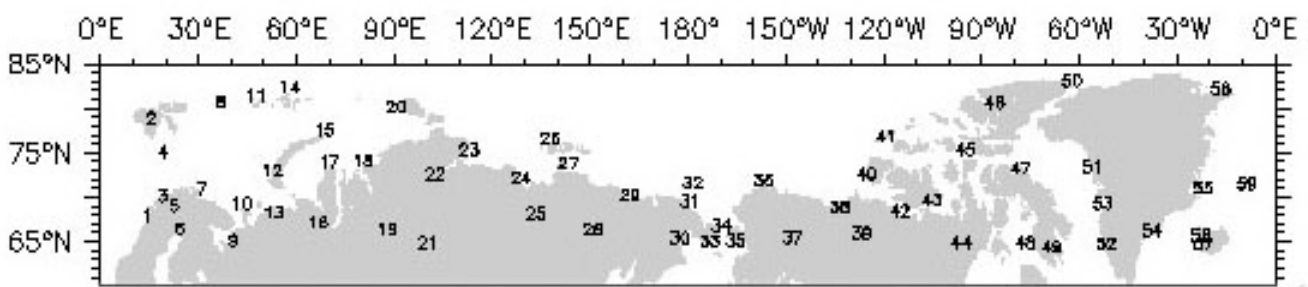


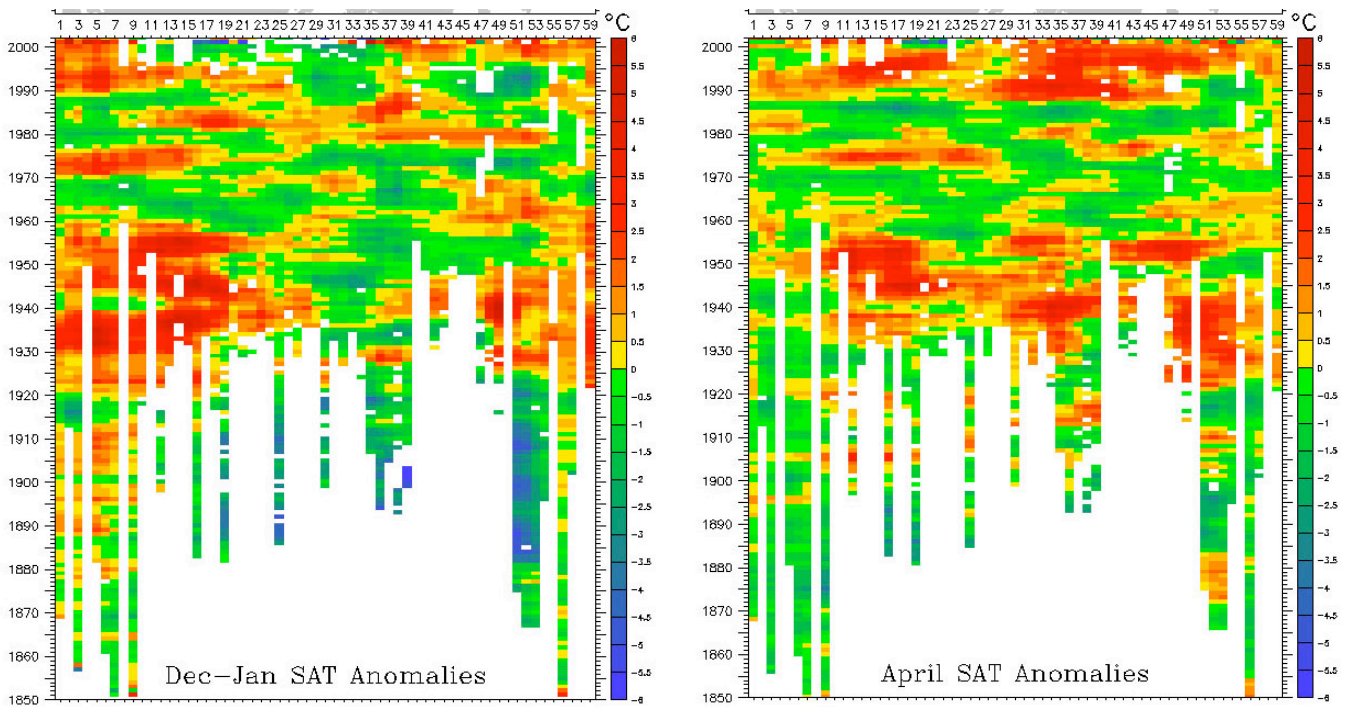
Figure 2.8 Surface air temperature anomaly map for 2005, showing that the whole Arctic was 2–4°C warmer than the normal and that the strongest warming was found in the northern Barents Sea. The scale is in °C (<http://nsidc.org>, 2006).

⁴ ECHAM: General Circulation Model developed by Max Planck Institute for Meteorology, Germany.

By analyzing climate anomalies in the model that are similar to those that occurred in the early twentieth century, it was found that the simulated temperature increase in the Arctic was related to enhanced wind-driven oceanic inflow into the Barents Sea with an associated sea ice retreat. The magnitude of the inflow is linked to the strength of westerlies into the Barents Sea. This study proposes a mechanism sustaining the enhanced westerly winds by a cyclonic atmospheric circulation in the Barents Sea region created by a strong surface heat flux over the ice-free areas. Observational data suggest a similar series of events during the early twentieth-century Arctic warming, including increasing westerly winds between Spitsbergen and Norway, reduced sea ice, and enhanced cyclonic circulation over the Barents Sea. At the same time, the North Atlantic Oscillation was weakening.



a



b

c

Figure 2.9 Circumpolar data records of surface air temperatures: (a) station map, (b) air temperature anomalies for December-January; (c) air temperature anomalies for April (Overland et al., 2004).

Of particular interest are atmospheric circulation contributions to the latest warm period, marked by less sea ice and changes in tundra conditions. Arctic cyclone activity (i.e., storms that bring warm, moist air to the Arctic) increased in number and intensity in the second half of the twentieth century, especially in summer, coupled with a general decrease in storminess in the mid-latitudes (Serreze *et al.*, 1997; Zhang *et al.*, 2004).

2.5 Polar Lows

Small cyclones forming over open sea during the cold season within polar or arctic air masses are called "polar lows." Typically several hundred kilometers in diameter, and often possessing strong winds, polar lows tend to form beneath cold upper-level troughs or lows when frigid arctic air flows southward over a warm body of water. In satellite imagery polar lows show characteristic spiral or comma shaped patterns of deep clouds, sometimes with an inner "eye" similar to those seen in tropical cyclones. Convective cloud bands occupy the surroundings (Fig. 2.10a and Fig. 2.11).

Polar lows last on average only a day or two. They can develop rapidly, reaching maximum strength within 12 to 24 hours of the time of formation. They often dissipate just as quickly, especially upon making landfall. In some instances several may exist in a region at the same time or develop in rapid succession. They represent a specific hazard to offshore operations since they develop quickly, provide extreme wind speeds and are difficult to forecast.

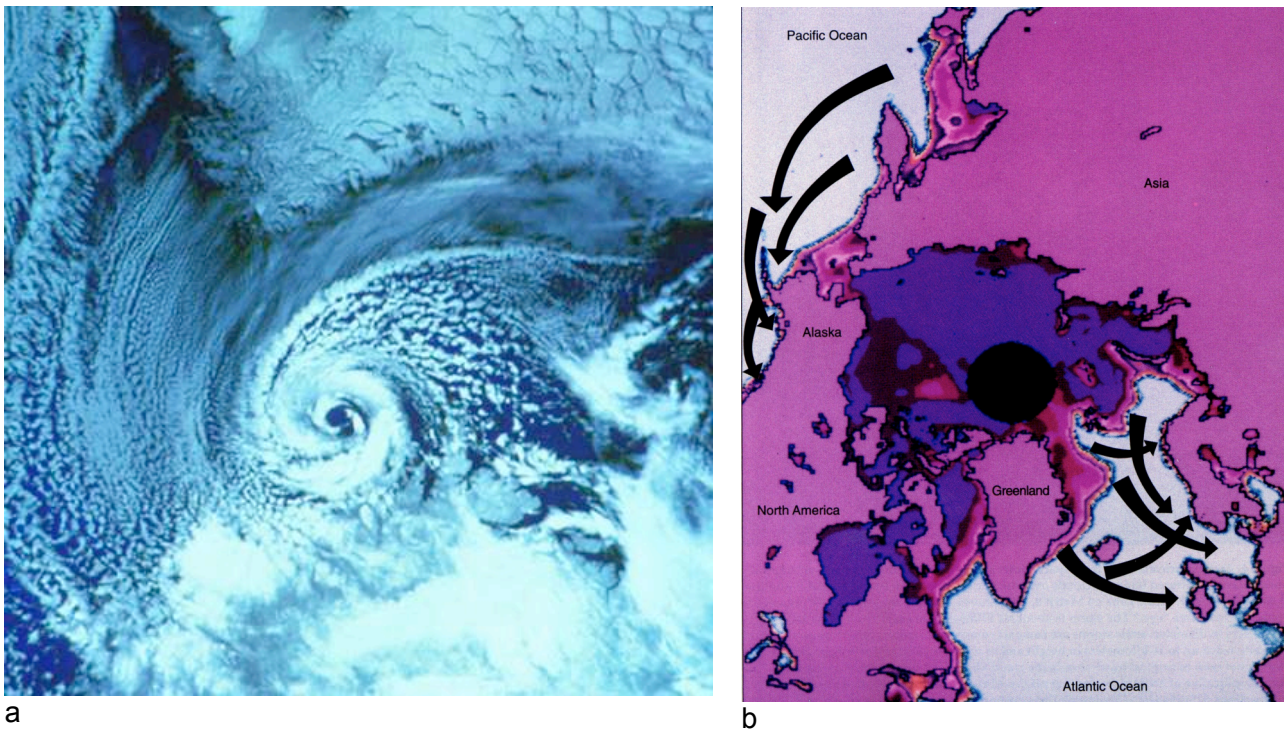


Fig. 2.10 (a) A NOAA-9 polar orbiter satellite image (visible band) of a polar low over the Barents Sea on 27 February 1987. The southern tip of Spitsbergen is visible at the top of the image. The polar low is centered just north of the Norwegian coast; (b) Map of the most common areas of Polar Lows (Courtesy: S. Businger, Department of Meteorology, University of Hawaii).

Analysis of aircraft and radiosonde data collected during field experiments reveals that polar lows may possess warm cores. This finding, coupled with their appearance in satellite imagery, has

prompted some investigators to refer to polar lows as "arctic hurricanes," although they seldom, if ever, possess hurricane strength winds.

Polar lows occur most frequently in the marginal ice zones in the North Pacific and in the Greenland, Norwegian and Barents Seas (Fig. 2.10b). Polar lows are difficult to predict even with current high resolution and high performing operational numerical models, because they usually occur in remote oceanic regions where data are too sparse to define the model initial state on a sufficiently fine scale. However, present-day models can depict synoptic-scale patterns favorable to the development of the smaller scale systems, allowing forecasters to use the predictions in conjunction with satellite imagery and conventional observations to make subjective forecasts of their occurrence.

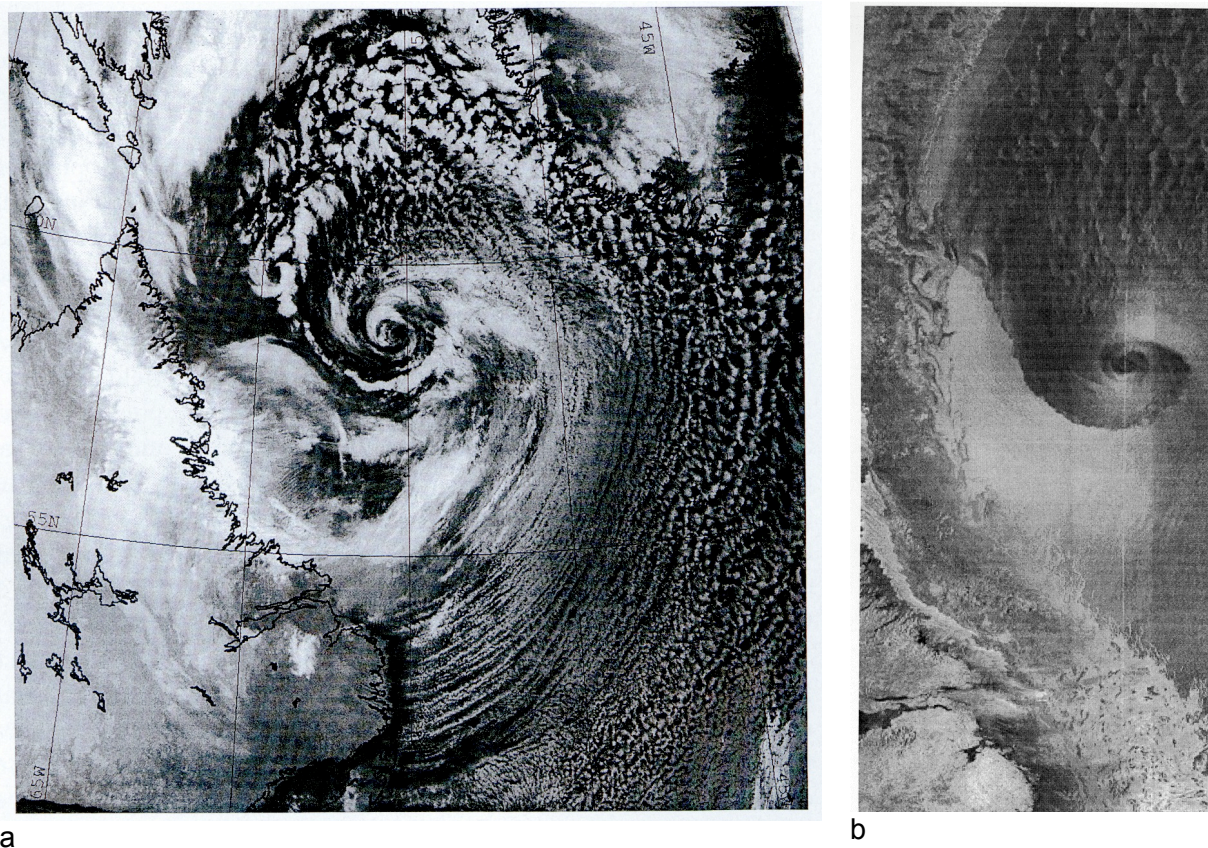


Figure 2.11. Polar lows observed in the Labrador Sea (a) from NOAA IR image, (b) from a RADARSAT ScanSAR image (courtesy Peter Guest, Naval Postgraduate School, Monterey, California; <http://www.weather.nps.navy.mil/~psguest/polarmet/geninfo/index.html>).

2.6 Clouds

Clouds are factors in climate that influence the radiation budget and therefore temperature. Clouds reflect a large fraction of solar radiation, resulting in surface cooling. On the other hand, clouds inhibit longwave radiation loss from the surface, which can lead to higher surface temperatures. The dominant process depends on many factors including cloud type and thickness, the magnitude of the solar radiation, and the albedo of the underlying surface. Clouds and precipitation undergo a seasonal cycle, as shown in Fig. 2.12 a and b, and a trend of increased cloud cover over the last decades (Fig. 2.12 c and d).

Clouds are composed of minute water droplets, ice crystals or a combination of the two that have condensed on such atmospheric particles as airborne dust, smoke, sea salt, chemical compounds, and meteoric fragments. Condensation on nuclei occurs at relative humidity near 100 percent. Many condensation nuclei such as salts are hygroscopic, that is, they have a special chemical affinity for water molecules and promote condensation at relative humidity under 100 percent.

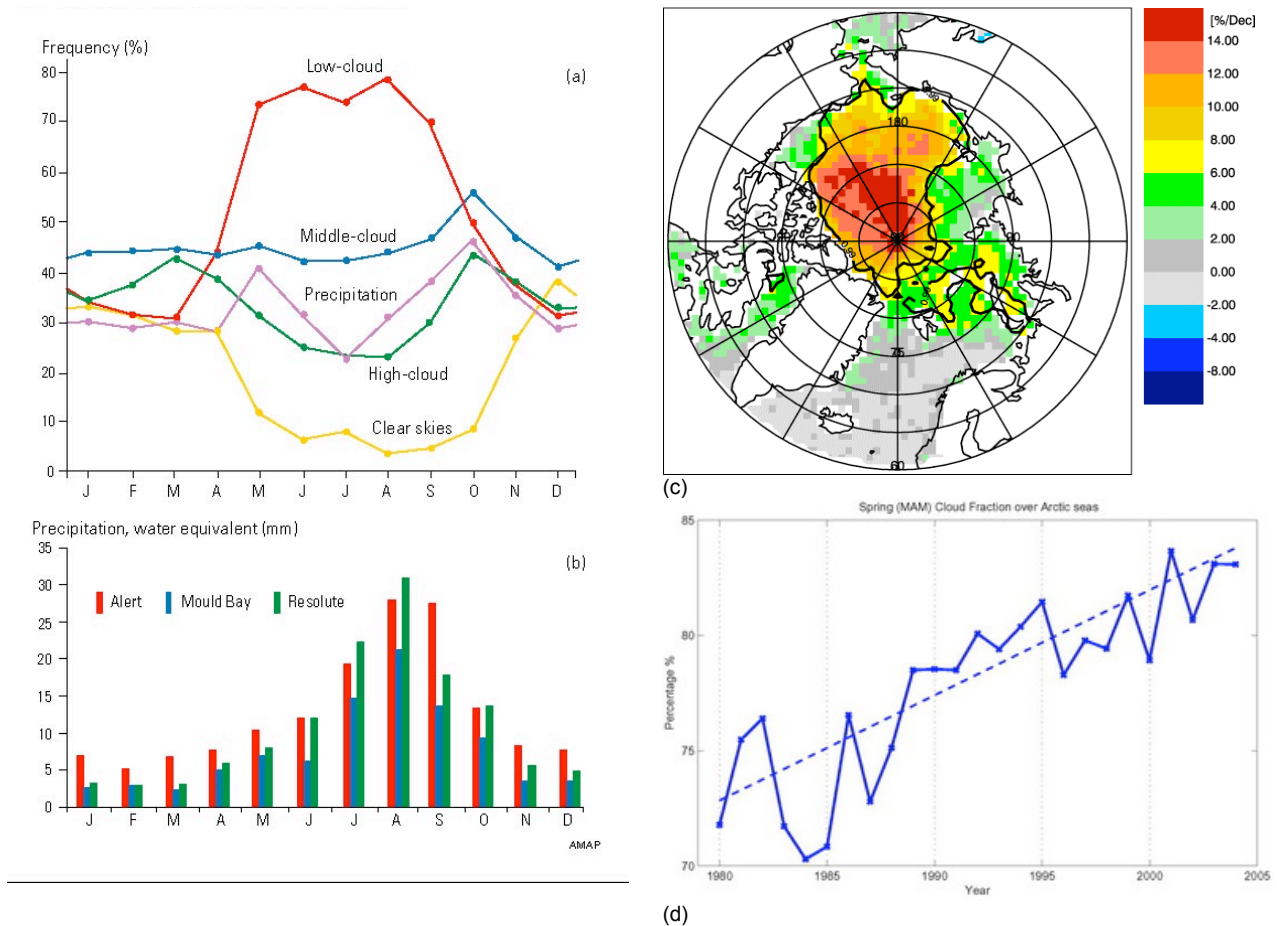


Figure 2.12. Seasonal variability of different cloud types (a) and precipitation (b) in the Arctic; Spatial distribution of trends in cloud cover over twenty years. (c); Time series of seasonally averaged cloud fraction (d) over the arctic seas in spring (March, April, May). (Schweiger, 2004 for c and d).

The most important characteristic of clouds in the Arctic is the summer stratus. From about mid-June to mid-September, the ocean area covered by sea ice is 80 to 90 percent covered with this cloud type. Summer stratus has important effects on the radiation balance of the surface.

The three main cloud layers, with approximate heights, are:

- * low: up to 2 kilometers (cumulus and stratus)
- * medium: 2 kilometers to 8 kilometers (altocumulus and altostratus)
- * high: 8 kilometers to 15 kilometers (cirrus, cirrostratus and cirrocumulus)

In general, much of the arctic sky is covered by low stratus and stratocumulus clouds. Total cloud cover is least extensive in December and January. Starting in May, cloudiness increases. Warm air over the water adjacent to ice, frequent temperature inversions, and fog, cause low level stratus clouds to form and persist through the entire warm period.

The most striking feature of low cloud cover during the winter months is the relative maximum over the northern North Atlantic. This manifests the uplift of air masses by the frequent cyclone activity in this area associated with the Icelandic Low. Low cloud cover is rather limited over central and eastern Siberia because of the general subsidence (downward motion) of air in the area of the strong Siberian high. During summer, the Icelandic Low and Siberian High weaken. Low cloud cover becomes more uniform, but with a distinct increase over the Arctic Ocean. The increase reflects the dominance of low-level stratus, which form as warm air masses moving over the ocean are chilled by the cold, melting sea ice cover. Then autumn months illustrate the transition back to the winter pattern. Total cloud cover combines low, middle and high clouds. While amounts of total cloud are hence greater than for only low cloud, it can be seen that most cloud cover is of the low variety.

Clouds are important to the Arctic climate because they trap warm temperatures and reflect sunlight in spring and summer. There has been a nearly linear increase in the cloud cover over the central Arctic in the previous two decades. The linear trend of the time series and the western Arctic location of the major changes contrast with the regime-like variation of the Arctic Oscillation. The difference between the linear trend of clouds and the behavior of the Arctic Oscillation highlights present uncertainties in understanding Arctic climate.

2.7 Precipitation

Precipitation, usually falling as snow, is the factor of arctic climate most important to the hydrological cycle. The principal forms of precipitation are rain, drizzle, freezing rain, snow, ice pellets (sleet), and hail. Precipitation form depends on the source cloud and the temperature of the air below the cloud. Moisture may be deposited not only by precipitation but as dew or hoar frost on a horizontal surface or on a vertical surface as rime crystals. Rain falling on a surface that is below 0° C forms glaze.

Cloud development is not always an indication of coming rain or snow. Although all precipitation occurs because of condensation, cloud physicists have determined that condensation alone cannot cause cloud droplets to grow into raindrops. This is because updrafts within clouds are usually strong enough to prevent cloud particles from leaving the base of a cloud and falling to the earth's surface. Even if droplets or ice crystals descend from a cloud, their downward drift is so slow that they might travel only a short distance before evaporating in the unsaturated air beneath the cloud. Cloud particles must grow large enough to counter updrafts and survive a descent to the earth's surface as raindrops or snowflakes without completely evaporating.

Once a raindrop or a snowflake leaves a cloud, it enters unsaturated air where either evaporation or sublimation can take place. In general, the longer the journey to the ground and the lower the relative humidity of the air beneath the clouds, the greater the quantity of rain or snow that returns to the atmosphere as vapor through evaporation or sublimation.

Eventually an ice crystal or water droplet becomes big enough (heavy enough) to start to fall. Often the particles will catch updrafts as they fall and circulate in the cloud a few times to pick up more water or ice. Many particles that start out as ice crystals never reach the ground. For instance, if the air is very dry, they simply evaporate, while relatively warm air will change ice into rain, and strong winds can break ice crystals into smaller fragments.

The amount of precipitation in a given region depends on the amount of available atmospheric water vapor (precipitable water), as well as on the processes that cause condensation, in particular

the uplift of air associated with cyclones and fronts, as well as convection. If all the water vapor in the atmosphere were condensed, the earth's surface would be covered, on average, with a 25 mm layer of water. However, since the amount of water vapor the atmosphere can hold decreases with decreasing temperature, the amount of water that can be condensed from the air generally decreases with latitude. In general, the amount of precipitable water in the humid tropics is more than 40 mm, while near the pole, it is often less than 5 mm.

In some parts of the Arctic, warm ocean currents bring heat and moisture to the air and frontal activity results in increased precipitation. For instance, southern Iceland, southern Alaska and parts of the Norwegian coast receive in excess of 3000 mm of precipitation per year. In contrast, inland areas of the Arctic with continental climate and lower temperatures receive less than 150 mm of precipitation per year.

The Intergovernmental Panel on Climate Change (IPCC, 2001) has consistently reported 20th-century increases in precipitation in northern high latitudes (55° – 85° N) as shown in Fig. 2.13. The increase is similar to that in Karl's (1998) "Arctic region", which includes the area poleward of 65° N but excludes the waters surrounding southern Greenland. In both cases, the greatest increase appears to have occurred during the first half of the 20th century. However, the time series are based on data from the synoptic station network, which is unevenly distributed and has undergone much change.

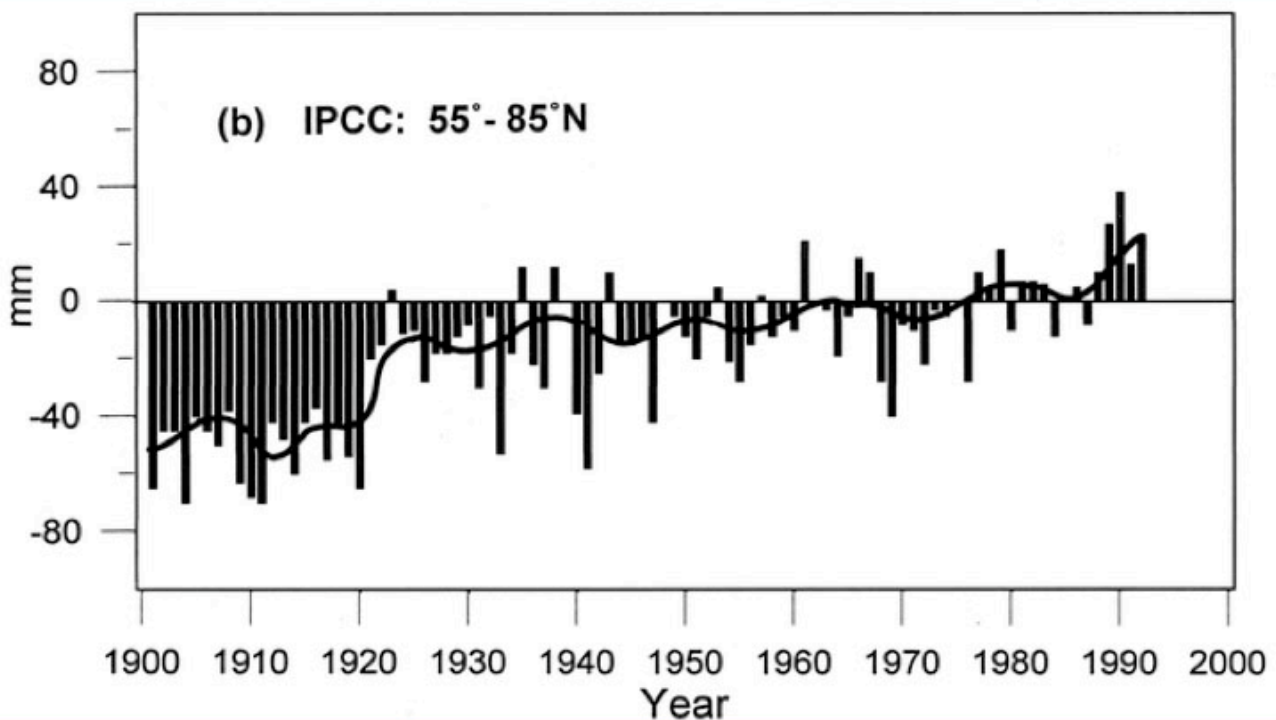


Figure 2.13 Mean annual precipitation between 55° and 85° N (IPCC, 2001).

Arctic precipitation has a characteristic the seasonal cycle (Fig. 2.12 b). During winter, precipitation is highest over the Atlantic sector. This represents the effect of frequent cyclone activity associated with the Icelandic Low. High precipitation totals are also found south of Alaska corresponding to the Aleutian Low. The lowest amounts are found over the central Arctic Ocean and land areas, where cyclone activity is uncommon and anticyclonic conditions are more the rule. From spring into summer, the pattern changes. The precipitation maxima over the Atlantic side and south of

Alaska weaken, attended by increases in precipitation over the Arctic Ocean and land. The increases over the Arctic Ocean correspond to the seasonal increase in cyclone activity in this area. This is also true for the increase in precipitation over land. Perhaps surprisingly given the high latitude, the summer maximum in terrestrial precipitation is also contributed to by convective activity (that is, by thunderstorms). Autumn shows the transition back to the winter regime. The maxima associated with the Icelandic and Aleutian lows is reestablished, and precipitation decreases over land.

The seasonal cycle of snow

The winter fields indicate greater snow depths over the North American side of the Arctic Ocean. This is because temperatures are lower in this region, so that snow falling during the autumn months tends to more readily accumulate compared to other areas. However, March shows a tendency for deeper snow cover towards the Atlantic side of the Arctic Ocean. This is because winter snowfall is comparatively high in this area due to the northward penetration of storms associated with the Icelandic Low. Moving through spring and summer, the pattern of greater snow depths on the North American side is reestablished. Again, this is because this region tends to be colder, but here the effect is to result in slower melt. Most of the snow is melted by August. The season's first snowfall tends to occur in September. Because snow densities are broadly similar across the Arctic Ocean, the seasonal cycle of snow water equivalent is similar to that of snow depth.

Land areas with high winter snow depths correspond in part to regions with fairly high elevations (for example, Alaska and parts of Siberia). This is understood in that higher-elevation areas tend to be somewhat cooler, so snow can more easily accumulate in autumn. Snowfall may also be enhanced by orographic uplift of air masses. For other areas, such as Northwestern Eurasia, large snow depths appear to be more directly a reflection of synoptic activity. Note the low winter snow depths over east-central Siberia, where the strong Siberian High suppresses precipitation. The seasonal melt of the snow cover occurs earlier over the North American side. By July, snow cover has essentially disappeared (Fig. 2.14).

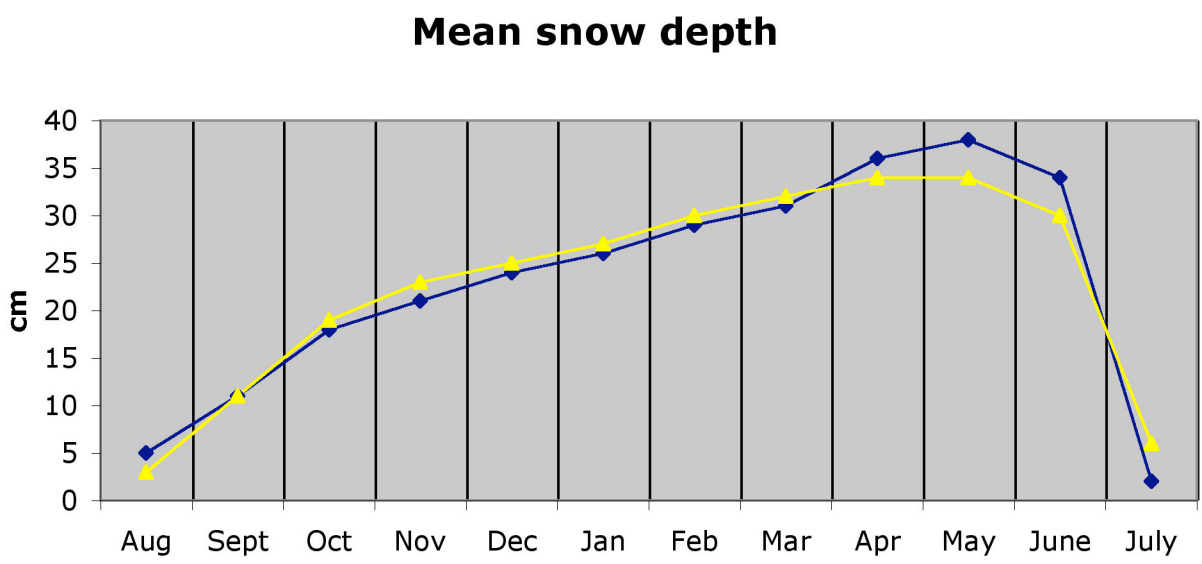


Figure. 2.14. Monthly mean snow depth over multiyear from Russian Polar Drifting station. The blue curve is from data before 1964, and the yellow curve is data up to early 1990s (Warren et al., 1999)

2.8 Feedback Loops: Interactions that Influence Arctic Climate

In the climate system a "feedback loop" refers to a pattern of interacting processes where a change in one variable, through interaction with other variables in the system, either reinforces the original process (positive feedback) or suppresses the process (negative feedback). In order to model and predict arctic (and global) climate variability correctly, feedback loops must be understood. Two major feedback processes that scientists consider in studies of arctic and global climate change are described below in simple terms. In nature, the processes are considerably more complicated.

2.8.1 Temperature—Albedo Feedback

The temperature-albedo feedback mechanism is illustrated in Fig. 2.15. It shows that rising temperatures increase melting of snow and sea ice, reducing surface reflectance, thereby increasing solar absorption, which raises temperatures, and so on. The feedback loop can also work in reverse. For instance, if climate cools, less snow and ice melts in summer, raising the albedo and causing further cooling as more solar radiation is reflected rather than absorbed. The temperature—albedo feedback is positive because the initial temperature change is amplified.

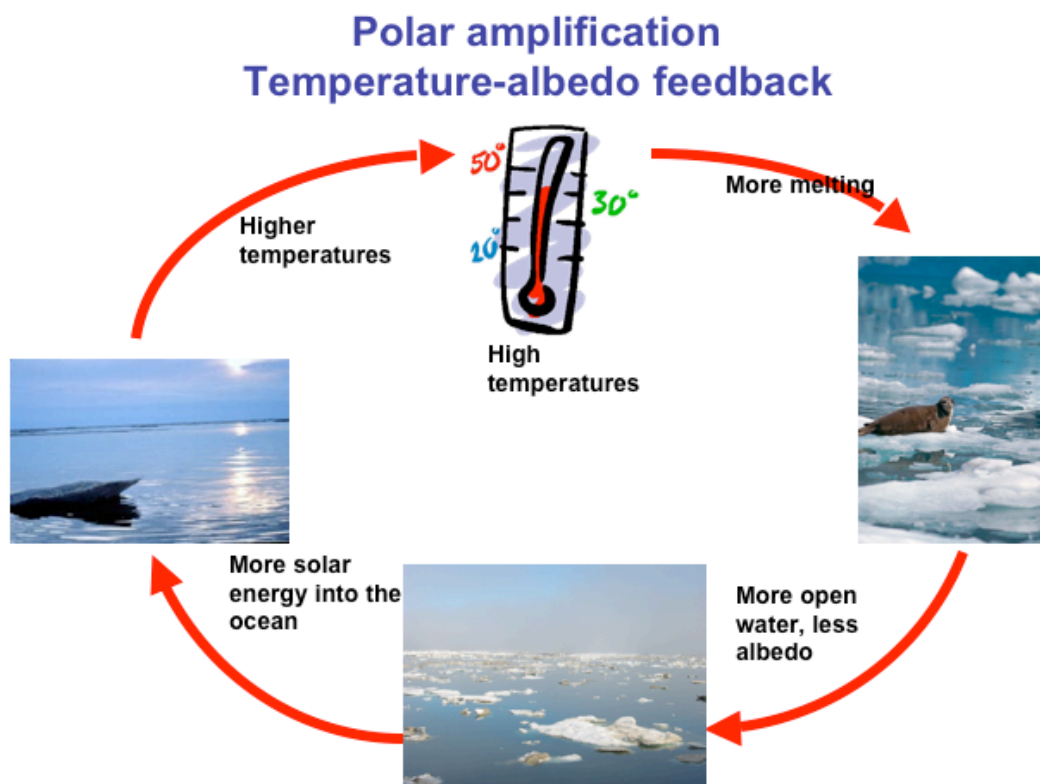


Fig. 2.15 Illustration of the temperature-albedo feedback cycle.

2.8.2 Temperature—Cloud Cover—Radiation Feedbacks

Another feedback mechanism is between temperature, cloud cover and radiation, which are potentially important agents of climate change (Fig. 2.16). However, they are not well understood but research in this area is active. It is thought that if climate warms, evaporation will also increase, in turn increasing cloud cover. Because clouds have high albedo, more cloud cover will increase the earth's albedo and reduce the amount of solar radiation absorbed at the surface. Clouds should therefore inhibit further rises in temperature. This temperature—cloud cover—radiation feedback is negative as the initial temperature change is dampened.

However, cloud cover also acts as a blanket to inhibit loss of longwave radiation from the earth's atmosphere. By this process, an increase in temperature leading to an increase in cloud cover could lead to a further increase in temperature - a positive feedback.

Knowing which process dominates is a complex issue. Cloud type plays a strong role, as do cloud water content and particle size. Another factor is whether the cloud albedo is higher or lower than that of the surface. Research indicates that the effect of this feedback in the Arctic may be different than in other latitudes. Except in summer, arctic clouds seem to have a warming effect. This is because the blanket effect of clouds tends to dominate over reductions in shortwave radiation to the surface caused by the high cloud albedo.

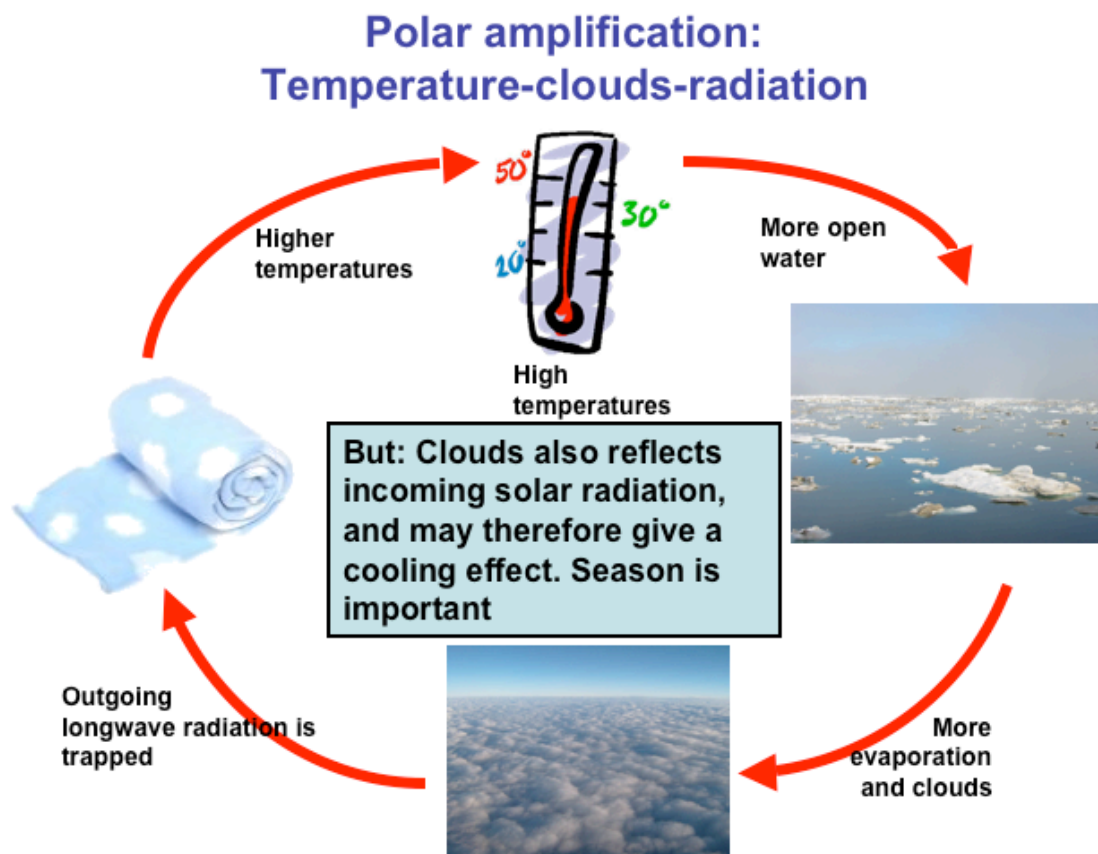


Figure 2.16 Illustration of the temperature-cloud-radiation feedback cycle.

2.9 Meteorological conditions of importance for operations and navigation

There are three major meteorological factors with impact on Arctic navigation and operations: horizontal visibility (related to fog, rain, snowstorm and duration of daylight), direct influence of wind speed and wind direction, and icing (from the combined influence of air and water temperatures, direction and speed of wind, direction and speed of ship, and state of the sea). The meteorological conditions in the Barents Sea, Kara Sea, Laptev Sea, East Siberian Sea and Chukchi Sea have been reviewed in the INSROP project (Proshutinsky and Weingarten, 1998). The main results of this report are presented in this chapter.

2.9.1 Visibility

Lack of visibility slows speed when a vessel is operating in conditions where the ice concentration is greater than 30%. Darkness, fog, and snowstorm are the defining factors for horizontal visibility in arctic waters.

The absolute air humidity in the Arctic is very low compared to sub-Arctic and mid latitude areas. Maximum mean monthly relative humidity is observed in summer (85 - 95%), while minimum is observed in winter (75 - 85%). Fog is related to high relative humidity. In winter, in spite of over-saturation by water vapor, the frequency of fog is low because of low absolute humidity and low number of condensation particles. In the presence of condensation particles (e.g. smoke and vehicle exhaust) frost fog can be observed.

In summer, the air is very close to a point of saturation by water vapor, and a small decrease in temperature is enough for fog formation. The fogs in the Arctic very often correlate with wind direction. This relationship is most visible in summer when advective fog prevails and the temperature difference between land and open sea is large. In coastal regions, the fog correlates well with winds from the open sea. For example, on the west coast of Novaya Zemlya the fog is usually brought into the area by westerly winds. There are no fogs during easterly winds. The opposite phenomenon is observed on the east coast of Novaya Zemlya.

For many regions of the Arctic, there is an inverse relationship between fog and wind velocity. Maximum fog events are observed with small or regular wind velocities (< 7 m/s). But in some coastal regions and straits fog can be associated with high winds. There is a strong relationship between fog and ice edge location in the arctic seas. There is a maximum frequency of fog in the northern part of the seas where the sea ice is located. The frequency of occurrence increases with increasing ice concentration up to about 80-90%. The maximum duration of fog with the lowest visibility is observed in summer in the coastal regions and around islands in the western part of the Barents Sea, where warm currents meet cold arctic air masses. Fog caused by evaporation occurs frequently in Kola Bay and other bays in the Barents Sea. From December to February up to 22 - 24 days of fog per month can occur. In Murmansk, 50% of the fog events are regular or strong fogs and about 20% are very strong fogs with visibility of less than 50 m.

A snowstorm is defined by wind velocity above 8 m/s and air temperature below 0°C, leading to visibility less than 2.5 km. In the coastal regions snowstorms occur usually from October through May. In the northern regions the snowstorm period can be longer. The annual number of days with snowstorm is 100 - 120 days in the Barents, Kara, and Chukchi seas, and 60 - 80 days in the East Siberian and Laptev seas. Fog and snowstorms are the main factors defining the horizontal visibility in addition to darkness in the mid-winter months. Very low visibility (less than 1 km) occurs in summer due to fog and in winter due to snowstorms and darkness. In June - August, low visibility in the open sea occurs 25 - 30% of the time, decreasing to 10% at the coast. In conditions of limited visibility there is increased risk for ships to lose their ice navigation channel, get stuck in ice, or break convoy motion.

2.9.2 Wind regime

The atmospheric pressure and circulation patterns as described in section 2.1 define the character of prevailing winds in the arctic seas. As an example of wind statistics, wind roses for January are presented in Fig. 2.17. In winter winds are often blowing from a south-southwesterly direction in the Barents and Kara Sea region. In the Laptev Sea, prevailing winds are from the south-southwest in winter.

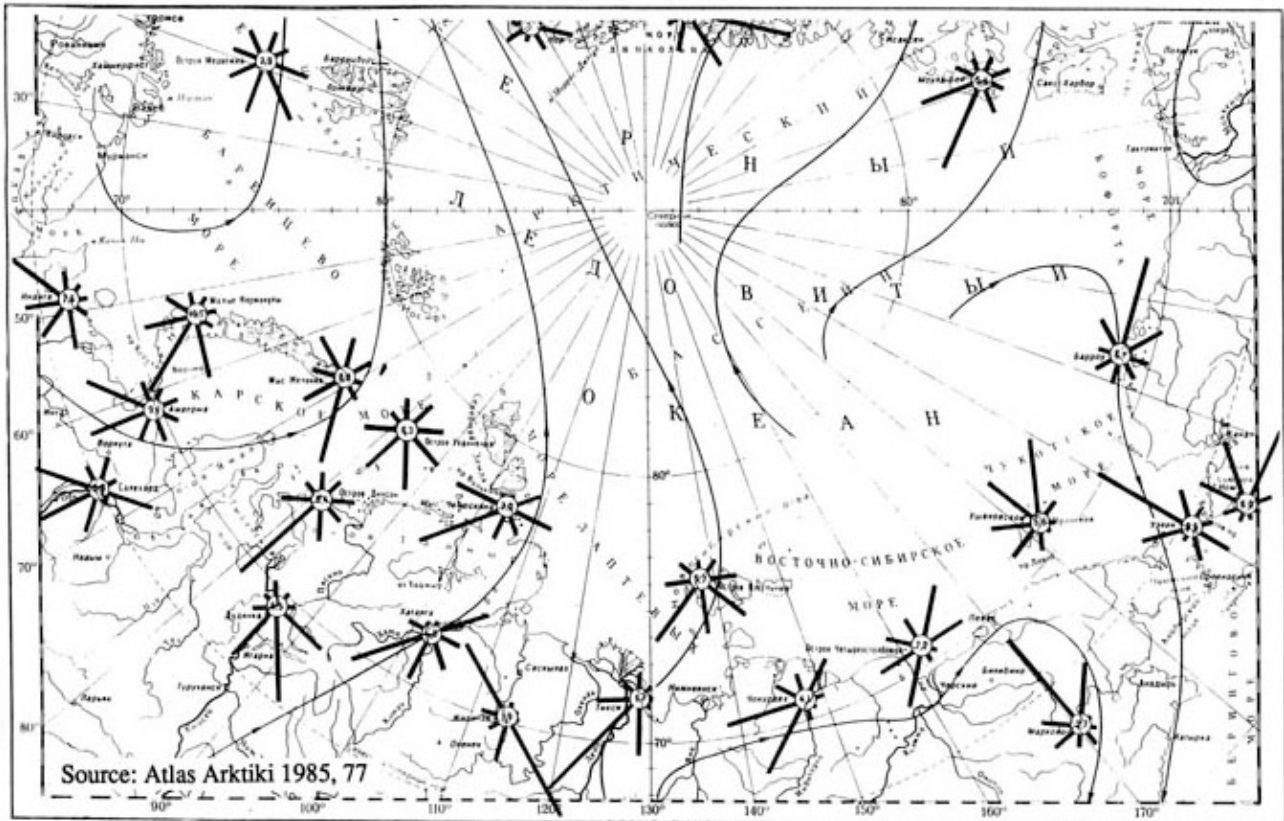


Figure 2.17. Wind roses for January in the Eurasian sector of the Arctic. The number in the center of the roses indicate mean wind speed in m/s. The length of the rays represent the probability of occurrence of wind direction in %.

Over the New Siberian Islands and in the East Siberian Sea, the winds are ranging from westerly to southerly and easterly. Northerly winds prevail in the Chukchi Sea with directions ranging from northwest in the western part of the sea to northeast in the eastern part. In the southeastern part of the Chukchi and Bering seas, northerly winds prevail in winter. The mean wind speeds are relatively small, 4 - 5 m/s, but show significant regional variability. For example, in the western and eastern regions the velocities are higher than in the central part. In winter, the highest mean monthly wind speed is observed in the Barents Sea (8 - 9 m/s), followed by the Kara Sea (6 - 8 m/s). In the Laptev Sea and in the western part of the East Siberian Sea, the mean wind speed is less than 5 m/s. In the eastern part of the East Siberian Sea and in the Chukchi Sea, the mean wind speed is 5 - 7 m/s.

During the arctic summer, the atmospheric pressure and wind regime is often opposite to the typical winter situation. Low pressure tends to prevail over the Siberian continent prevail, while

high pressure prevail over the arctic seas. The summer monthly mean wind speed is more or less uniform (5 - 6 m/s) along the entire Russian Arctic. In both winter and summer, wind speeds typically increase near capes, in straits and in bays. High wind speeds (> 15 m/s) are observed more often in winter than in summer. In the Barents Sea, there are about 6 - 8 stormy days in January, while the Kara Sea has 4 - 6 stormy days. In the Laptev and East Siberian seas, the number of stormy days is lower, 2 - 5 days per month. In the Chukchi Sea, 6 - 10 storm days occur per month.

In summer, an average of 1-2 stormy days occur per month, but 10 - 12 stormy days can occur per month in specific places where topography enhance the wind speed. The duration of storm events for all the polar stations ranges from 6 to 24 hours. In winter, however, stormy weather can last 8-14 days in extreme cases. There are several places in the Russian Arctic where orographic effects generate increased wind speeds. Maximum catabatic wind speeds have been observed to be 50 - 56 m/s at Rudolph Island, 70 m/s at the Karmakuly, 49 m/s at Mys Stolbovoy, and more than 80 m/s at Pevek. In summer, these winds can bring warm air masses with strong temperature increase (up to 20-25 °C per day) according to (e.g. Dementev, 1985).

Wind is an important factor affecting ice conditions, especially the drift and deformation of ice. The wind conditions can be classified as "push-off" and "push-on" according to their effect on the ice drift. Push-off winds will weaken or remove the pressure in the icepack, while push-on winds will do the opposite. Along the Siberian coast, push-on winds are, with few exceptions, blowing from northerly directions. In the western Siberian coast push-on winds occur in 60 - 70% of the days in June and 33 - 35% in August. In the eastern East Siberian and Chukchi seas the occurrence rate of push-on winds increases towards the end of the navigation period (October-November). Push-on winds are usually followed by push-off winds or by low winds normally lasting for several days. The most severe push-on area is to the west and east of Vilkitsky Strait and in the vicinity of New Siberian Islands where more than 15 days of push-on winds can occur. The longest duration of push-on winds, lasting for 32 days, was observed in the western part of the Laptev Sea and in the area to the west of Vilkitsky Strait. The occurrence rate of winds with a speed of less than 12 m/s (up to 15 m/s in gusts) is greatest in the northernmost parts of the Siberian Coast, especially at the end of the navigation season. The occurrence of push-on winds varies considerably from year to year.

2.9.3 Icing on vessels

Many lives and ships have been lost after ships sank or became disabled, after the accretion of ice on decks and superstructures (Fig. 2.18). The extra weight from ice accretion can cause capsizing, extreme rolling and pitching and topside flooding. Icing is particularly dangerous for fishing vessels and other small ships. Also navy ships with high superstructures and low freeboard are vulnerable to icing.

There are two types of icing which can occur on vessels in cold weather regions: atmospheric icing and sea-spray icing. The most severe type is sea-spray icing, which can be a serious hazard for marine operations on polar regions.

Probability of icing

Icing on a structure at sea requires the several simultaneous conditions. The main element in the phenomenon of icing at sea is a supply of water or moisture at subfreezing temperatures on surfaces above sea level. This can be fresh water in the form of dry or wet snow, supercooled water droplets, or salt water in the form of sea spray or shipped water on deck.

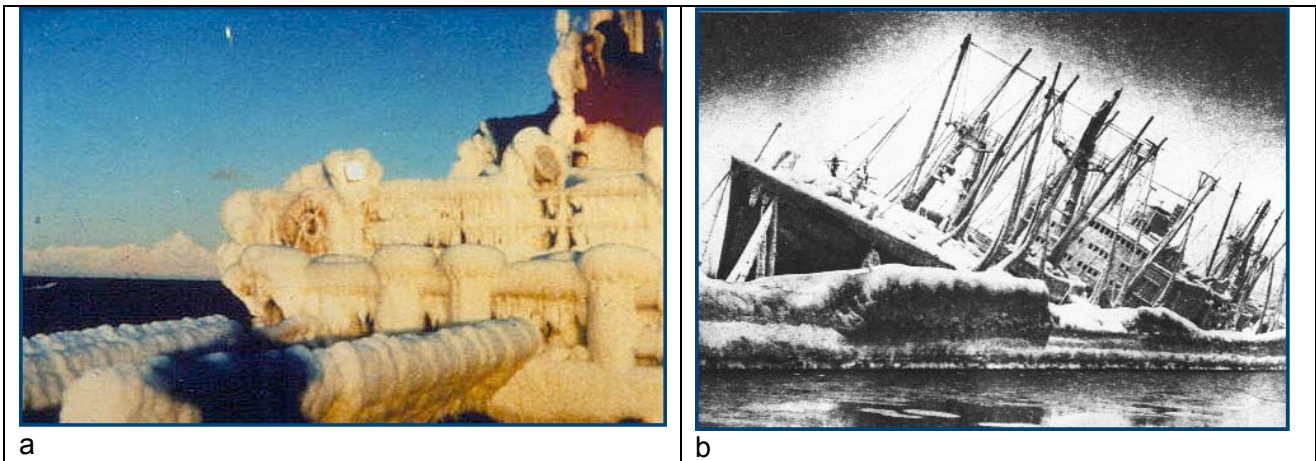


Figure 2.18. Photographs of icing on vessels operating in the Arctic. Photographs provided by Peter Guest.

There are two major types of sea icing: atmospheric and saltwater. Atmospheric icing is related to precipitation. Dry snow does not usually adhere to a surface so it poses no hazard. However, sea spray or sleet dampens the snow, the wet snow freezes to the surface. The ice thus formed is porous, with low mechanical strength, so it can usually be removed.

Water that is supercooled freezes to ice by contact with a cold surface. Supercooling occurs in its liquid phase at temperatures far below the freezing point. Supercooled droplets exist in the form of frost smoke, supercooled fog, or freezing rain and drizzle. These are the most common sources of atmospheric icing.

Opinions on the seriousness of atmospheric icing differ. In some reports this is scarcely mentioned, but in others it is referred to as the feared "black frost". Atmospheric icing produces a uniform layer of ice on all surfaces. This may pose various problems in operations, communication, and navigation. For smaller vessels especially, black frost can cause a critical reduction of stability. If atmospheric icing occurs at the same time as sea spray icing, the increase beyond the amount caused by sea spray alone could be the decisive factor in an accident.

Saltwater icing (icing caused by sea spray) is the most frequent and most important form of icing in the sea. Another cause of saltwater icing is shipped water, which enters the deck of a vessel over the bow or sides. The latent heat content of this water, even if its temperature is near the freezing point, is sufficient to avoid freezing if it flows off the vessel quickly. This water will, in addition, contribute to the melting and flushing away of ice which has already formed on deck. But if the scuppers freeze or the railings are covered with ice, the waters may be trapped and frozen.

Sea spray icing accounts for by far the largest number of icing cases, and the most serious. Sea spray is formed in two ways. The most important with regard to icing is sea spray generated by the vessel or structure itself as it meets waves. The other type of sea spray is created when the wind blows droplets of water off the wave crests. This phenomenon depends on the form and steepness of the waves and wind speed. It begins to occur at speeds of 8-10 m/s. The stronger the wind, the higher the spray is lifted. Usually the height of sea spray icing is limited to 15-20 m above the sea surface; however, there have been reports of sea spray icing at up to 60 m above the sea surface.

Certain ranges of air temperature, water temperature, and wind speed must be met to cause a significant accumulation of superstructure icing. These conditions are:

- air temperature less than the freezing point of seawater (-1.7°C to -1.9°C , depending on salinity of the water, down to about -30°C);
- wind speed of 10 m /s or more, and
- seawater temperature colder than 8°C .

The most important areas in the Northern Hemisphere are the Norwegian Sea, the Barents Sea, the Labrador Sea, the Bering Strait, Gulf of Alaska and Sea of Okhotsk (Fig. 2.19a).

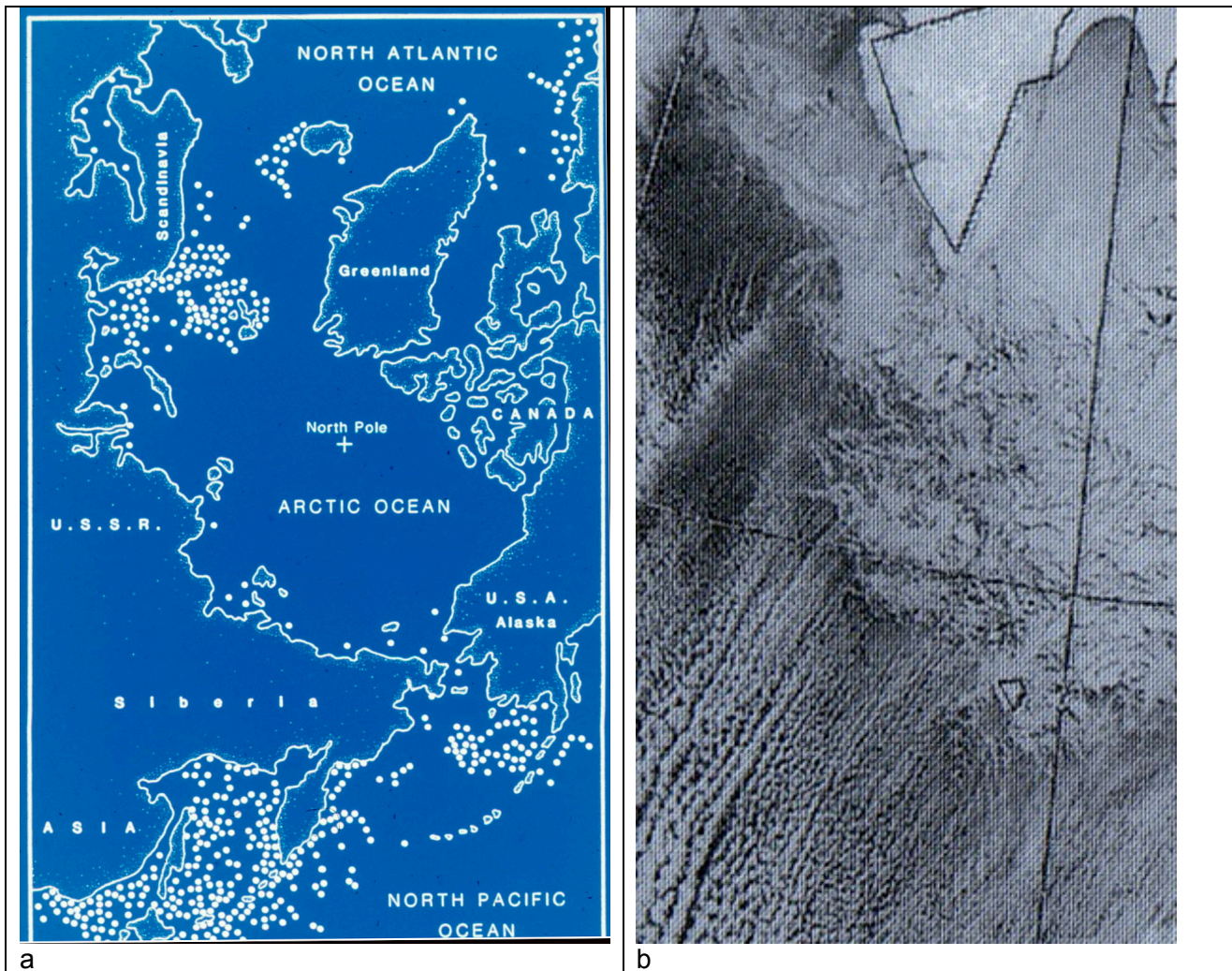


Figure 2.19. (a). Map of the areas with most frequent occurrence of icing on vessels in the Arctic areas (white dots); (b) example of cold advection observed in an NOAA AVHRR image where cold air masses flow out in open water areas generating characteristic convection cells. This example is from the western Barents Sea (courtesy P. Guest).

Icing can occur in all Marginal Ice Zones, in the Great Lakes, the Black Sea, the Caspian Sea and the Baltic Sea, wherever water is $< 5^{\circ}\text{C}$. In the Northern Sea Route icing is generally not a serious problem for large cargo ships, but along some routes (Murmansk-Dudinka) icing may be very

dangerous, especially during a long cruise at the end of autumn or in winter when air temperatures are below zero and there is no ice cover on the sea surface.

The main vessel characteristics are speed, heading (with respect to wind, waves and swell), length, freeboard, handling and cold soaking. Threshold wind speeds for icing to occur on various length of ships is shown in the following table:

Parameter	Threshold values					
Vessel length (m)	15	30	50	75	100	150
Significant wave height (m)	0.6	1.2	2.0	3.0	4.0	6.0
Wind speed at 200 km fetch (m/s)	5.0	7.4	9.8	12.5	15.0	20.0

The table is only a rough guide for ships steaming into the wind and waves. The actual potential for icing depends on the type, load, and handling characteristics of a particular ship. Any captain or bridge officer who is familiar with a ship should be well aware of the wind speeds which cause sea spray to reach the deck and superstructure, and should base his/her assessment on the potential for icing on this knowledge.

A forecasting algorithm for icing has been developed by Jim Overland (Overland et al., 1986). For vessels from 20 to 75 meters in length the following formula can be applied:

$$PPR = \frac{V_a(T_f - T_a)}{1 + 0.3(T_w - T_f)}$$

where

- PPR = Icing Predictor (m^0Cs^{-1})
- V_a = Wind Speed (m s^{-1})
- T_f = Freezing point of seawater
(usually -1.7°C or -1.8°C)
- T_a = Air Temperature ($^\circ\text{C}$)
- T_w = Sea Temperature ($^\circ\text{C}$)

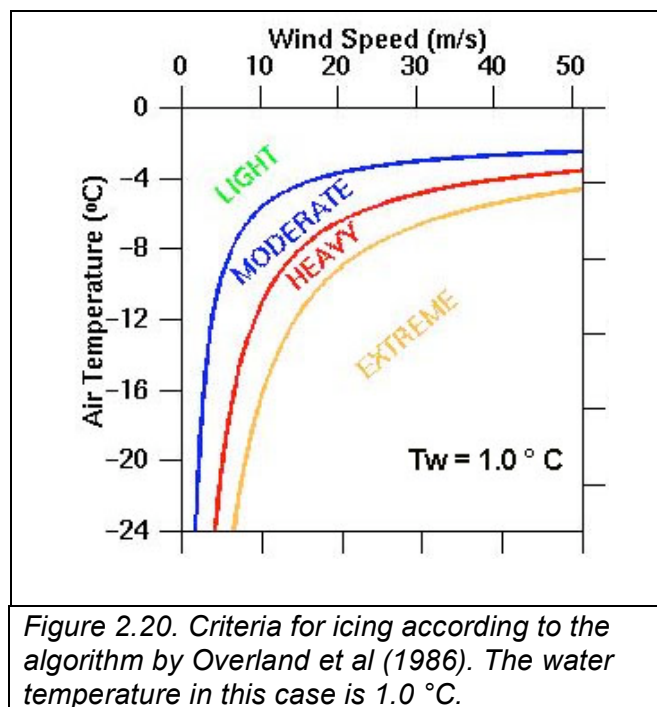


Figure 2.20. Criteria for icing according to the algorithm by Overland et al (1986). The water temperature in this case is 1.0°C .

By using forecasts of wind and temperature, the algorithm by Overland can be used to predict icing class and icing rates for a given vessel. A graphical presentation of icing classes is shown in Fig. 2.20. Icing class and icing rates for different PPR is shown in Table 2.1.

Table 2.1 Icing predictor for vessels from 20 to 75 m.

PPR (m^0Cs^{-1})	< 0	0-22.4	22.4 – 53.3	53.3 – 83.0	> 83.0
Icing class	None	Light	Moderate	Heavy	Extreme
Icing rates (cm/hour)	0	< 0.7	0.7 – 2.0	2.0 – 4.0	> 4.0

3. Sea ice processes

3.1 Trend and variability in sea ice extent in the Arctic

Sea ice is a sensitive component of the climate system, influenced by conditions in both the atmosphere and ocean. Variations in sea ice may in turn modulate climate by altering the surface albedo; the exchange of heat, moisture, and momentum between the atmosphere and ocean; and the upper ocean stratification in areas of deep water formation. The surface albedo effect is considered to be one of the dominant factors in the poleward amplification of global warming due to increased “greenhouse gas” concentrations simulated in many climate models (e.g., IPCC 2001).

Observational studies of sea ice extent indicate that variability on timescales of weeks and longer tends to be organized into large-scale geographical patterns that are closely associated with the dominant structures of atmospheric circulation variability, particularly during winter (e.g. Walsh and Johnson, 1979, Prinsenberg et al., 1997, Deser et al., 2000). The consensus of the observational studies is that “interannual variability in sea ice conditions is caused by the variability in the large-scale atmospheric circulation which locally manifests itself as surface air temperature and wind anomalies” (Prinsenberg et al. 1997).

Over the past 3–4 decades, the dominant patterns of wintertime atmospheric circulation variability in the Northern Hemisphere, particularly the Pacific–North American and the North Atlantic oscillation (NAO) or Arctic oscillation (AO) teleconnection patterns, have exhibited trends that are unprecedented in the observational record. The NAO may be regarded as a subset of the spatially broader AO (Thompson and Wallace 1998). Sea level pressures have decreased over the central Arctic and over the climatological Icelandic and Aleutian low centers, and increased farther south. The most pronounced reductions of sea level pressures over the central Arctic has occurred since 1988 (Walsh et al. 1996). Associated with these circulation changes, winter surface air temperatures over land (Eurasia in particular) have increased to record values while those over the oceans have cooled slightly (Thompson et al., 2000). The latter authors hypothesize that anthropogenic forcing may be a contributing factor to the recent unprecedented strengthening of the polar vortex (reflected by the AO) and associated warming over the Northern Hemisphere continents.

The Marginal Ice Zone is defined according to the location of the ice edge, and the ice edge varies both seasonally and interannually. With passive microwave satellite data obtained for nearly three decades the ice edge position has been monitored very accurately day by day in all polar regions. Monthly mean ice concentration maps from satellite data are presented in Figure 3.1. With retreat of the Arctic sea ice during summer, the Marginal Ice Zone in areas such as the Barents and Kara Seas have been extended further north.

During 2005, each month except May showed a record minimum sea ice extent in the northern hemisphere for the period 1979–2005. The extent of the sea ice cover is typically at or near its maximum in March and its minimum in September. The ice extent in March 2005 was 14.8 million km². In September 2005 the ice extent was 5.6 million km². In comparison, the mean ice extent for March and September, for the period 1979–2005, was 15.7 million km² and 6.9 million km², respectively (Fig. 3.2). It is notable that in March 2005 the ice extent fell within the median contour at almost every location. In September 2005, the retreat of the ice cover was particularly pronounced along the Eurasian and North American coastlines.

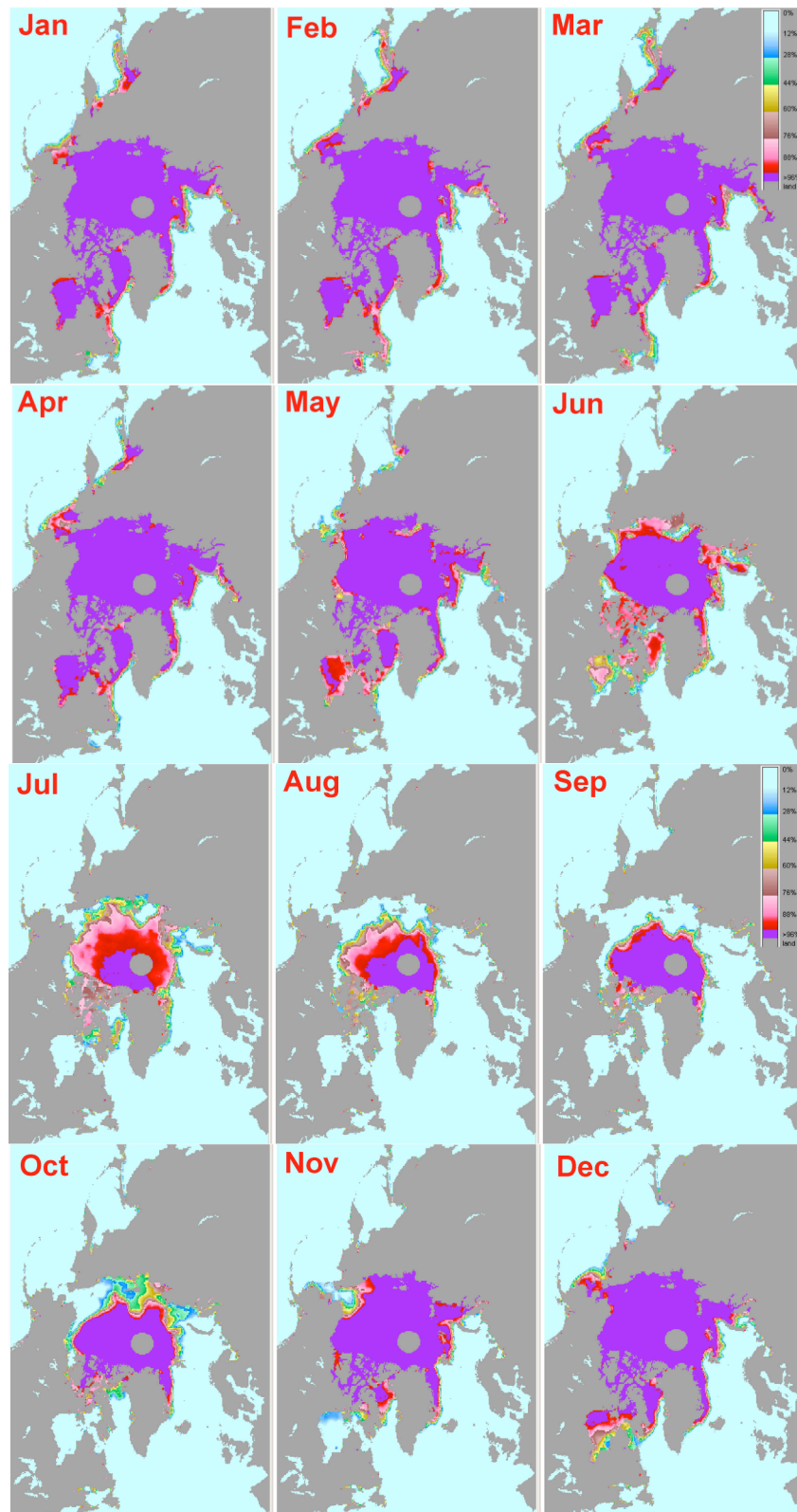


Figure 3.1 Sea ice extent in the Arctic for each month in 2005 based on passive microwave satellite data (SSM/I data). The colour scale indicates ice concentration intervals (Adapted from National Snow and Ice Data Center web site, <http://nsidc.org/>.)

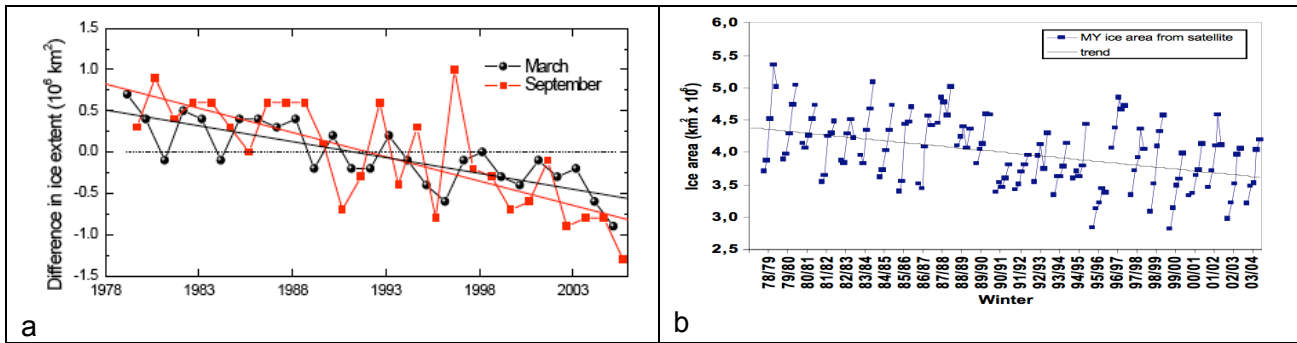


Figure 3.2: (a) Time series of the difference in ice extent in March (maximum) and September (minimum) from the mean values for 1979–2005 from SSM/I data. Based on a least-squares linear regression, the rates of decrease in March and September were 2% per decade and 7% per decade, respectively. Recent data from March 2006 are also shown and represent a new record minimum for the period of observation (<http://nsidc.org>). (b) Time series of multiyear ice area for the winter months derived from SSM/I data (Johannessen et al., 2004).

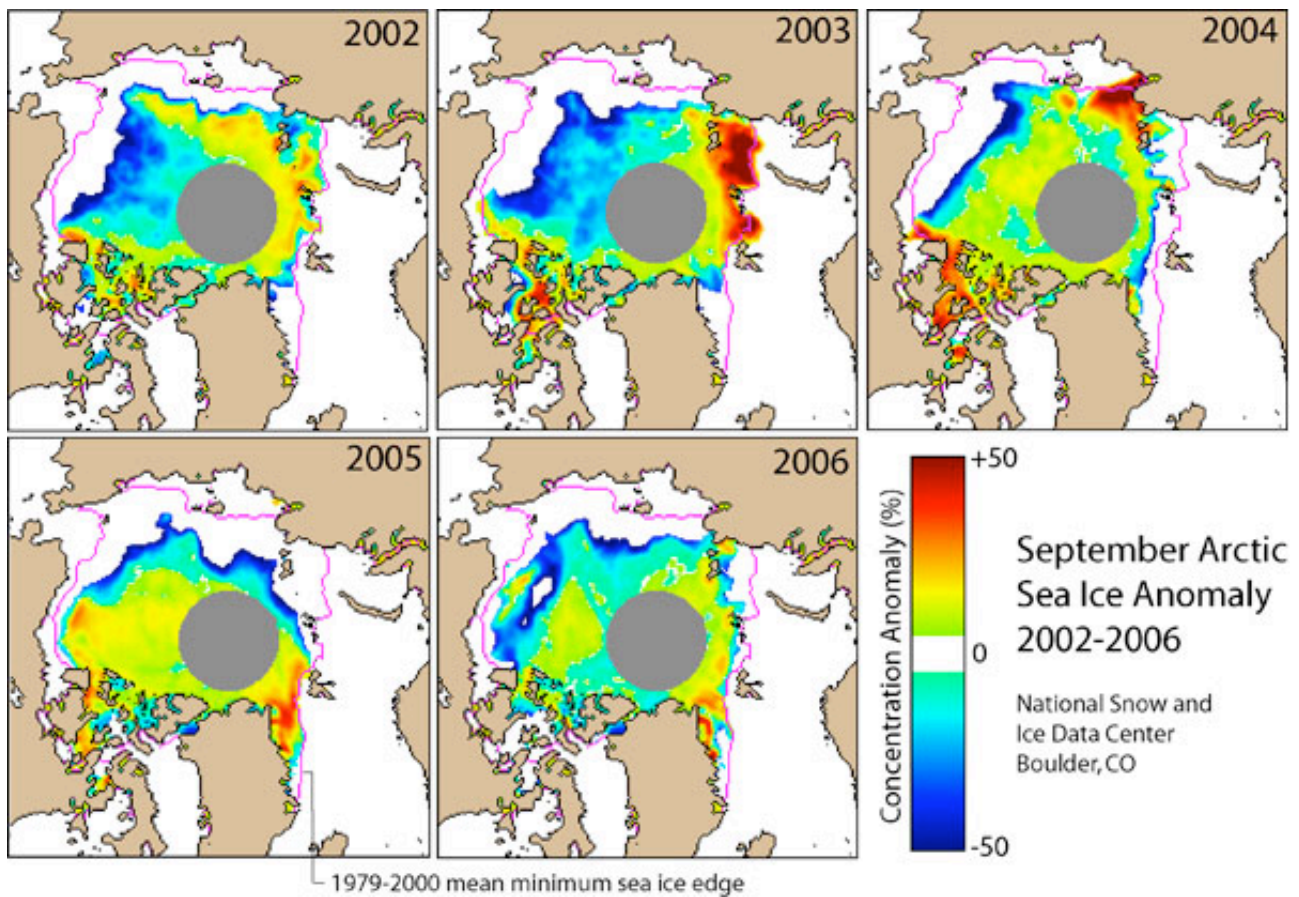


Figure 3.3 Sea ice conditions for September 2002, 2003, 2004, 2005, and 2006, derived from the NSIDC Sea Ice Index. Each image shows the concentration anomaly (key at lower right) and the 1979-2000 mean September ice edge (pink line). For each year, the ice edge is well north of its mean position off the coasts of Alaska and Siberia. Image provided by National Snow and Ice Data Center, University of Colorado, Boulder (<http://nsidc.org>).

Recent data from winter 2006 indicate a further reduction in the maximum ice extent, reaching 14.5 million km² in March. To put the 2005 minimum and maximum ice extents into context, the time series of the variability of ice extent in March and September for 1979–2005 are presented in Fig. 3.2. In both cases, a negative trend is apparent, with a rate of 2% per decade for March and 7% per decade for September. The summers of 2002–2005 marked an unprecedented series of extreme ice extent minima, as shown in Fig. 3.3 (Stroeve *et al.*, 2005).

The reduction in sea ice area can be estimated for each of the Arctic Shelf seas, and analyses of satellite data for the Barents Sea are shown in Fig. 3.4. There is a large interannual variability as well as a general reduction over the period. By including historical ice edge observation, which are less accurate and systematically collected compared to satellite data, it has been possible to reconstruct the variability of the ice edge position in the past (Divine and Dick, 2006). Example of ice edge variability in the period 1850–1899 are presented in Fig. 3.5.

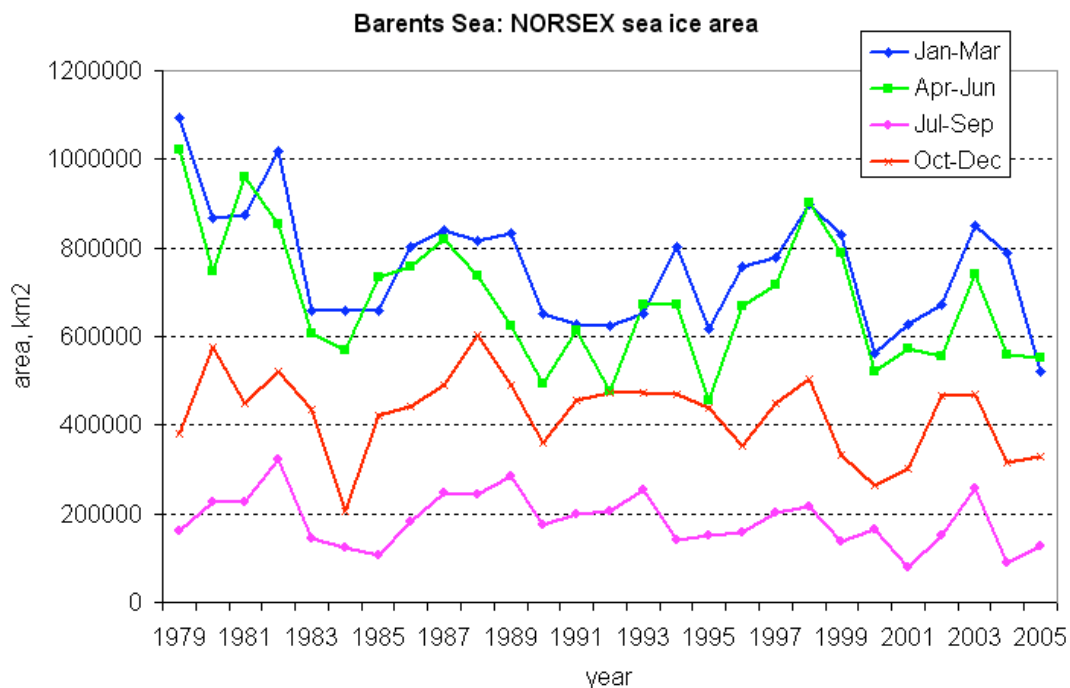


Figure 3.4 Time series of three-monthly mean ice area in the Barents Sea for the period 1978 – 2005, obtained from satellite passive microwave data.

Historical ice observations in the Nordic Seas from April through August have been used to construct time series of ice edge position anomalies spanning the period 1750–2002 (Divine and Dick, 2006). While analysis showed that interannual variability remained almost constant throughout this period, evidence was found of oscillations in ice cover with periods of about 60 to 80 years and 20 to 30 years, superimposed on a continuous negative trend. The lower frequency oscillations are more prominent in the Greenland Sea, while higher frequency oscillations are dominant in the Barents. The analysis suggests that the recent well-documented retreat of ice cover can partly be attributed to a manifestation of the positive phase of the 60–80 year variability, associated with the warming of the subpolar North Atlantic and the Arctic. The continuous retreat of ice edge position observed since the second half of the 19th century may be a recovery after significant cooling in the study area that occurred as early as the second half of the 18th century.

Given the last cold period observed in the Arctic at the end of the 1960s, the results by Divine and Dick (2006) suggest that the Arctic ice pack is now at the periodical apogee of the low-frequency

variability. This could explain the strong negative trend in ice extent during the last decades as a possible superposition of natural low frequency variability and greenhouse gas induced warming of the last decades. However, a similar shrinkage of ice cover was observed in the 1920s– 1930s, during the previous warm phase of the low-frequency variability, when any anthropogenic influence is believed to have still been negligible. Therefore, during decades to come as the negative phase of the thermohaline circulation evolves, the retreat of ice cover may change to an expansion.

The state of the sea ice cover is intrinsically linked to the state of the ocean and atmosphere. This is confirmed by the observation that during this same period (1979–2005), the annual surface temperatures over land areas north of 60°N have generally been rising and have been above the mean value for the twentieth century since the early 1990s.

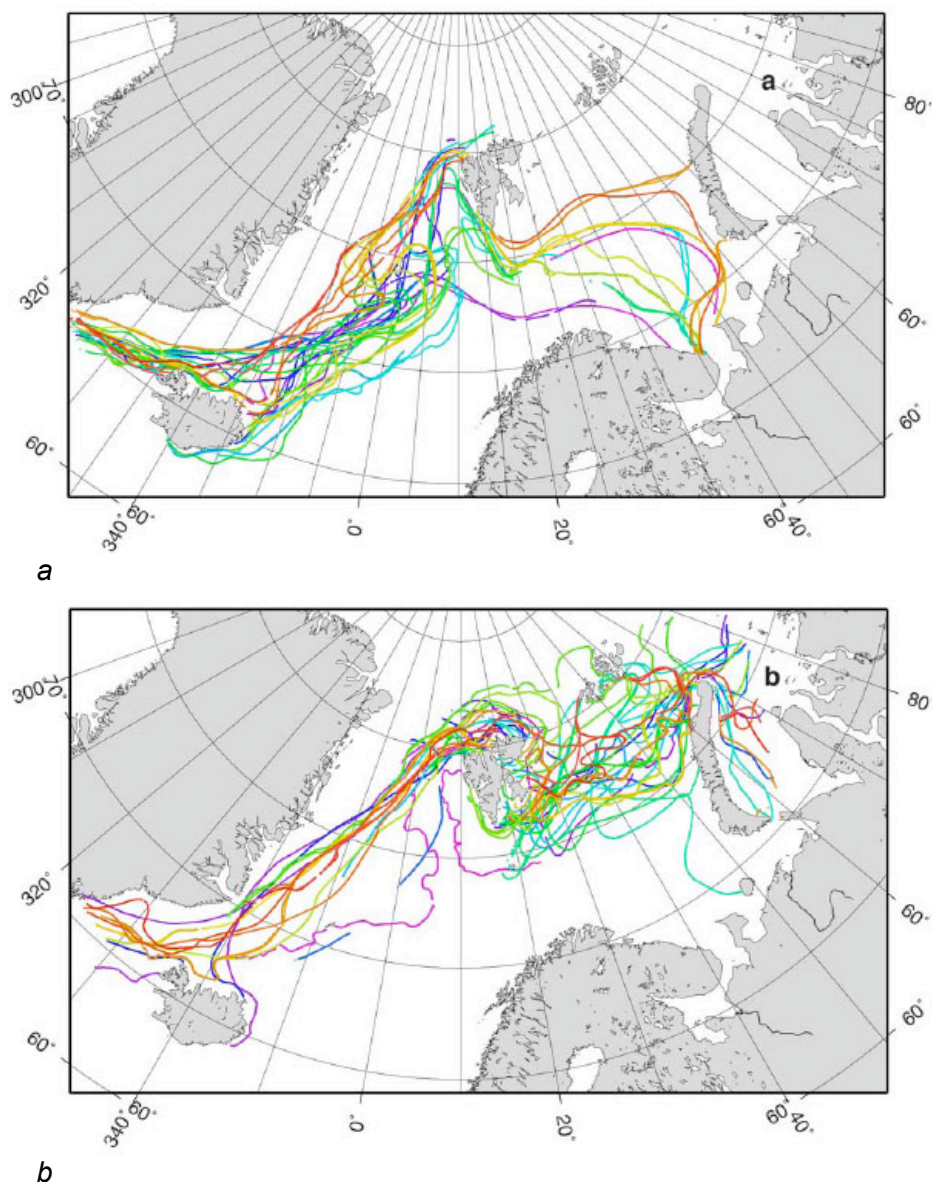


Figure 3.5. Historical ice edge position in the Barents and Norwegian/Greenland seas in the period 1850 -1899 for (a) April and (b) August. The observations are based on reports from sealers and whalers (from Divine and Dick, 2006).

Ice thickness is more difficult to monitor than ice extent. With satellite based techniques only recently introduced (Laxon *et al.*, 2003; Kwok *et al.*, 2006), observations have been spatially and temporally limited. Data from submarine based observations indicate that at the end of the melt season the permanent ice cover (the ice located toward the center of the Arctic basin that survives year round; see Fig. 3.6, right panel) thinned by an average of 1.3 m between 1956– 1978 and the 1990s, from 3.1 to 1.8 m (Rothrock *et al.*, 1999).

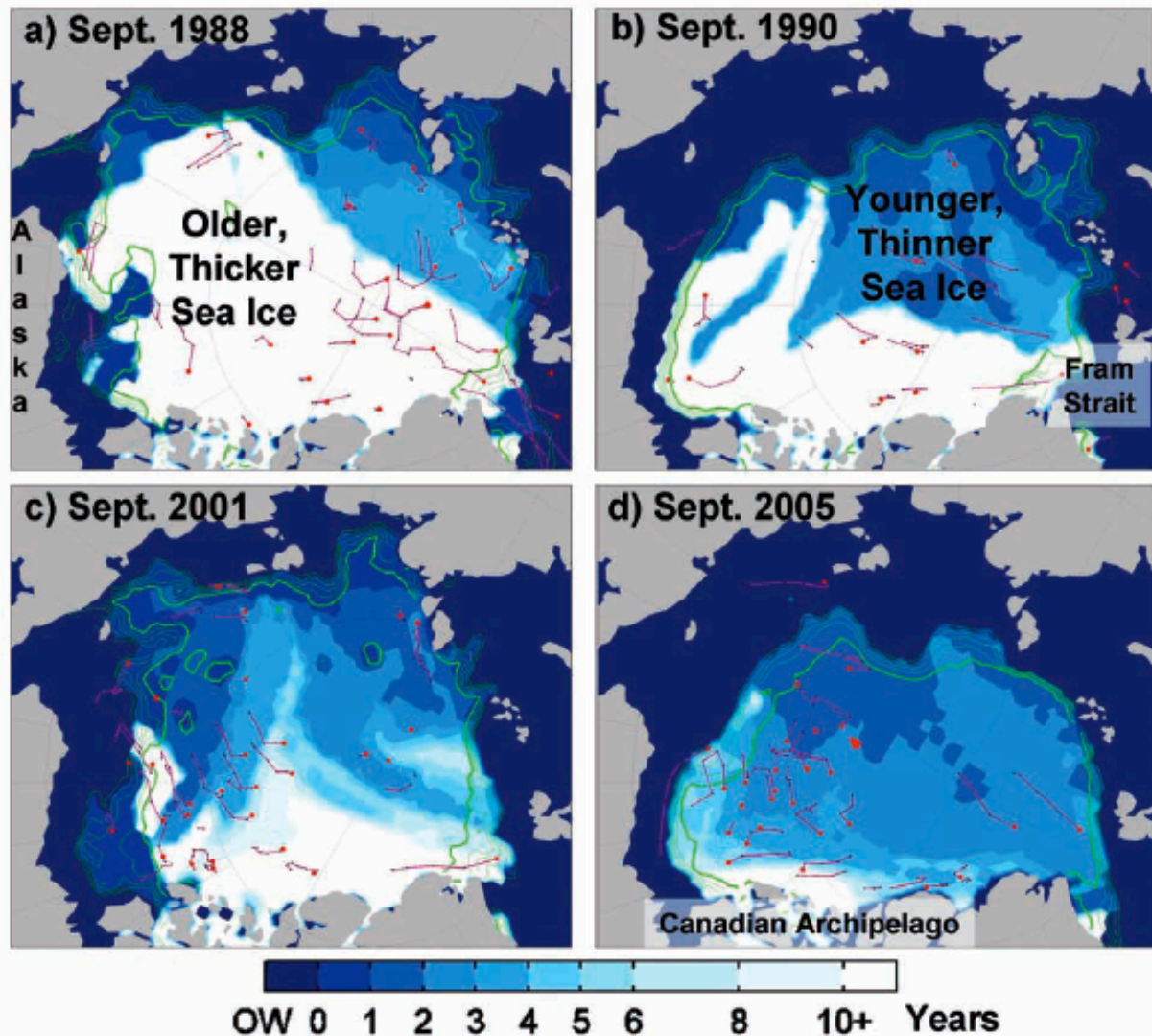


Figure 3.6: Change in the age of ice on the Arctic Ocean, compared for September and based on results from a simulation using drifting buoy data and satellite-derived ice concentration data (Rigor and Wallace, 2004). Open water (OW) is shown in dark blue, and the oldest ice is shown in white. The darker green line marks 90% ice concentration, and the lighter green lines mark ice concentrations of 80, 70, 60, and 50%. This sequence shows that (a) most of the Arctic Ocean was covered by older, thicker sea ice in September 1988; (b) coincident with a transition to high-AO conditions in 1989 (Fig. 2.5), most of the older, thicker sea ice was rapidly flushed out of the Arctic Ocean through Fram Strait, so that by 1990 only 30% of the Arctic Ocean was covered by older, thicker sea ice; (c) the relative distribution between older, thicker and younger, thinner sea ice persisted during the 1990s, in spite of a shift back towards a more neutral AO in the mid-1990s; and (d) the average ice age over the Arctic Ocean apparently continued to decrease through 2005, with older, thicker ice now limited to the area north of the Canadian Archipelago.

On the other hand, measurements of the seasonal ice cover (the ice around the periphery of the Arctic basin that melts during the summer) do not indicate any statistically significant change in thickness in recent decades (Melling *et al.*, 2005; Haas, 2004; Polyakov *et al.*, 2003). The trends in the extent and thickness of the cover are consistent with observations of a significant loss of older, thicker ice out of the Arctic via Fram Strait (e.g., Rigor and Wallace, 2004; Pfirman *et al.*, 2004; Yu *et al.*, 2004) in the late 1980s and early 1990s (Fig. 2.38). This event coincided with the strong, positive AO period that extended from 1989 to 1995 (Fig. 2.5). When the AO is positive, atmospheric and oceanic conditions favor a thinner ice cover. A younger, thinner ice cover, such as the one left behind from this event, is more susceptible to atmospheric or oceanic warming. It is of great interest to observe whether the sea ice cover will continue its decline or rebound under the recent, more-neutral AO conditions.

The Arctic sea ice variability and its association with surface air temperature (SAT) and sea level pressure (SLP) in the Northern Hemisphere has been investigated by Deser *et al.* (2000). Forty years (1958–97) of reanalysis products and corresponding sea ice concentration data were analyzed using empirical orthogonal function (EOF) analysis. The dominant mode of winter (January–March) sea ice variability exhibits out-of-phase fluctuations between the western and eastern North Atlantic, together with a weaker dipole in the North Pacific. The time series of this mode has a high winter-to-winter autocorrelation (0.69) and is dominated by decadal-scale variations and a longer-term trend of diminishing ice cover east of Greenland and increasing ice cover west of Greenland. Associated with the dominant pattern of winter sea ice variability are large-scale changes in SAT and SLP that closely resemble the North Atlantic oscillation. The associated SAT and surface sensible and latent heat flux anomalies are largest over the portions of the marginal sea ice zone in which the trends of ice coverage have been greatest, although the well-documented warming of the northern continental regions is also apparent. The temporal and spatial relationships between the SLP and ice anomaly fields are consistent with the notion that atmospheric circulation anomalies force the sea ice variations. However, there appears to be a local response of the atmospheric circulation to the changing sea ice cover east of Greenland. Specifically, cyclone frequencies have increased and mean SLPs have decreased over the retracted ice margin in the Greenland Sea, and these changes differ from those associated directly with the North Atlantic oscillation.

The dominant mode of sea ice variability in summer (July–September) is more spatially uniform than that in winter. Summer ice extent for the Arctic as a whole has exhibited a nearly monotonic decline (-4% per decade) during the past 40 years. Summer sea ice variations appear to be initiated by atmospheric circulation anomalies over the high Arctic in late spring. Positive ice–albedo feedback may account for the relatively long delay (2–3 months) between the time of atmospheric forcing and the maximum ice response, and it may have served to amplify the summer ice retreat.

The Russian started already in 1970 to measure area-averaged ice thickness derived from field-based measurements of surface elastic-gravity waves from Russian North Polar drifting stations 1970–91, when regular measurements of ice surface vibrations were made in the central Arctic Ocean (Nagurnyi *et al.*, 1994). Long elastic-gravity waves (on the order of 1 km) in the sea-ice cover arise from the interaction with ocean swells. These elastic-gravity waves can propagate for hundreds to thousands of kilometers before dampening out. Based on a linear theory of free vibrations of the sea ice cover, the measured wavelength, wave period and direction are then related to thickness through a wave-energy dispersion relation. The ice thicknesses determined from different propagation directions are averaged to provide a basin-wide mean thickness estimate (Nagurnyi *et al.*, 1994). The values compare well to those observed in the regional ice cover (Romanov, 1995) and their interannual variability correlates well with modelled arctic ice volume (e.g. Hilmer and Lemke, 2000). The thickness estimates have also been found to correlate

strongly (~ 0.88) to the satellite-derived area of the perennial, MY ice cover in winter (Johannessen et al., 1999), suggesting moreover that the decreases found in MY ice area represent a mass balance change rather than merely a peripheral effect.

Figure 3.7 a shows the 20-yr time series of area-averaged ice thickness, 1970–91, from which trends for winter and summer are derived (Fig. 2.39 b). The mean thickness estimates are ~ 2.9 – 3 m in winter and ~ 2.5 – 2.6 in summer (i.e. seasonal cycle ~ 40 cm). The linear trend of anomalies from 1971–90 indicates a decrease of only ~ 10 cm (less than 4%) over 20 yr. This is comparable with some observational and modelling analyses (e.g. Holloway and Sou, 2002), but is much less than the 1950s/1970s to 1990s sonar data analysis (Rothrock et al., 1999) upon which the IPCC based its statement that the arctic ice thickness has been reduced 40% during summer in recent decades. The large variability inherent in the arctic sea-ice–climate system, coupled with the problem of obtaining ice thickness data, renders the evaluation of ice thickness trends from the available observational data an open question..

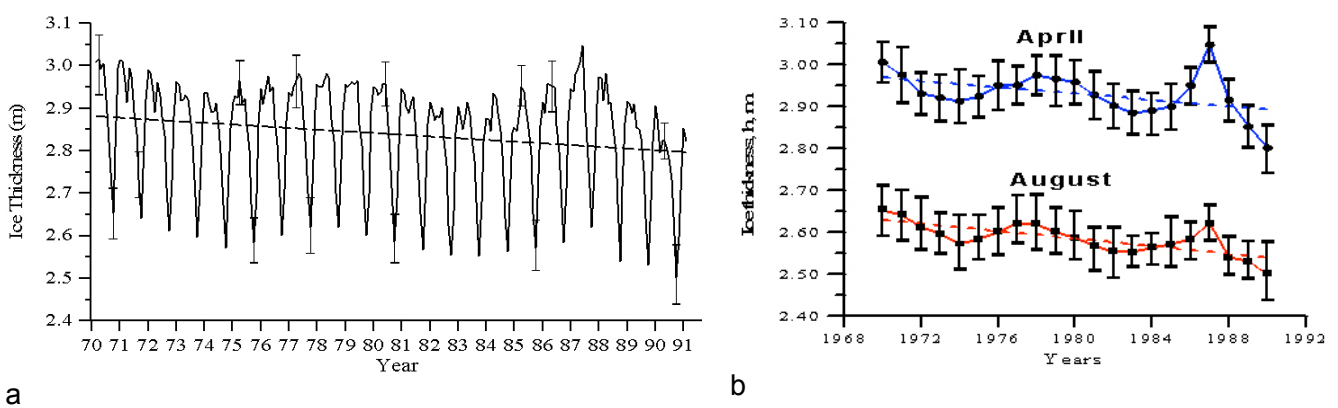


Figure 3.7 Arctic sea-ice thickness variability from 1970-1990. (a) Monthly area-averaged thickness estimates as derived from surface-based measurements of ice-surface vibrations made from Russian North Pole drifting stations in the perennial pack ice of the Arctic Ocean (Nagurnyi et al., 1994, Johannessen et al., 2004). (b) Interannual variability and linear trends for winter (April) and summer (August), with error bars denoting the 95% confidence interval of the ice thickness estimates.

3.2 Sea ice conditions of importance for operation, navigation and oil spill events

3.2.1 Sea ice types and properties

Ice concentration, thickness, and pressure are the major direct factors influencing ship speed. Ice pressure is one of the most important factors in slowing ship speed or even stopping an icebreaker. For offshore construction, the drift of ice as well as its thickness and mass are key parameters to estimate for ice loading calculations. Other sea ice conditions, which also have impact on oil spills and recovery of oil spills, include fast ice, different stages of ice growth and deformation, leads, polynyas, floe size and melting-freezing processes. The different sea ice conditions and nomenclature for sea ice is defined by WMO (2005). An illustration of the seasonal evolution of sea ice is shown in Fig. 3.8.

Fast ice, or landfast ice, floats on the water adjacent to the shoreline and can extend up to hundreds of kilometres, typically ending where water depth reaches over 20 m. Fast ice may range

in thickness from less than one metre to many metres, with irregularities in both the surface and underside based on the movement of air and water around it. This ice is attached to the shoreline and does not move unless released into the current (at which point it becomes drift ice).

Drift ice is essentially any floating sea ice that is not fast ice. There are many different drift ice formations, but they can be divided into four major categories: pack ice; drift ice; grease, frazil and brash ice; and snow. Ice coverage in any area may change among these categories on a daily basis, or one kind of ice may dominate for a season (such as pack ice persisting through the winter). Pack ice describes any concentrated ice cover that is not attached to land and exceeds 60-70% coverage (WMO 2005, Dickins and Buist 1999). Pack ice may range from less than one to several metres thick. This ice typically moves with the water current. Dynamic drift ice, which is sometimes referred to as "broken ice" may exist in the transition phases of freeze-up or break-up, persist throughout the winter in areas that do not reach full pack ice coverage, or exist at the edge of pack ice in the marginal ice zone.

Dynamic drift ice includes brash or slush ice as well as larger ice floes that move with the water current and wind. Irregular floes, often with "grease" ice or slush on the water's surface in between them, are impacted by wind and wave action, which may be greater closer to open water. Dynamic drift ice can be considered to be a collection of chunks of ice *up to 60-70% coverage* (above this would be pack ice,). Dynamic drift ice includes pancakes, ice cakes, and floes, all terms referring to different sized pieces of floating ice. In the spring melt, the chunks of ice may become "rotten" and honeycombed as the ice disintegrates.

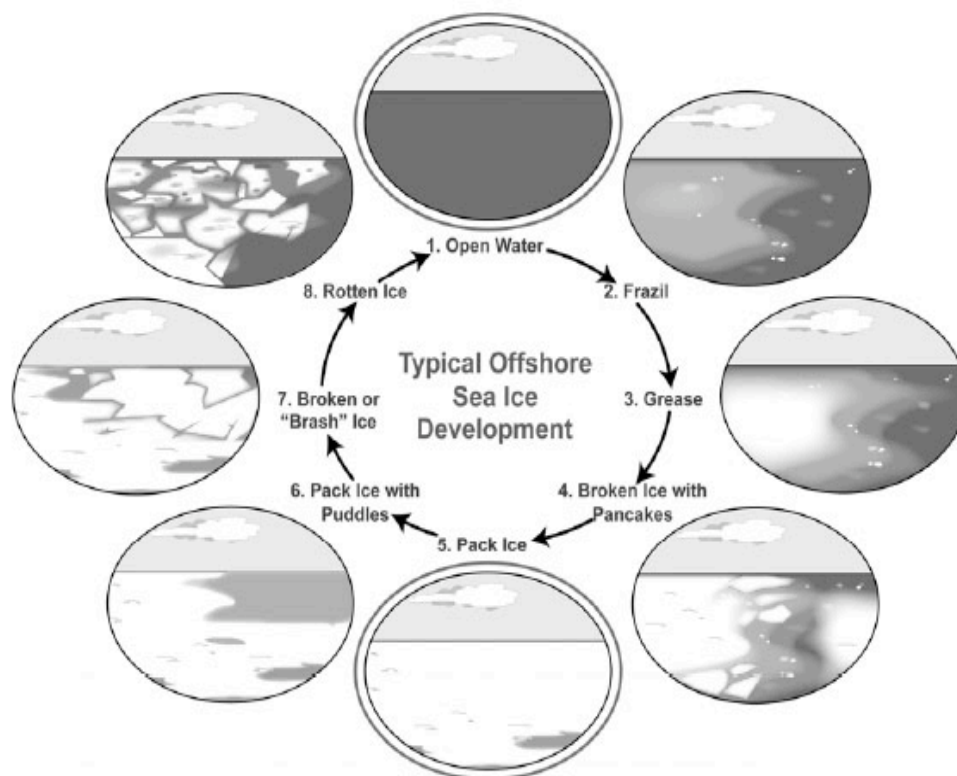


Figure 3.8 The stages in ice formation, growth and evolution of sea ice during a winter season (DeCola et al., 2006)

Grease, frazil, and brash ice are smaller pieces of ice floating on the surface in thin (frazil), or thick (grease), slushy layers. Grease ice may solidify during freeze-up or diurnal temperature cycles to create pancake ice. Frazil or grease ice can appear anywhere there is open water, including between chunks of ice, or on leads or polynyas. These terms refer to ice during freeze-up; brash ice is the breaking-up ice chunks on the surface of the water during melt.

Drift ice can have areas of open water, which may be covered with grease ice during freeze-up and winter. It may feature large "ice keels" which protrude below its irregular surface and can gouge the sea floor as the ice moves. The underside of pack ice may be very rough and irregular. The outer edge of pack ice can be designated separately as the MIZ, often an area of intense biological activity at the edge of open water.

Snow begins as loose and granular precipitation. After collecting on land or ice-covered waters, it is highly variable based on diurnal and seasonal temperature changes, wind, precipitation or wave spray, and depth. Very deep snow can harden into ice (Owens *et al.* 2005). Snow landing on water may create a slushy layer.

During freeze-up, the water surface may be covered with a thin slurry of ice, or a thicker slushy layer. As this ice solidifies into ice pancakes and then floes, a dynamic drift ice field is formed. It may solidify fully into a pack ice formation, or remain as chunks of drifting ice. The process is not necessarily linear (some stages may not happen), and the amount of time each stage takes will vary considerably. The actual ice development process depends on a wide range of factors specific to any one location, including sea state.

In addition to being characterized by variability and transition, sea ice may feature several unique structures or formations that exist within and among the types of ice described above. For example, leads and polynyas are openings that can occur where fast and pack ice meet.

Polynyas are caused by offshore wind conditions blowing sea ice away from the coasts, leaving open water that can refreeze. Polynyas can also be generated away from coasts where the ice field is diverging due to wind forcing. Polynyas are variable features, and may open and close depending on wind conditions.

Leads are elongated openings in the ice cover, associated with divergence in the ice field. Leads can open and close varying with changing forcing by wind and currents. Leads can also be created using ice-breaking or ice management vessels.

Multiyear ice is ice that has survived at least one summer melt season. Multiyear ice is usually thicker and stronger than first-year ice and represents a more severe obstacle to navigation and operations compared to first-year ice.

Sea ice processes in the MIZ includes dynamical processes such as ice edge eddies, ice tongues and jets, ice bands, and breaking of the ice into smaller floes due to waves. Furthermore, freezing and melting of ice is important in the MIZ.

To support offshore operations it is very important to have specific data on the various ice parameters in specific regions where ice operations are planned. Polynyas and fast ice have rather regular behaviour and evolve as function of wind and temperature regimes during the winter season. Fig 3.9 gives an overview of the fast ice areas and the main polynyas along the Siberian coast, obtained from Russian literature. Note that the Russian literature gives geographical names to the polynya areas.

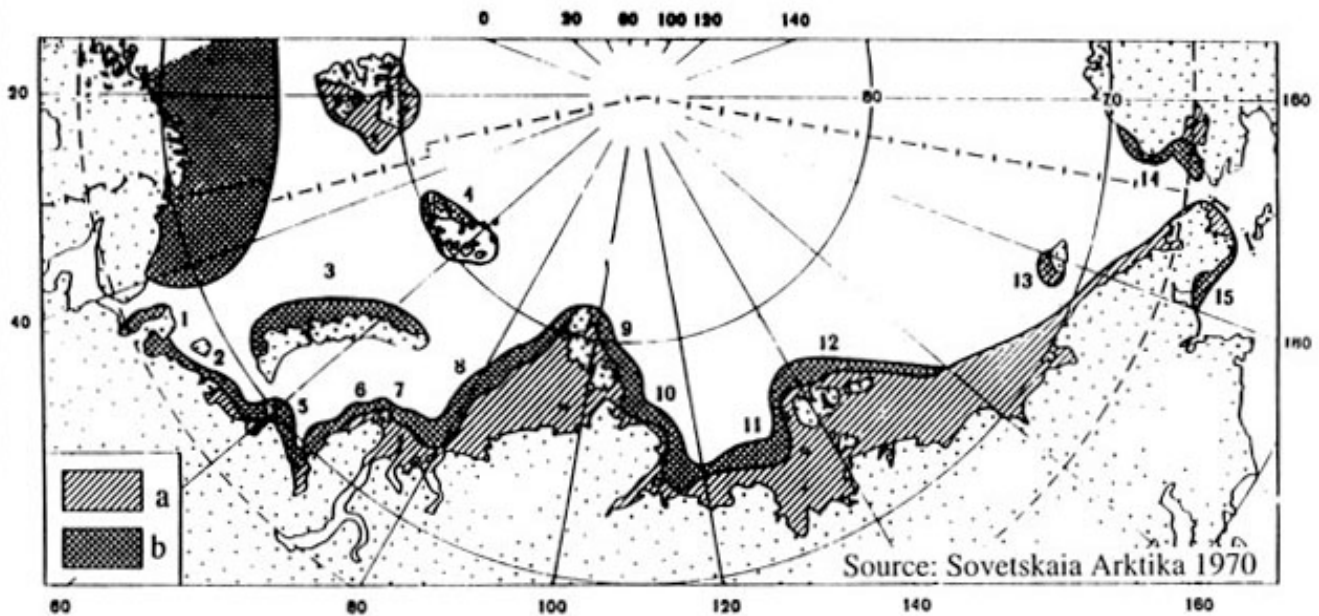


Figure 3.9. Map of fast ice (a) and coastal polynyas (b) in the Russian Arctic during the winter season. Names of the coastal polynyas include 1: Cheshkaya, 2: Pechorskaya, 3: Zapadno-Novozemelskaya, 4: More Victorii, 5: Amdermingskaya, 6: Yamalskaya, 7: Ob'-Eniseyskaya, 8: Zapadno-Severozemelskaya, 9: Vostochno-Severozemelskaya, 10: Taymirskaya, 11: Lenskaya, 12: Novosibirskaya, 13: Zavragelevskaya, 14: Alaskinskaya, 15: Anadirskaya.

An example of fast ice, polynya and other first-year ice characteristics in the Kara Sea observed in a RADARSAT ScanSAR image is shown in Fig. 3.10. This image demonstrates late winter ice conditions in the Kara Sea from the Ob estuary in the west to the shores of Taymyr in the east, with temperature between -10° to -15°C and winds of about 10 m/s from NE. The image has a complex pattern of ice types, and several areas are difficult to interpret with certainty. Large areas with fast ice are seen with a gray signature off the coasts and around the islands. In these areas the backscatter varies considerably and depends on the salinity, ice age and roughness. In general, strong backscatter indicates that the ice is fresher and rougher. The image interpretation could be done by use of *in situ* observations from the expedition.

The image can roughly be divided into three regions: medium and thick first year ice in the upper part of the image (1 and 2), polynya areas with various types of new and young ice including open water (3, 4 and 5), and finally the landfast ice regions near the coast and the islands (6 and 7). Area (1) consists mainly of large thick first year ice floes (darker), with smaller areas with young ice (brighter) and nilas (very dark) in-between. Some of the darker small areas might also be water. Some areas have strongly deformed thin and medium-thick first year ice (2), with some inclusions of young ice (light gray). The very bright parts of the polynya area (3) consists of deformed young ice, while areas (4) and (5) are most likely a mixture of water and thin ice types such as grease ice and nilas. Areas (6) and (7) show landfast ice of various age and deformation. The darker signature the more level and undeformed ice, while brighter backscatter suggests more roughness at the surface from the ice deep into estuaries may be due to a lower salinity of the river water. It is also hypothesized that the freshwater of the inner parts of the bays can be responsible for the high backscatter in these areas.

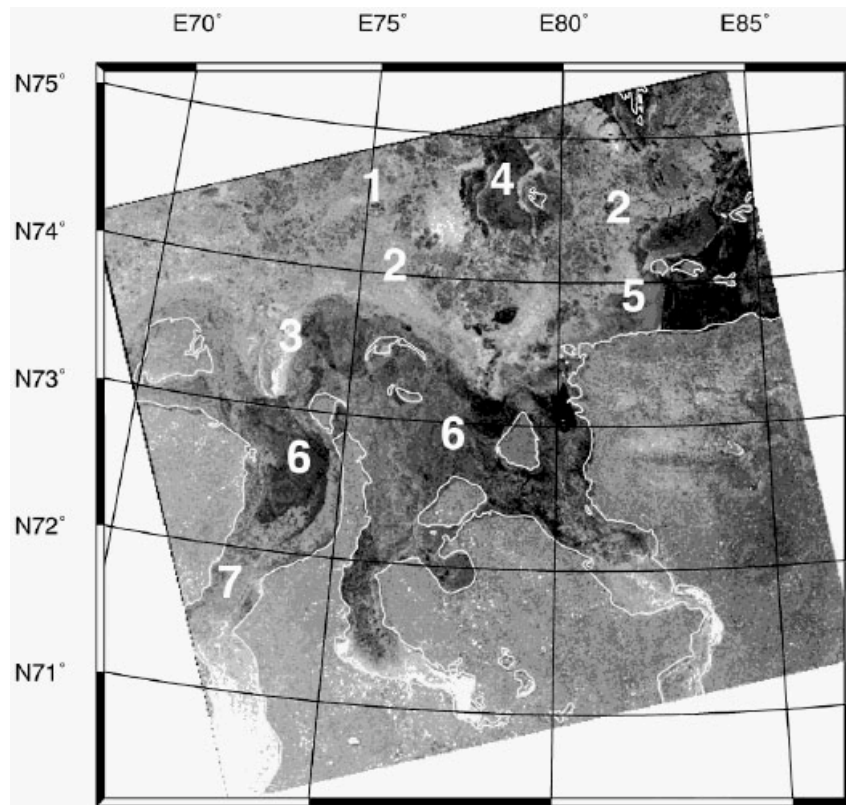


Figure 3.10. RADARSAT ScanSAR image of April 30, 1998, showing sea ice in the area where the Ob and Yenisei rivers enter the Kara Sea. The ice types 1-6 are discussed in the text (Shuchman et al., 2004).

Starting in autumn, the fastice is formed near at the coast of the arctic seas. During the winter, the fastice boundary extends further offshore. Maximum development of fast ice is observed in the shallow waters of depths up to 20-25 m. The bathymetry determines how far offshore the fastice can extend. Close to coastlines with deeper waters, the width of fast ice is only about 10-20 km. The fast ice is usually formed by firstyear ice. But in the regions of Franz Josef Land, Spitsbergen, and the East Siberian Sea, two-year old ice may also be found in the fastice areas.

Along the Siberian coast it is common to have polynyas or passage ways between the fast ice and the pack ice (Fig. 3.9). The polynyas changes with time under the influence of varying wind conditions. They can be very long and have variable width. During push-off winds, flaw zones of thin ice are formed beyond the landfast ice and may exist for a long time as open polynyas. Refreezing of the polynyas can occur with formations of up to 70 cm thick ice. Refrozen polynyas up to 50 km in width can occur in the Kara Sea and in areas to the west and north of the New Siberian Islands. Such zones are less developed in the East Siberian and Chukchi seas where the width is less than 15 miles.

There are many stamukhas in the landfast ice. Stamukhas are ridges that form in shallow water and becomes stuck at the seafloor as the they grow deeper during the winter season. Examples of rafting and ridging of sea ice are shown in Fig. 3.11. There are two dominant regions of landfast ice along the Siberian coast: the Severnaya Zemlia region (area 8 – 9 in Fig. 3.9) and the New-Siberian Island region (area 10 – 12 in Fig. 3.9). These two areas contain more than 80 % of the total landfast ice in the arctic seas. Landfast ice is usually in the range of 1.50 to 2.00 m thick. Wide leads with thinner ice, cracks, and hummocks, are frequently observed in the landfast ice.

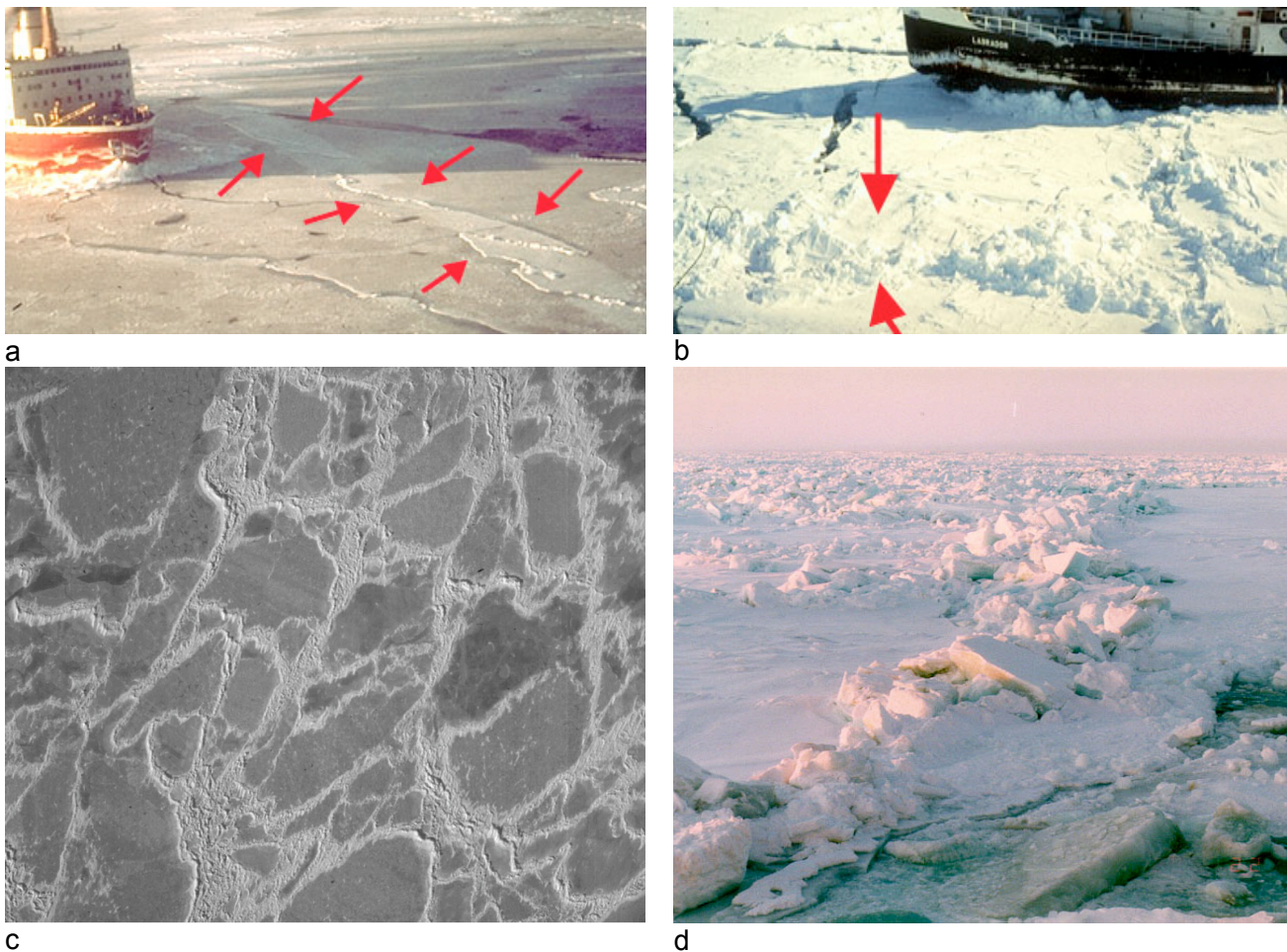


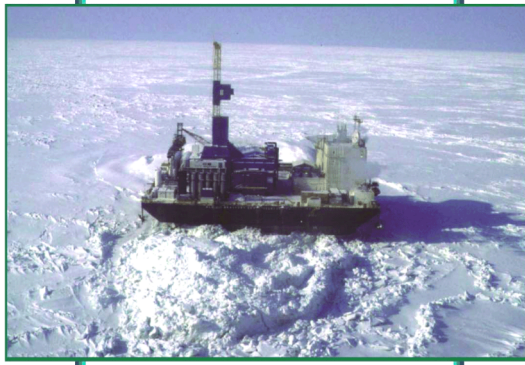
Figure 3.11 Examples of photographs of ridging and rafting of sea ice: (a) rafting where one ice sheet is pushed on top of another, (b) a ridge of about 1 m height, (c) vertical photograph of ridge pattern in first-year ice, (d) heavily ridged area of first-year ice.

The drift ice area is located immediately beyond the zone of thin ice. Thick first-year (1.2-1.6 m) ice occupies 30 – 35 % of the drift ice area. Perennial ice of the Arctic Basin enters into the Siberian coastal seas. Such ice is 2 to 3 m thick and is characterized by higher strength. Most of the total sea area occupied by perennial ice on the Siberian coastal shelf is concentrated in the East Siberian Sea where such ice occupies 15--20% of that area. In other Arctic shelf seas this ice normally occupies less than 5% of the areas.

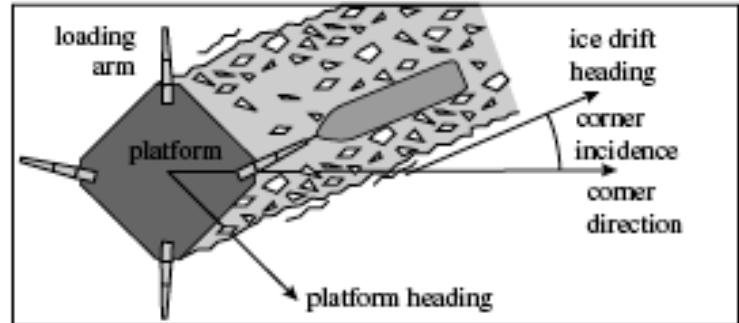
The ice drift responds to the wind direction within 3 to 6 hours after changes of wind direction. Ice drift results in ice exchange between the Arctic shelf seas and the Arctic Basin. In winter the ice is transported out of the Kara and Laptev seas and into the Chukchi Sea. This ice drift continues in May and June, although weaker. The ice drift to the Chukchi Sea continues, while the ice drift from the southwestern Kara Sea almost stops. The amount of ice transported from the northwest to the East Siberian Sea increases.

For offshore operations, there are two main situations which require handling of the ice. The first situation is in shallow waters (5 – 20 m) where constructions are built on the seafloor and designed to withstand the forces of drifting sea ice (Fig. 3.12 a). The sea ice is often attached to the

seafloor, but ice motion can occur during strong winds when ice can pile up and form stamukhas. The other situation is when operations takes place in deeper water covered with ice which is freely drifting and ships can operate in the area. Drifting ice passing by a fixed construction will leave an open lead in downstream direction (Fig. 3.12 b and c) and ice-going vessels can operate in this lead. An example of stamukhas is shown in Fig. 3.12 d where ice has piled up more than 10 m.



a



b



c



d

Figure 3.12 (a) photograph of a fixed bottom-mounted platform in sea ice in the Beaufort Sea, (b) illustration of drifting sea ice surrounding a fixed platform where loading to a ship takes place in the lead, (c) drifting ice around an artificial island built for drilling in the Caspian Sea, (d), photograph of a large stamukhas (courtesy D. Mayne, AGIP).

Sea ice thickness is the least know of the main sea ice parameters, because data on ice thickness are scarce and systematic measurements of ice thickness do not exist in many areas. Local knowledge of thickness including ice ridges and keels are essential for design of platforms to be operated in seasonal ice-covered areas. Recently, electromagnetic (EM) sounding from helicopter flights has become a well-established technique for measuring ice thickness on local and regional scale. Large data sets representative for regional ice regimes can be gathered for determination of the of ice thickness distribution as shown in Fig. 3.13 a,b (Haas and Eicken, 2001). The EM technology is under further development and will allow repeated systematic surveys in regions where helicopters can operate and there is need for detailed measurements of sea ice thickness and ridge distribution.

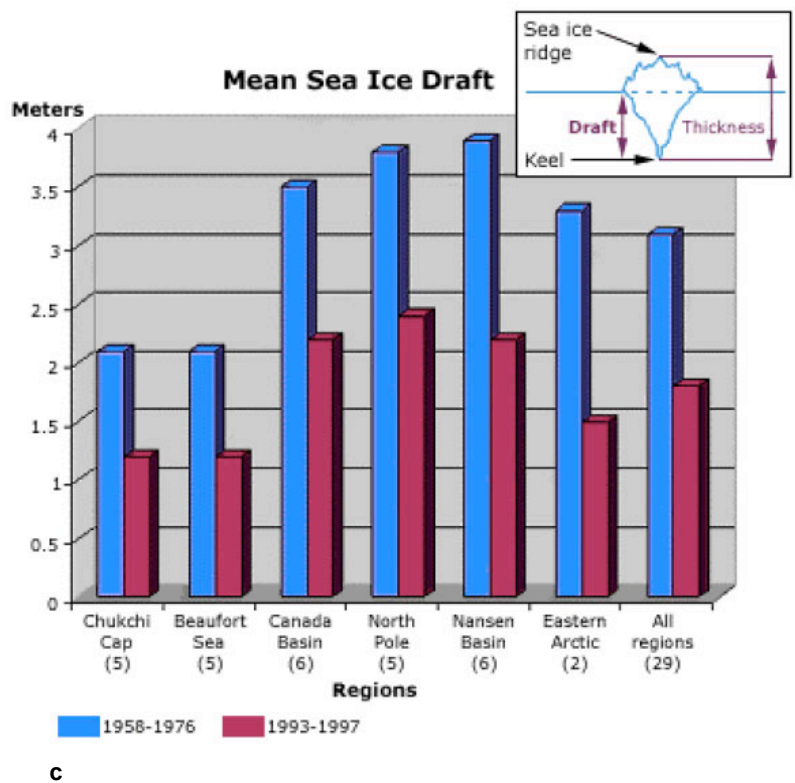
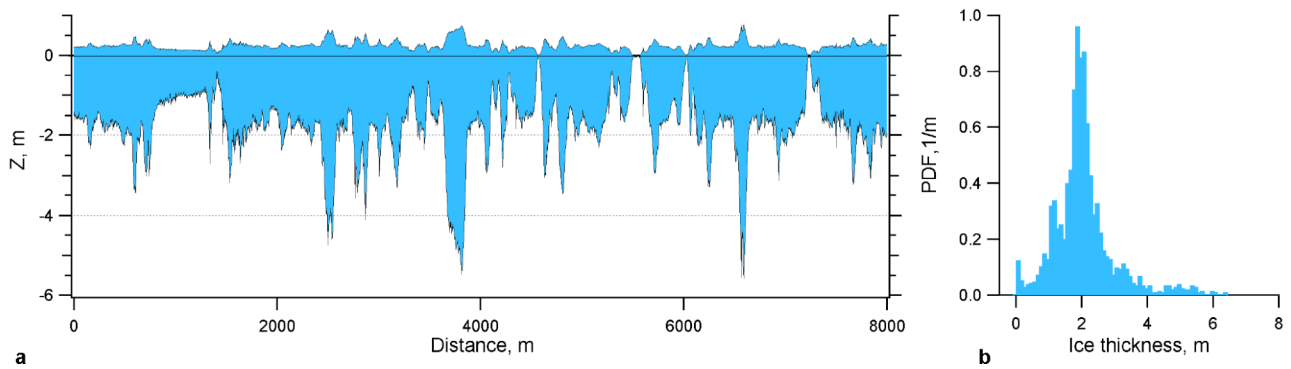


Figure 3.13. (a) Data on ice draft and ice surface height from helicopter electromagnetic induction profile, (b) ice thickness distribution function for the data presented in (a). The figures are provided by C. Haas, AWI, (c) is a comparison of mean ice draft in different Arctic seas obtained from submarine cruises from 1958 to 1997, showing a significant reduction in ice thickness over the last decades.

3.2.2 Sea processes in the MIZ

In the Marginal Ice Zone the abrupt transition to open water gives rise to unique processes including water mass formation, oceanic upwelling, wave propagation into the ice, eddy formation and atmospheric boundary layer processes (e.g. Johannessen et al., 1994). The ice edge morphology can vary from a regular line with compacted floes to a diffuse transition between open water and ice. The ice edge is highly variable and exhibits rapid dynamic and thermodynamic responses. Table 3-1 summarizes various ice edge structures.

Variations in ice concentrations along the edge result from wind drag, tides, ocean circulation, ice ablation, or freezing and can vary on a daily, monthly, seasonal, or yearly basis. Ice edges are classified as either compacted or diffuse. Compacted edges are clearly defined due to wind and/or currents moving toward the pack. Diffuse edges are poorly defined, and are usually associated with the downwind side of the pack. The type of ice edge structure can be best identified using SAR images for satellites, because these images have high resolution and are independent of cloud and light conditions. The ice edge is characterized by observing the change in ice concentration within the outer ice edge region that is made up of small floes. These small floes, ranging from 20 to 100 m in size, occur along the ice edge as a result of ablation, freezing, and gravity-wave/ice interaction and eddy induced collisions, which break up large floes. When an on-ice wind event occurs, the ice edge becomes very compact, the ice concentration approaches 100%, and the backscatter intensity values become large. When an off-ice wind event occurs, the ice edge becomes diffuse, the ice concentration reduces to values as low as 20% and the average backscatter intensity average reduces considerably.

Table 3-1. Ice edge structures

Definition	Description
Compacted ice edge	Close, clear-cut ice edge compacted by wind or current; usually on the windward side of an area of pack ice.
Diffuse ice edge	Poorly defined ice edge limiting an area of dispersed ice; usually on the leeward side of an area of pack ice.
Tongue	A projection of the ice edge up to several kilometers in length, caused by wind or current.
Bight	An extensive crescent-shaped indentation in the ice edge, formed by either wind or current.
Ice Field	An area of drift ice consisting of floes of any size and having an area greater than 10 km across: Small Ice Field: 10-15 km across Medium Ice Field: 15-20 km across Large Ice Field: Greater than 20 km across
Ice Patch	An area of drift ice less than 10 km across.
Belt	A large feature of drift ice arrangement; longer than it is wide; from 1 km to more than 100 km in width.
Strip	Long narrow area of drift ice, about 1 km or less in width, usually composed of small fragments detached from the main mass of ice and run together under the influence of wind, swell or current.

The dynamics of the ice edge as imaged by SAR can be illustrated in Figure 3.14, an area of the Greenland Sea. Each SAR strip, which is 500 km long and 100 km wide, covers the same geographical area in the ice-edge region between 76° to 80°N, and 8°W to 4°E. This series of annotated ERS-1 images and corresponding interpretation maps shows how the ice-edge location and features changed during the period from 13 to 16 January 1992. During this period, oceanographical investigations in the area were conducted from the R/V Håkon Mosby showing a number of shallow surface tongues of colder and fresher water associated with the ice tongues in Figure 3.14 (Johannessen, et al., 1994).

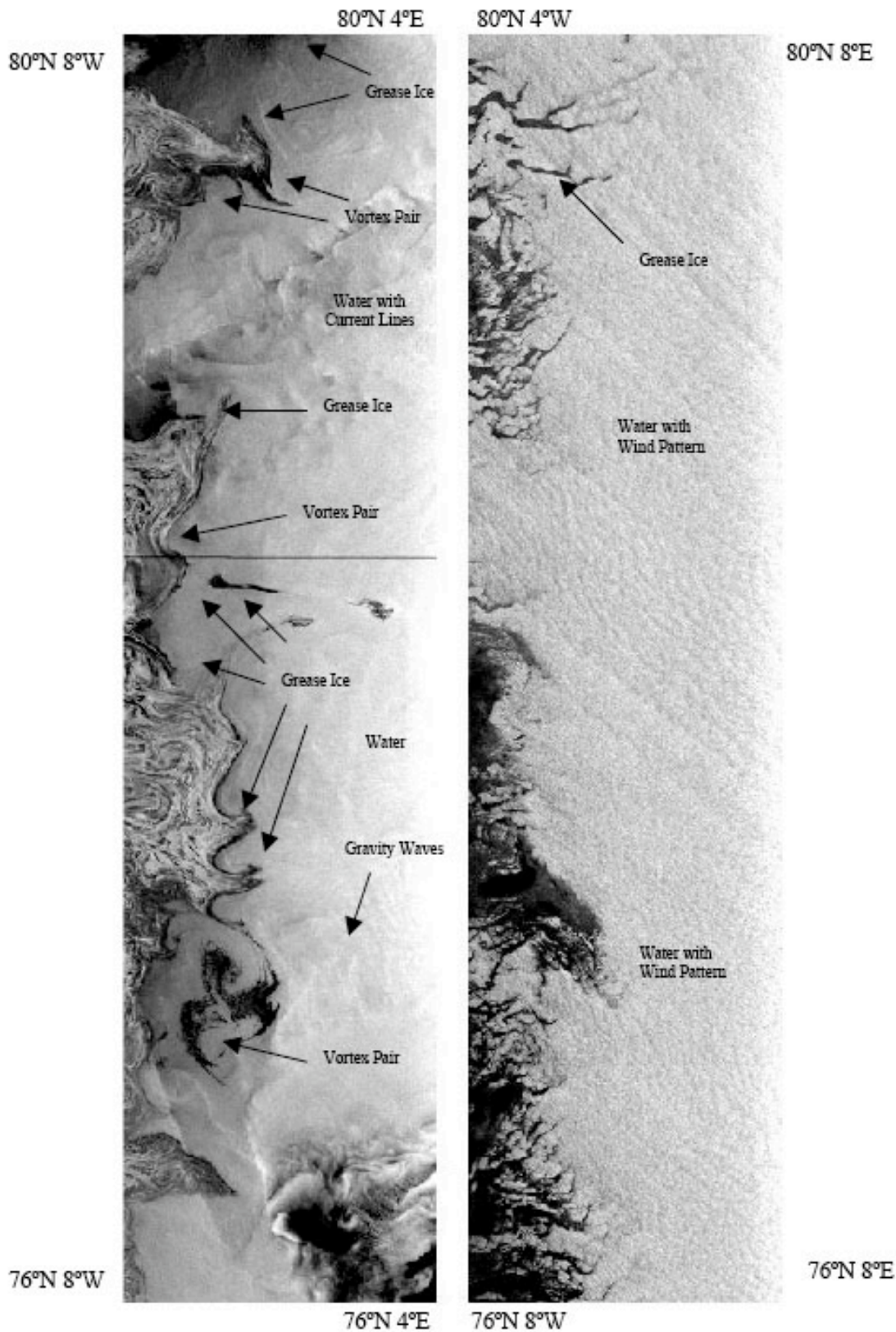


Figure 3.14. ERS-1 SAR Example of rapid ice edge variability in the Greenland Sea – Fram Strait area as a result of strong off-ice winds. Left image: 13 January 1992 with calm to moderate wind. Right image: 16 January 1992 with strong NNW winds of 20 m/s (Johannessen et al., 1994).

SAR images with 25 m resolution were the only data capable of providing accurate ice edge location in a period of almost no daylight. SAR images transmitted to the ship in near-real time were used to route the ship to positions near the edge of the ice. Without SAR imagery, the R/V Håkon Mosby would not have been able to operate close to the edge of the ice, as the wind conditions were variable and included storm events with wind speeds exceeding 25 m/s. During southeasterly winds, the ice edge was pushed towards the west. From 10 to 13 January, the wind began as northerly and then shifted to southerly, resulting in a more eastward location of the edge. On 16 January the effects of a north-northwest wind is made visible by ice streamers in the open ocean oriented parallel to the wind. Three days later, westerly winds produced an ice edge that is very diffuse. The rapid change in edge location and detailed ice features as characteristic of this area, could only be observed from a time series of SAR images. The repeat period for the ERS SAR coverage was three days.

Figure 3.14 also shows how wind speed is a determining factor in discerning the ice edge on SAR images. High wind and wave conditions will cause the open ocean to produce a large return making the intensity value similar to sea ice.

The delineation of the ice edge on SAR imagery at the marginal ice zone in winter is complicated by the formation of new ice. Grease ice first forms followed by frazil, which then transitions into pancakes. Due to continued freezing and wave action the pancakes then grow from a few centimeters in diameter to meter plus size. The SAR backscatter return from these features also varies greatly. The grease ice dampens the ocean wind generated Bragg waves, thus causing dark radar returns. The pancake floes also shown in Figure 3.15 have rough edges at the water interface and thus are brighter SAR backscatter values on the satellite imagery.

Ice edge eddies in the Greenland Sea and Fram Strait area were investigated for the first time during the MIZEX program using remote sensing in combination with *in situ* observations (Johannessen, et al., 1992, 1994) The ice edge eddies, a result of warm and cold ocean water masses interacting, are important for several reasons, i.e. as a mechanism to exchange to heat and mass between open water and ice covered regions, in controlling the position of the ice edge, and to advect water masses trapped in the eddies. Mesoscale eddies, which have a typical scale of 20-40 km in the Greenland Sea area, can also elevate intermediate water masses to the surface and contribute to deep-water formation; hence, they are important to the oceanic uptake of atmospheric carbon dioxide and other climatic gases. Eddies are also an area of typically higher than normal ambient acoustic noise due to ice floe collisions. Eddies are most readily observed along the ice edges where SAR images show a sharp contrast between ice and water. An example of ice edge eddies in the MIZ of the Barents Sea observed by SAR is shown in Fig. 3.16. SAR can be used to locate eddies in this region because individual ice floes act as tracers mirroring the ocean circulation. When they occur within the ice pack, they are much more difficult to detect in the SAR images. In regions of open water, it is necessary to use infrared or visible imagery to look for sea surface temperature gradients or color contrast to locate vortex-pairs.

Other processes in the MIZ include wave propagation into the ice cover, which is further described in section 5.4.1. SAR is also a useful instrument to observe waves in ice because the wave lengths are long, typically 100 – 200 m. This allows us to observe the wave field in ice in SAR imagery with high resolution, e.g. 10 – 20 m pixel size. Example of wave propagation in sea ice is shown in Fig. 5.5. A consequence of the waves acting on the ice cover is that the ice floes are broken into smaller floes, ranging from 10 to 100 m. The ice cover in the MIZ, consisting of many small floes, obey different dynamical laws compared to the interior of the ice pack, leading to different ice rheology formulations, which is further described in chapter 4.



Figure 3.15. Photo of Odden from the R/V Håkon Mosby showing pancake and grease ice. The pancake floes (bright circular features) are approximately 25 cm in diameter (Shuchman et al., 2004).

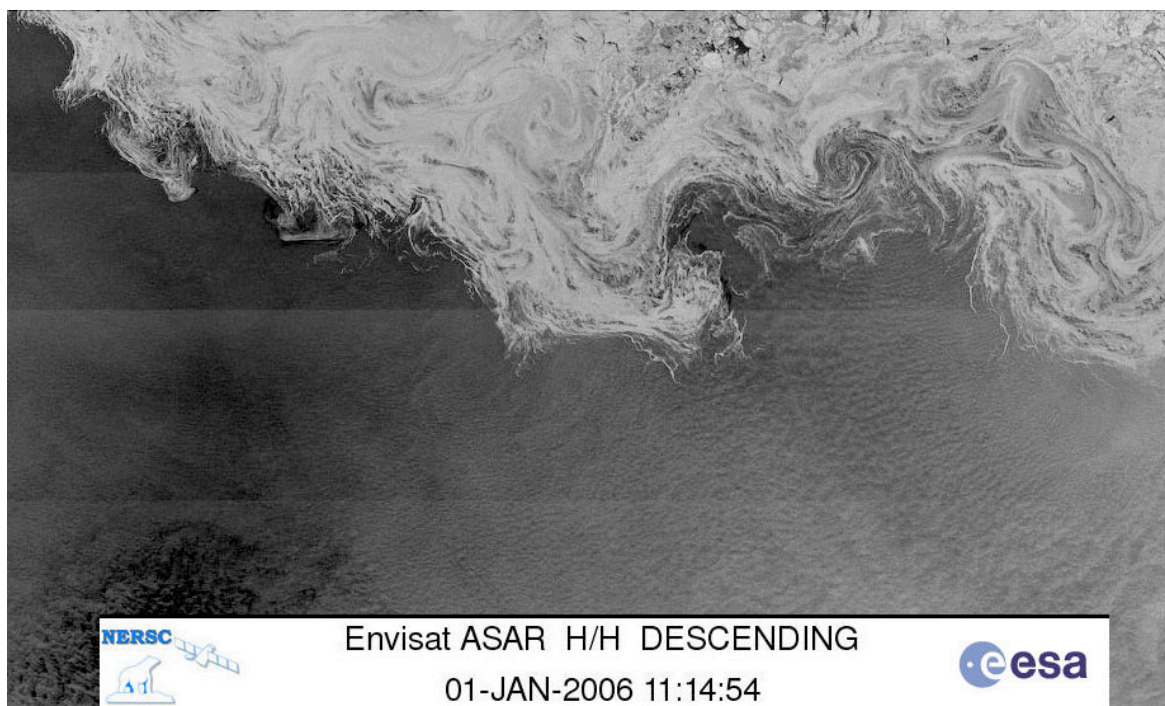


Figure 3.16. SAR image from ENVISAT showing ice edge eddies in the MIZ of the Barents Sea.

3.3 Icebergs

Icebergs, which are originating from glaciers, are commonly found off eastern Canada, around Greenland, in the Barents Sea and several places in the Russian Arctic (Fig. 3.17). They can be very dangerous for ships and oil rigs because most of the ice mass is below the surface. Smaller icebergs, with horizontal scale of typical 100 m, can be difficult to detect. Observations of sea ice and icebergs are obtained by several methods: aircraft/helicopter surveys, ship observations, reports from coastal and meteorological stations, data from drifting buoys and satellite data. The International Ice Patrol is responsible for observing and reporting icebergs in the Northwestern Atlantic (<http://www.uscg.mil/lantarea/iip/home.html>). In the European Arctic, there is a need to establish a monitoring and forecasting system for icebergs to support the offshore oil and gas exploration.

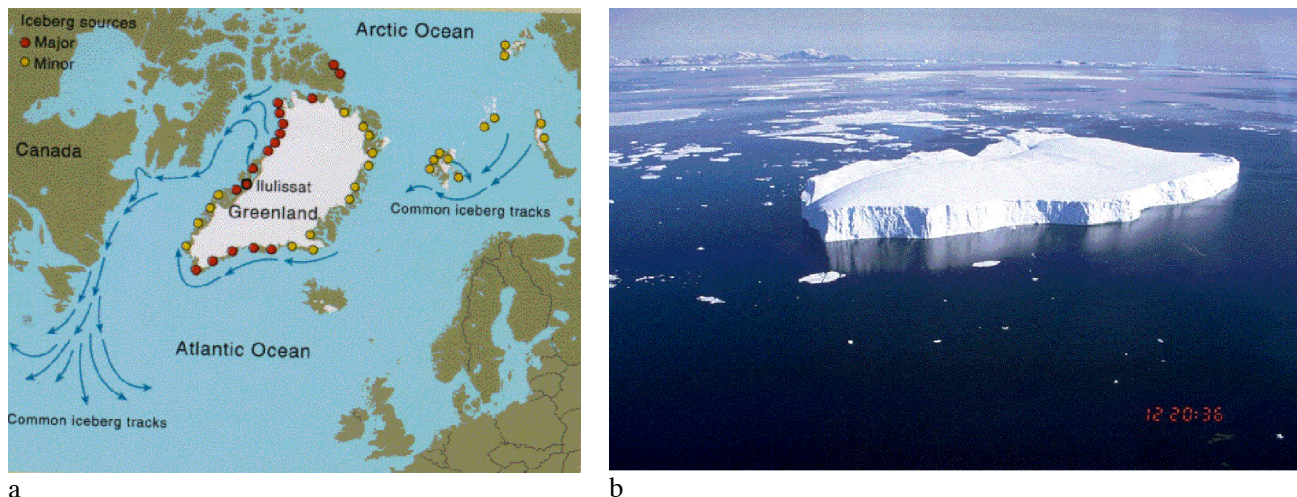


Figure 3.17. (a) Map of the main iceberg-producing areas in the European Arctic and the major drift paths for icebergs, (b) photograph of a characteristic tabular iceberg in the Barents Sea, with horizontal scale of about 100 m and freeboard height of 6 – 8 m.

Systematic monitoring of icebergs in the Arctic have been conducted by Russian aircraft surveys in previous decades, and results of these monitoring projects were presented in several reports as part of the OKN IDAP project 1988 – 1994 (Spring, 1994). Systematic observations by aircraft stopped in the 1990s. In the last 10 – 15 years, there have only been occasional observations of icebergs in connection with expeditions.

An overview of the aircraft iceberg surveys in the Barents and Kara Sea conducted by Arctic and Antarctic Research Institute in the period 1970 – 1989 has been provided by Abramov and Zubakin (1992). This report shows that more than 1500 flights were conducted in the 20 year period and icebergs were observed in more than 1000 of the flights. The flight tracks are shown in Fig. 3.18. More than 16000 icebergs were observed in total and the annual and monthly distribution of the observations (Abramov and Zubakin, 1992). In addition to this report, the Iceberg Atlas for the Arctic by Abramov (1996) gives the best overview of icebergs from early 1900 and up to about 1993. The aircraft surveys were normally performed at a flight altitude between 100 and 500 m, with an observing range of 20 – 30 nautical miles. A main question is how large part of the icebergs are captured by this observing scheme. It is obvious that large parts of the areas that potentially can have icebergs are not covered by the surveys. The data presented in Table 2 is underestimating the total amount of icebergs, and the question is by how much. Another issue is the size distribution of the icebergs. Previous investigations show that most of the icebergs in the Barents Sea have size less than 100 m. This has impact on the detection capability using aircraft surveys as well as satellite observations.

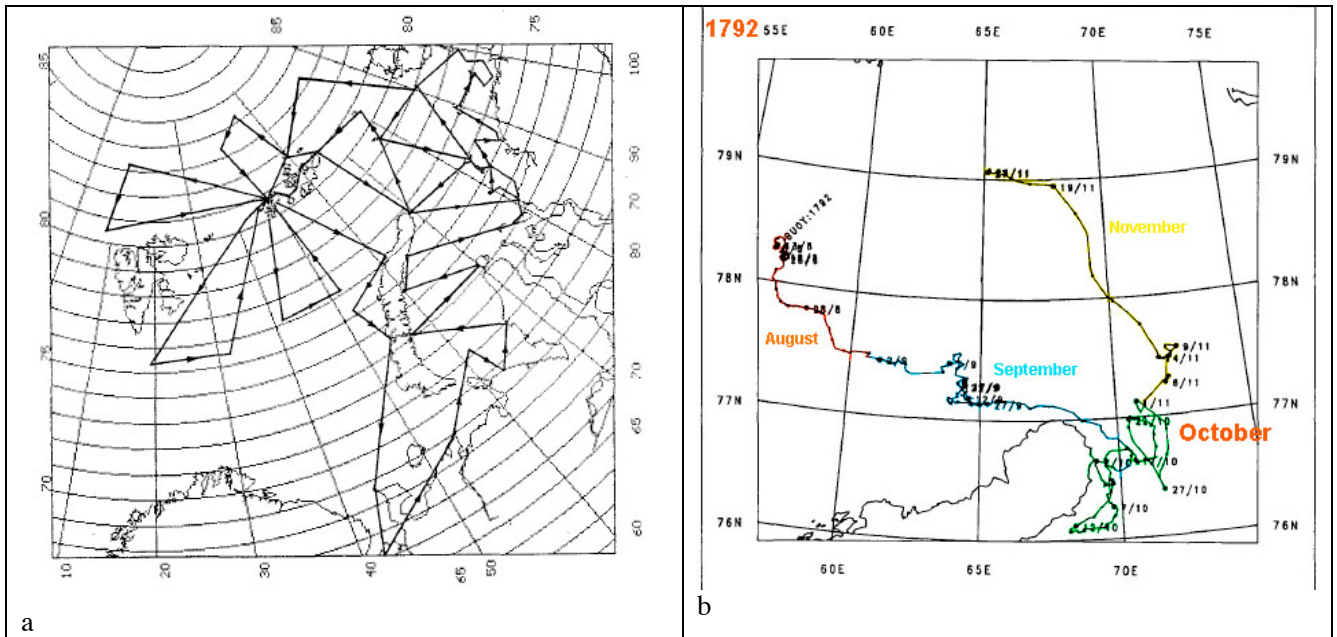


Figure 3.18. (a) Map of standard aircraft flight tracks used for icebergs surveys 1970 – 1989); (b) example of iceberg drift pattern using Argos positions during IDAP investigations (Abramov and Zubakin, 1992).

As observed in Fig. 3.19, the number flights and consequently the number of icebergs were at a minimum in the dark winter month November, December, January and February. Maximum observations in the winter season was in April, while summer observations were at maximum in August and September. Fig 3.20 shows the annual variability in total number of observed icebergs. There are noteworthy minima in 1974-75, 1981-82, and 1987-88. These minima are correlated with lower number of survey flights, as shown in Fig. 3.21

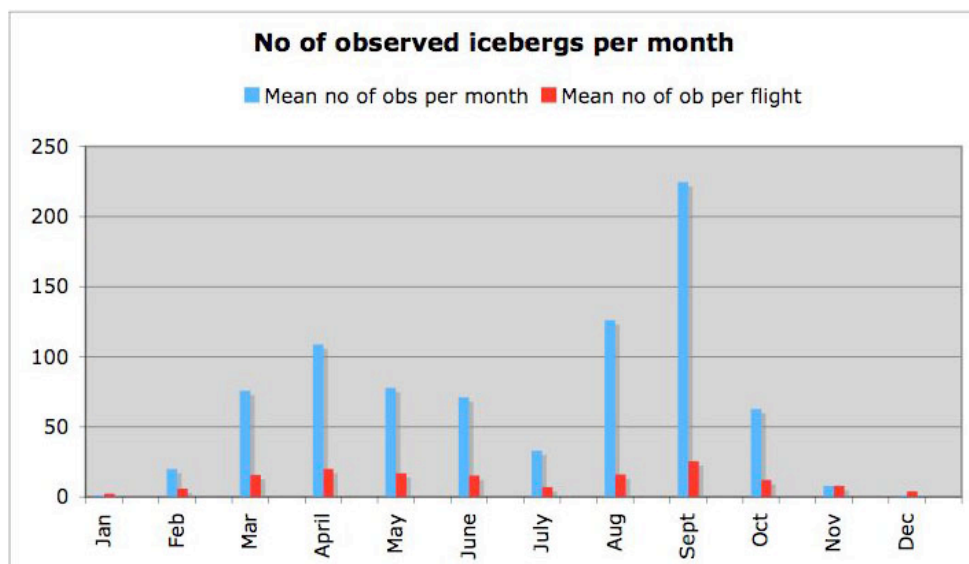


Figure 3.19 Mean number of observed icebergs per month (blue bars) and mean number of observations per flight (red bars)

It is noteworthy that the years with lowest number of observed icebergs in Fig 3.20 (1974-75, 1981-82 and 1987-88) also have the lowest number of flights. In addition, 1974, 1981 and 1982 had the lowest number of observations per flight. 1989 is remarkable because the number of observations per flight is significantly higher than all the other years. By comparing total number of flights with total number of observed icebergs is possible to assess if there has been a trend in iceberg occurrence over the 20 year period. The years 1970-73 is characterized by high number of observations and high number of flights. If we compare this with the next period of high number of observations (1983-1986), we see that relatively more icebergs were observed by a lower number of flights. Except for the extreme year 1989, it can be concluded that iceberg occurrence in the survey area showed large interannual variability and this variability is to a large extent correlated with the number of flights.

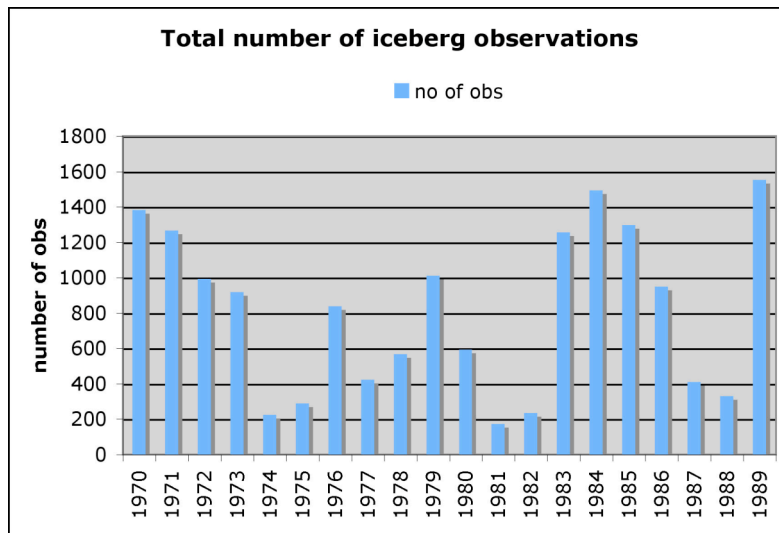


Figure 3.20 Total number of observed icebergs per year in the Barents and Kara Seas

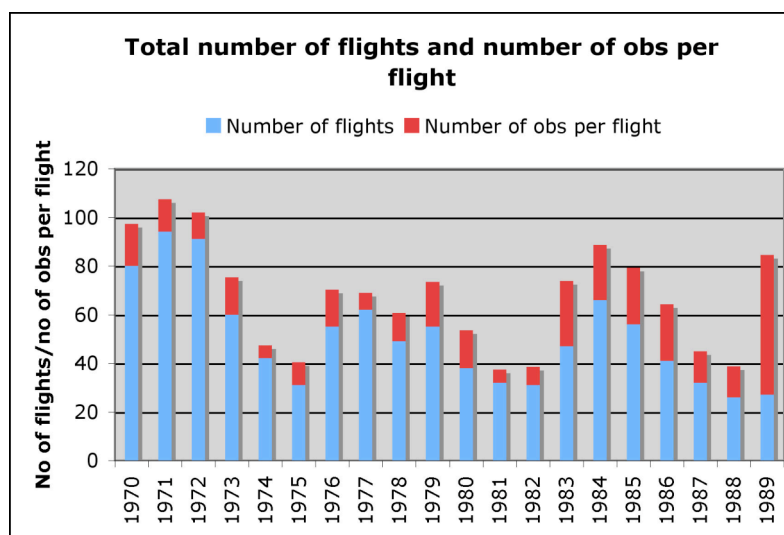


Figure 3.21 Total number of survey flights per year (blue bars) and total number of observations per flight (red bars);

The observations of icebergs from the aircraft surveys have been used to produce iceberg occurrence probability maps (e.g. Abramov and Zubakin, 1992). A more extensive compilation of iceberg data have been published in the Atlas of Arctic Icebergs by Abramov (1996). In this atlas monthly maps of iceberg distribution probability are presented. Also annual occurrence probability maps have been produced (Fig. 3.22) showing that the Northern Barents Sea, Kara Sea and part of the Laptev Sea have the highest probability of icebergs. Maximum iceberg occurrence is found around Franz Josef Land, northern Novaya Zemlya and Severnaya Zemlya.

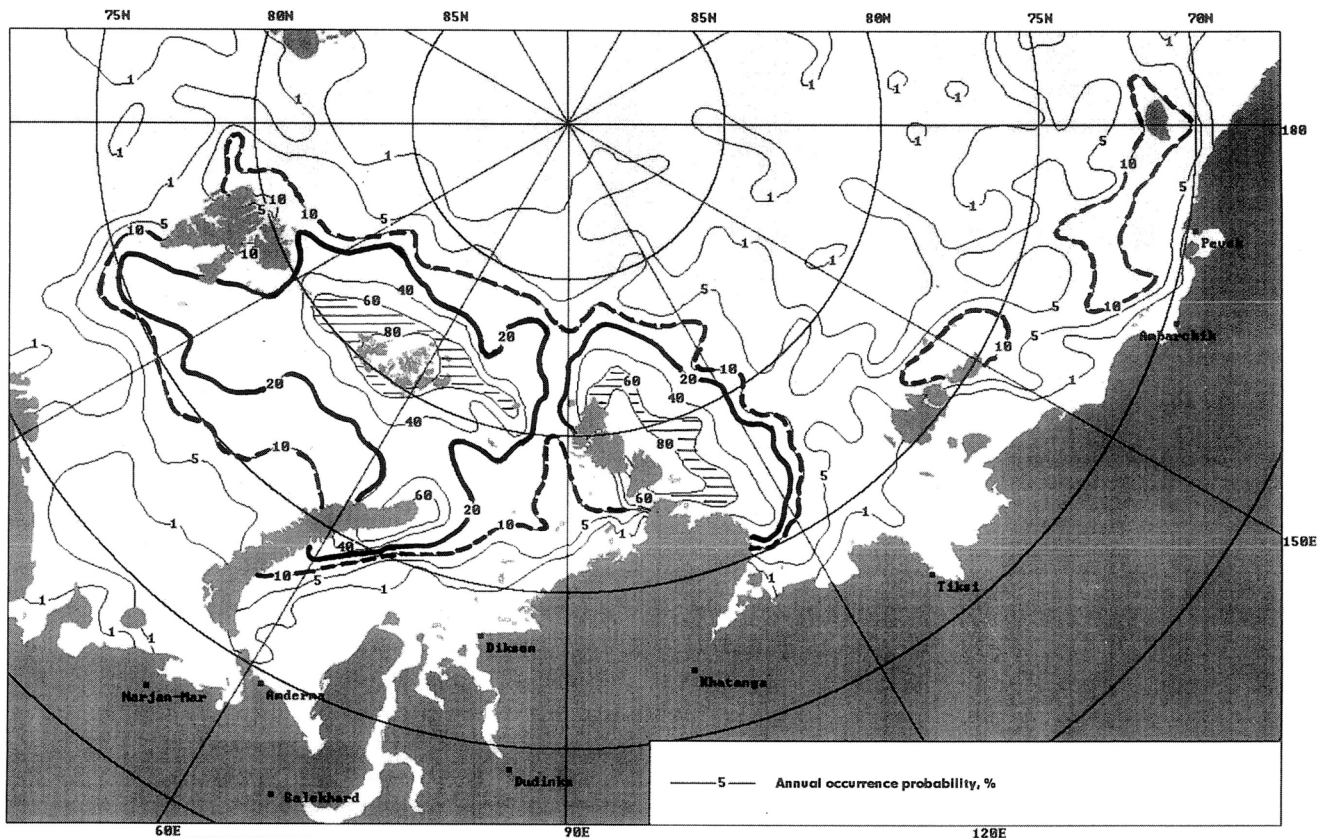


Figure 3.22. Annual iceberg occurrence probability from the Abramov Atlas (1996).

In May 2003, surprisingly many icebergs were observed in the Shtokman area south to 72 N (Zubakin et al., 2004). From ship radar observations, 109 iceberg and bergy bits were found in the area between 71 and 75 N and between 40 and 46 E. The largest iceberg was 190 by 430 m. Before this event, the iceberg occurrence probability for the Shtokman area was that 7 icebergs would occur once in ten years. After May 2003 this probability rose to 19 icebergs occurring once in ten years.

Since the iceberg distribution can vary strongly from year to year, it is important to have good monitoring and tracking systems for the icebergs. Such systems are not in operation for most parts of the Arctic today. Extreme events can happen from year to year and there is no direct method to predict when and where icebergs occur and how they drift in the ocean.

4. Sea ice modeling of the marginal ice zone

4.1 Introduction to sea ice modeling

The Marginal Ice Zone (MIZ) is the region between the open ocean and the perennial ice pack. It is a region which is very dynamically active compared with the oceanographic conditions in the central Arctic. A strict definition does not exist, but a loose definition of the MIZ is given by Wadhams (1986); "The part of the ice cover which is close enough to the open ocean boundary to be affected by its presence." The MIZ can be seen as a transitional region, with atmospheric and oceanic conditions changing rapidly as one moves across the MIZ. In the MIZ, the atmosphere still feels the presence of the relatively warm surface waters of the open ocean. Relative to the central Arctic atmospheric conditions, the MIZ usually experiences a mild climate. The ice cover in the MIZ is also very much influenced by the proximity of the open ocean. Storms in the open ocean generate ocean waves and swells which penetrate into the ice covered waters. As a consequence, waves in the open ocean strongly affect the sea-ice properties of the region by breaking up the pack-ice originating in the Central Arctic Ocean into small floes typical of the MIZ.

The width of the MIZ varies spatially from being narrow, on the order of kilometers, and wide, on the order of hundreds of kilometers. This large variation stems from the different factors that create and shape the MIZ. It is for instance strongly related to atmospheric conditions. Winds normal to the sea-ice edge can quickly diffuse or compact the MIZ. These properties make the MIZ a quickly changing region, making it a challenging region to forecast on short time scales. Many industries operating in the proximity of the sea-ice edge have very little capability of operating within the ice itself, so accurate predictions of the MIZ and ice edge are perhaps the most important element in sea-ice forecasting. This necessitates the improvement of sea-ice models. Today's sea-ice modelling tools provide good results on large scales, with the ice dynamics model of Hibler III (1979) and variants of it being the most commonly used models in climate and operational sea-ice modelling. For instance, the sea-ice forecasting products of the TOPAZ system Bertino et al. (2005), presently uses the EVP model of Hunke and Dukowicz (1997), which can be seen as a variant of the model of the model of Hibler III (1979). An illustration of the sea-ice forecasts from TOPAZ modeling system is shown in Figure 4.1.

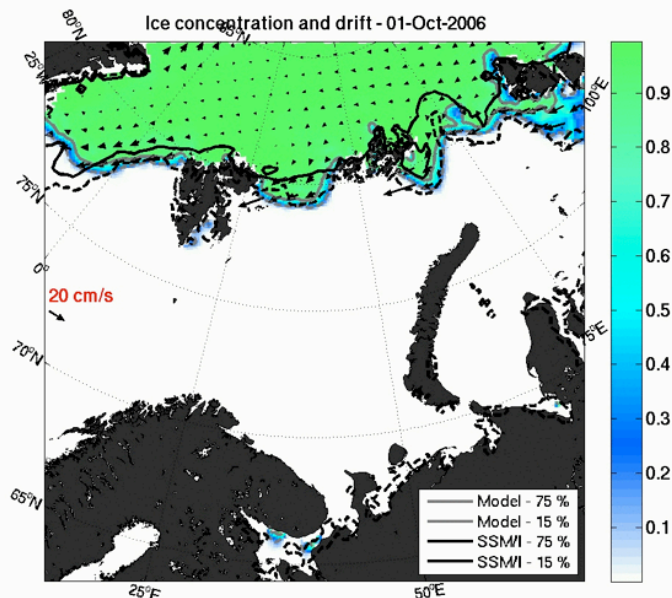


Figure 4.1. Sea ice forecast from the TOPAZ system. The color scale is model ice concentration, contour lines are the 15% ice concentration contour from model and observations. The ice drift vectors are shown by arrows.

A problem with the Hibler (1980) model is that it is well suited to the properties of the interior ice pack, whereas it is not that suited to the properties of sea-ice in the marginal ice zone. The interior ice pack generally has large sea-ice floes on the order of kilometers, whereas the marginal ice zone contains ice floes with sizes varying from meters to hundreds of meters. The different properties of the MIZ versus the interior ice pack leads to fundamental changes in how the ice responds to external forces. In the interior ice pack, converging ice floes create so-called pressure-ridges, where the resistance to this converging motion depends mainly on transformation of kinetic energy (ice motion) to potential energy (raising of sea-ice ridges) (Thorndike et al., 1975). In the MIZ, on the other hand, the resistance to the converging motion is mainly due to inelastic collisions between sea-ice floes. Furthermore, the effect of waves is another aspect of the MIZ that needs to be examined when modelling the MIZ.

4.2 Model tools and sea ice rheologies

The model tools which will be used at NERSC consists of the Hybrid COordinate Ocean Model (Bleck, 2002, HYCOM;), coupled with an ice model describing the dynamics and thermodynamics of the sea-ice edge. Currently the NERSC version of HYCOM is coupled with the elastic viscous – plastic (EVP) sea-ice dynamics model (Hunke and Dukowicz, 1997).

The ocean model

The ocean model used is the Hybrid Coordinate Ocean Model (HYCOM v2.1) introduced by Bleck (2002) as an extension of the previous Miami Isopycnal Coordinate Ocean Model (MICOM) by Bleck and Smith (1990). HYCOM is isopycnal⁵ in the open, stratified ocean, but reverts smoothly to fixed vertical coordinates (z-levels or terrain-following coordinates) in unstratified waters. Such a model combines the advantages of the three different types of vertical coordinates. The isopycnic layers allow for high resolution in areas of large density gradients and the fixed coordinates at the top of the water column allow for a good representation of the mixed layer processes. The prescribed vertical mixing is solved using the KPP vertical turbulence closure scheme developed by Large et al. (1994). The advection of momentum uses a combination of Laplacian and biharmonic horizontal friction and the horizontal advection scheme is the second order flux corrected transport (FCT2).

Sea ice dynamics models

The modelling of sea-ice dynamics can be loosely divided into two categories, Lagrangian and Eulerian, although a mix of these two methods is also possible (Rheem et al., 1997). The Eulerian approach is the more traditional approach, where the sea-ice drift velocity is calculated in fixed locations, in a finite element or a finite difference approach. In geophysical applications the latter is the more frequent. Another approach is the Lagrangian approach, where the sea-ice floes are allowed to move freely about, and where the motion depends on the contact between the individual ice floes.

The Eulerian approach

The traditional approach to modelling sea-ice dynamics on geophysical scales is to model it as a two-dimensional fluid (Gray and Morland, 1994). The motion of this fluid u is given by the momentum equation of sea-ice

$$m \left(\frac{\partial u}{\partial t} + u \cdot \nabla u \right) = mfk \times u + A\tau_a + A\tau_o + S + \nabla \cdot \sigma \quad (4.1)$$

⁵ Isopycnal: constant density

where m is the mass of the ice, f is the coriolis parameter, A is the fraction of the ocean surface covered by sea ice, τ_o and τ_a are the stresses from the ocean and atmosphere, S is the effect of the sea-surface tilt, and σ is a matrix which determines the forces due to sea-ice deformation. Of the different components in (4.1), their values and formulation can change markedly in the MIZ. For instance, the specification of the stress from the atmosphere on the ice, τ_a , is known to be different in the MIZ relative to the interior ice pack. It is for instance known to depend on the stability of the atmosphere, which can change markedly as one moves across the MIZ. This is due in part to the heat fluxes from the ocean to the atmosphere, which are very high over open ocean, but which are markedly reduced as one moves across the MIZ towards the more densely packed pack ice. The insulating properties of sea-ice is the main reason for this drop in heat fluxes. Another effect which is of potential importance is the term $u \cdot \nabla u$. Although this term is included in the basic equations of sea-ice motion, it is often neglected in Eulerian sea-ice dynamics models (Hunke and Dukowicz, 1997). Neglecting this term is based on a scale analysis of the forces in the central Arctic, but for high-resolution modelling of the MIZ this term should probably be included as well.

Rheologies

One of the main elements for improved ice modelling is the final term in equation (4.1). This relates deformation of the ice pack (for instance during shear flow or convergence) to the forces which arise due to this deformation. The formulation of this term is well known to be of a different nature in the central ice pack relative to conditions in the MIZ, and we will briefly describe some of the fundamental differences below. In considering the relation between deformation and forces, it is important to consider that sea ice rheologies are based on “geophysical” scales (> 1000m) and not on scales that we are commonly used to, which is on the order of meters. On scales of meters, there are no fundamental differences between the rheological properties of sea-ice whether it is in the central Arctic or in the MIZ. In fact, on these scales the sea-ice behaves as an elastic fluid under short-term low loading, and a viscous fluid under long-term loading Mellor (1986). For higher loads on the sea-ice it will eventually crack and form smaller sea-ice floes. When we talk of the sea-ice rheology in the following, we will refer to the geophysical scales, where other effects than the material properties contribute as well. On larger scales, the rheological properties of sea-ice depend on stress-generating mechanisms of a set of sea-ice floes, which again depends on the composition of the ice cover. A loosely packed field of small sea-ice floes will for instance have different dominating stress-generating mechanisms compared to a densely packed field of very large sea-ice floes. The stress-generating mechanisms in a sea-ice field mainly arise due to five physical mechanisms defined by Lepparanta (2005) and listed in Table 4.1.

Table 4.1 Stress generating mechanisms for sea ice

1.	Floe collisions
2.	Floe break-up
3.	Shear friction between floes
4.	Friction between ice blocks in pressure formation
5.	Potential energy production in pressure formation

At any time in different parts of the sea-ice pack, these mechanisms will contribute to how stresses are transferred within the ice, and how the matrix σ should be formulated.

As already mentioned, the forces acting between sea-ice floes have different properties in the MIZ relative to the interior ice pack. Whereas these forces in the interior ice pack relate to the increase of potential energy and loss through friction energy as ridges form, the MIZ is more strongly connected to inelastic collisions between sea-ice floes, and ridging plays a smaller part in the

balance of forces. The change in properties from the central ice pack to the MIZ is illustrated in Figure 4.2. This figure illustrates how the central Arctic ice pack consists of relatively large sea-ice floes, separated by linear features. These features are regions with open water and freshly formed ice, arising due to local divergence in the sea-ice field. In the central Arctic, sea-ice floes are often so large that the large scale-motion is set up by the constant motion (rotation and translation) of individual sea-ice floes with divergence and shear occurring between sea-ice floes (plug flow). The floe arrangement in the Central Arctic should be contrasted to the situation in the MIZ, Fig. 4.2. In the MIZ, the sea-ice floes are much smaller in size, an effect which is due to the melting of sea-ice floes as they get closer to the open ocean, and the effect of open ocean waves as they penetrate into the sea-ice cover. The width of the MIZ depends on local conditions, but in the region marked in fig. 4.2, the MIZ width appears to be significant. Note that Fig.4.2 is only indicative of the MIZ. Floes in the MIZ are often of a size much smaller than can be seen from space.



Figure 4.2. Illustration of a wintertime situation near Svalbard in 2003. The properties of the central ice pack and the MIZ are illustrated, with the MIZ consisting of a more broken-up ice field and a more granular appearance. (Image courtesy of NASA)

Plastic Rheologies

The specification of the sea-ice stresses are related to the deformation rate of the sea-ice pack. The relationship between stresses and the deformation is often referred to as the constitutive relationship of the ice pack, they describe the forces as a function the strain rate, $\dot{\epsilon}$ of the material

$$\sigma = F(\varepsilon) \quad (4.2)$$

where σ are the stresses; ε and σ are both tensors. The main difference between the rheologies in the central Arctic and in the MIZ lies in the specification of plasticity of the materials. The ice in the central Arctic has been modeled with the use plastic rheology variants (Hibler III, 1979; Hunke and Dukowicz, 1997). In the plastic rheologies, the stresses in the ice have an upper limit. In a strictly plastic rheology the sea-ice will not deform until the stresses reaches maximum value. Above this limit, deformation occurs, but the stresses do not increase any further. This means that an increase in the deformation of the ice material does not necessarily lead to an increase in the forces opposing it. This is contradictory to many common fluids, such as water, where the resistance to deformation always increases in response to the deformation. The plastic rheologies puts an emphasis on items 5 and 4 in the list in Table 4.1. Today, variants of the plastic rheologies are the main model in use by the climate modelling community. They are also in frequent use by operational forecasting models such as the TOPAZ model system Bertino et al. (2005).

Based on experiences with medium and high-resolution models, the TOPAZ model and its nested model components appear to give good results in the Arctic. However, one of the main problems appear to be the modelling of the MIZ, where the transition from 0% ice coverage to 100% ice coverage is often too abrupt, whereas observations tend to show a smoother transition from open water to a fully packed sea-ice cover. This is illustrated in Figure 4.3, which shows a comparison of ice concentration derived from microwave satellite sensors (SSM/I) with a 4-km resolution sea-ice model of the Barents Sea. The figure illustrates how the satellite data has a somewhat smoother transition from a fully packed ice cover to open water. The figure also illustrates how this is not necessarily a resolution-dependent feature in the ice model. Although there are several effects that may contribute to the abrupt transition in our model system, we believe that the choice of rheology is an important issue here.

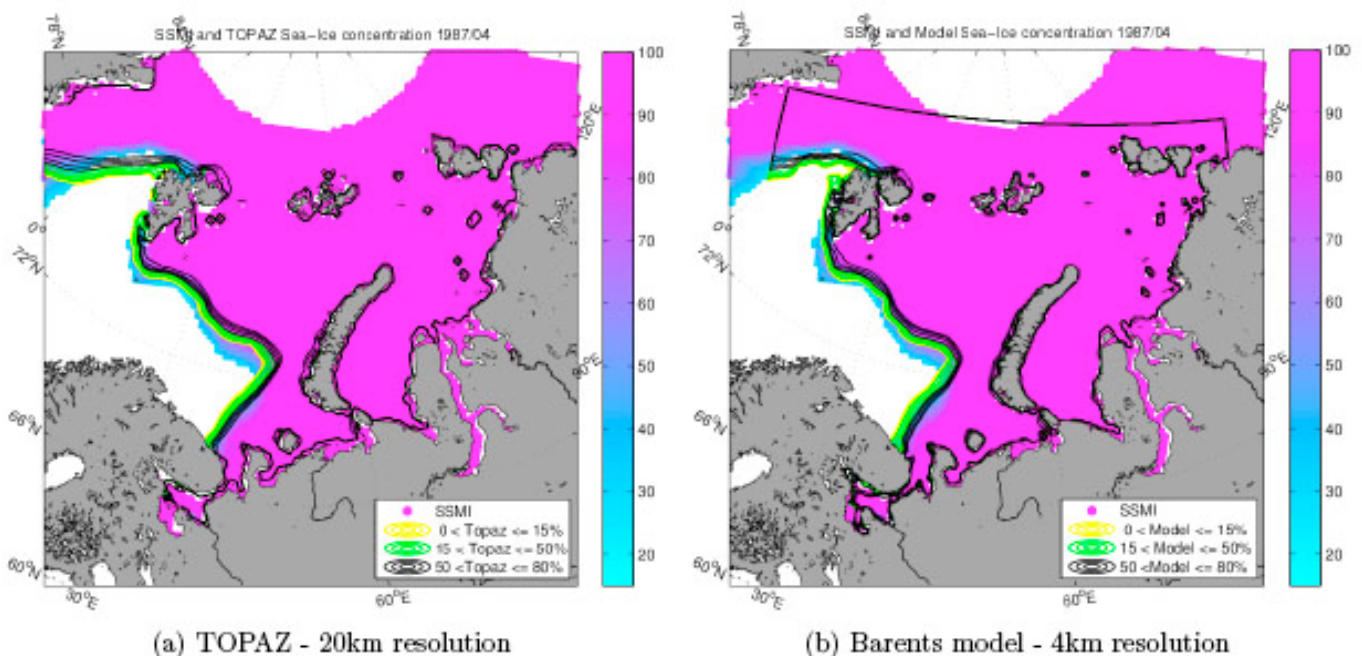


Figure 4.3. Comparison between ice concentration in the Barents Sea from observations (color scale) and model (contour lines). (a) shows the comparison with a model which has 20 km resolution, whereas (b) is a comparison with a model of 4 km resolution.

Collision-induced rheologies

As mentioned, the plastic rheologies have led to good results when modelling the central ice pack. However, a rheology that is suited for the central Arctic may not be that well suited for the MIZ. This is related to the changes in floe arrangement in the MIZ, where the floes are generally smaller, and the sea-ice field may consist of a chaotic field of floes of varying sizes, interspersed with severely broken-up ice and slush ice. This has led to the suggestion that it is not mainly the deformation and creation of ice ridges which restrict the motion in the MIZ, but rather the (inelastic) collisions between ice floes. In other words, item 1 in Table 4.1 is the main stress-inducing mechanism for the flow in the MIZ. As a result, the formulation of collision-induced rheologies have been developed. The idea was first proposed in the 1970s by Ovsienko (1976), and a theory was developed in the 1980s by Shen et al. (1986). It is assumed that the MIZ consists of a large number of identical sea-ice floes of thickness h and diameter d . In a shear flow of the sea-ice, random fluctuations in the velocity field give rise to floe collisions, the frequency of which depends on the ice compactness and the fluctuation velocities. Integrated over a large area, these random fluctuations give rise to a rheology description, connecting the large-scale deformation with the stresses. One of the main elements of this rheology description is that the stresses in the MIZ rheology are much lower than in the plastic rheology, for sea-ice fields with identical ice thickness and compactness. Due to this the MIZ can diffuse and compact much quicker when using this rheology, as compared to the plastic rheologies.

Despite the fact that this rheology gives good results in the MIZ (Shen et al., 1986), it has been rarely used in sea-ice modelling. As mentioned, the plastic rheologies are the most frequently used, even in applications involving the MIZ. The main reason for this is probably that many applications focus on the interior of the ice pack, where the plastic rheologies give reasonably good results. There have been some attempts at merging the plastic and collision-induced rheologies. In a paper by Lu et al. (1989), this was done, and the results did show interesting results near the ice edge. However, there does not appear to have been any further development of this model. For fine-scale applications in the Barents Sea, the position of the sea-ice edge becomes an important parameter to predict. In order to do that, a rheology model which is best suited for the MIZ should be employed.

Lagrangian approach

Lagrangian approaches to sea-ice modelling differ considerably to the Eulerian models. Instead of needing to specify a ice rheology as in the Eulerian approach, the Lagrangian approach models the sea-ice field as a collection of ice elements, where the contact forces between these elements are modeled directly. This approach gives interesting results in the central Arctic, where the size of ice floes are quite large. In these regions, it is therefore possible to model the movement of individual sea-ice floes. Several implementations of this type exists Hopkins (1996); Løset (1993).

The Lagrangian element method reveals spatial structures which are similar to those found in the central ice pack. An example from the formulation of Hopkins (1996) is shown in Figure 4.4. The different gray-shaded areas denote individual floe elements. Comparing Figure 4.2 in the central Arctic ice pack with Figure 4.4 reveal features which are quantitatively similar in the Lagrangian model. One of the problems with the Lagrangian approach is that as the elements break up the total number of elements increase, this of course increases the numerical work needed to advance the model solution. The problem can therefore quickly become unmanageable. Fortunately, methods have been developed to re-initialize the elements from time to time, so that the total number of elements does not increase too much.

It is, however, unclear how well the Lagrangian approach would work for the MIZ, since it becomes impractical to directly model floe-sized elements in this environment due to the smaller size of floes

in the MIZ. Methods which mix Eulerian and Lagrangian approaches do exist, and may be an alternative (Rheem et al., 1997). The so-called Particle-In-Cell (PIC) method so far appears to be among the more promising of these methods Huang and Savage (1998).

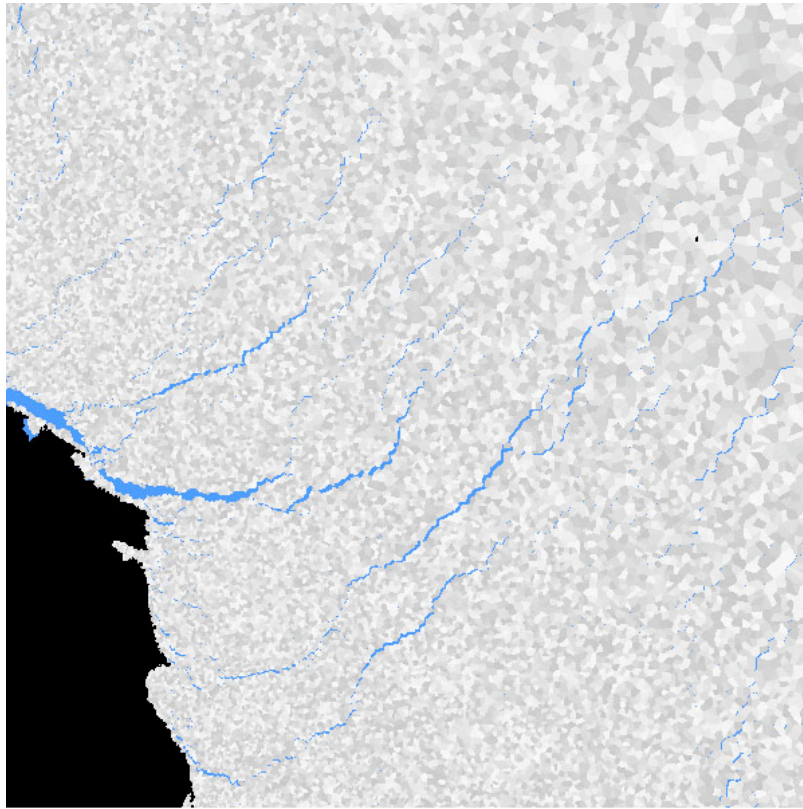


Figure 4.4. A field of individual particles from a Lagrangian model of the ice pack. The formation of leads (light blue areas) during large-scale deformation of the ice field is apparent. The black area is land. Note that the floe size increases with distance from the coast (Courtesy Mark Hopkins, CRREL).

4.3 Ocean-ice interaction

The ocean plays an important part in the ice dynamics in the MIZ, and deserves to be mentioned here as well. The model used at NERSC, HYCOM, was briefly described in the previous section. Although ocean currents are important for the entire sea-ice cover, especially on long time scales, it becomes especially important in the MIZ because of the large mesoscale activities close to the ice edge. In 1983 and 1984, a large field experiment, the Marginal Ice Zone Experiments (MIZEX), was performed in the Fram Strait. The MIZEX experiment showed how the mesoscale activity is especially pronounced in the Fram Strait, with several mechanisms contributing to the complicated ocean currents. It is believed that barotropic instability, baroclinic instability and topographic control all contribute to the generation of ocean eddies in the Fram Strait MIZ. The scales of the ocean eddies vary depending on local oceanographic conditions, but in Johannessen et al. (1987) the typical scale varies from 5 to 80 km, depending on the mechanisms generating them. The eddies can have a significant effect on the sea-ice edge by embedding sea-ice into the eddy, or the eddies can transport warm surface waters under the sea-ice, thereby enhancing melt of sea-ice.

In addition to eddies which are generated in open ocean conditions, there are also an important mechanism for eddies which is directly connected to the interplay between the ice cover and the

ocean. This is related to the surface winds, and differences in the way these exert a drag force on the ice and ocean surface. In general, the atmospheric drag force is larger over ice than over open water, due to the roughness of the ice cover. This leads to upwelling and downwelling events near the ice edge (Røed and O'Brien, 1983). The mechanism leading to these upwelling or downwelling events can be explained as follows. A wind blowing along the sea ice edge, will cause a differential transport of water masses, leading to these events, an effect also known as Ekman pumping. An along-ice edge wind with the open ocean to its left hand side will cause a horizontal transport of water masses toward the ice pack. Since the wind drag is larger on the ice, the water masses under the ice will be transported faster than the water masses in open water. The net result of this is a local divergence in the horizontal transport of the surface water masses, a local divergence which is then accompanied by a upward transport of water masses. The opposite situation (horizontal convergence and downwelling) occurs when the wind is blowing along the ice edge with the open ocean to its right.

This Ekman-induced lifting and lowering of density surfaces in the ocean leads to a change in the horizontal pressure gradients of the ocean, which again results in ocean currents developing. Depending on the situation these ocean currents can become instable, and eddies may emerge near the sea-ice edge. This process has been studied in numerical model by Røed and O'Brien (1983) and Hakkinen (1986). The latter found that downwelling situations led to a more instable situation with formation of mesoscale eddies which further affect the ocean field.

Ocean waves

One of the main features which separates the MIZ from the central ice pack is the size of the sea-ice floes. The ice floes in the MIZ are generally smaller and more circular than those in the central ice pack, a result of floe collisions and break-up. One of the main reasons for this is the proximity of the MIZ to the open ocean, and the effect of ocean waves (Wadhams, 1986; Gascard et al., 1988).

As waves approach the sea-ice edge, its presence can modify the ocean waves in several ways. It can reflect the ocean waves, which means less wave energy is transported into the marginal ice zone. The ocean waves can be refracted, which means the wave direction changes as it meets the MIZ. Also, as waves penetrate the MIZ, the ice floes strongly affect how the waves are transported further into the ice pack. The properties of the MIZ also leads to attenuation of ocean waves and to the spreading of the wave directional spectra.

During the 1984 MIZEX program, the study of ocean waves penetrating into the MIZ was performed (Wadhams et al., 1986). The study showed how the ice edge, and the marginal ice zone significantly affects the spread, damping and directional spectra of waves. The directional spectra of short-wavelength waves were seen to change as the waves penetrated the ice edge into the MIZ. Within the space of a few kilometers, these short waves had lost most of their initially narrow direction spectrum, and the wave direction spectrum was more or less isotropic. For longer waves (swells), the situation was different, and these waves were seen to propagate farther into the MIZ without losing their directional "preference". Differences between short and long wavelengths were also seen in the attenuation of waves, where short waves were attenuated more quickly than long waves. A simple equation which illustrates the wave energy and its dependency on distance from the ice edge is given by

$$E(x) = E(0) \exp(-\lambda x), \quad (4.3)$$

where λ increases with wave frequency (Wadhams, 1978). This illustrates how the wave energy at the ice edge, $E(x)$, is reduced exponentially as one progresses into the MIZ (increasing x). A portion of the energy deficit at penetration distance x will be due to energy loss as waves are

breaking up the sea-ice field, and due to inelastic collisions between neighboring ice floes. The ocean waves certainly contribute to the break-up of the ice field in the MIZ, and for realistic modelling and forecasting applications, the effect of ocean waves are probably necessary to provide accurate ocean forecasts.

4.4 Conclusion of sea ice modelling in the MIZ

The Marginal Ice Zone is a dynamically active region of the Arctic. The effect of open ocean waves and swells, open ocean eddies and the effect of coupled ice-ocean mechanisms all contribute to making the modelling of the MIZ and the sea-ice edge a challenge. As an effect of the open ocean proximity, the properties of the sea-ice change fundamentally in the MIZ, relative to the pack ice. Whereas pack ice usually has large sea-ice floes and much of the work done by the ice cover comes through the formation of pressure ridges, the MIZ is less constrained by these mechanisms. In the MIZ, work is done mainly through inelastic collisions between smaller sea-ice floes. This, in effect, leads to a MIZ which is much less restrained by the stresses generated in shear deformation, relative to what we observe in the central ice pack. The traditional sea-ice rheology of Hibler III (1979), was formulated to model pack ice in the central Arctic, and not meant to model sea-ice in the MIZ. Still, the Hibler model is presently the most frequently encountered sea-ice model formulation in use, both when modelling sea-ice on regional and global scales, and in the MIZ. In our opinion, the consequences of this "mis-use" of the Hibler-model has not been sufficiently explored, and needs to be assessed, especially for regional scale models, and for forecasting applications. Moreover, due to the large heat fluxes which occur over open-water in the Arctic, the MIZ may be important for the global heat budget as well, and by extension, for global warming scenarios. To our knowledge, no assessment has been done on this effect.

5. Ocean processes

5.1 Water masses and currents

The Arctic Ocean with the adjacent shelf seas are influenced by relatively warm and saline water from the Atlantic Ocean, advecting through the Fram Strait and the Barents Sea into the Arctic Ocean. Polar water masses of relatively low salinity and low temperature are supplied through Bering Strait from the Pacific. River run-off from the continents adds a significant amount of fresh water. The water of Atlantic origin circulates within the Arctic Ocean on different paths whereby it undergoes intensive modifications. The waters exiting the Arctic Ocean supply the source waters for the formation of North Atlantic Deep Water, which plays a significant role in the global thermohaline overturning circulation. The Fram Strait represents the only deep-water connection between the Arctic Ocean and the Nordic Seas. This strait is characterized by a northward flow of deep waters from the Greenland and the Norwegian Sea entering the Arctic Ocean, and deep waters from the Arctic basins flowing southward to the Nordic Seas. The source waters for the North Atlantic Deep Water formation leave the Nordic Seas as overflows between Greenland and Scotland.

The oceanic circulation in the Arctic Ocean is driven by a combination of wind and thermohaline forcing. The air pressure distribution is basically determined by a high-pressure system over the Beaufort Sea and low pressure over the Nordic Seas leading to an anticyclonic circulation pattern. However, it is strongly modified by the topographical structure of the basins which gives rise to internal circulation cells (Alekseev et al., 2004). The Arctic Ocean and adjacent seas are covered by a seasonally varying ice cover, which moves by wind forcing and ocean currents. The anticyclonic circulation in the Beaufort Gyre, often called the Beaufort High, and a less well-established cyclonic counterpart over the European Arctic feed into the Transpolar Drift. The latter provides the major export of sea ice through Fram Strait into the Nordic Seas where most of it

melts and affects the stability of the water column. Due to the large-scale sea level inclination there is a net flow from the Pacific Ocean into the Atlantic.

A major shift in the atmospheric pressure system and the ice drift pattern has been observed during the 1980s and 1990s, where 1) the Beaufort High has decreased and shifted towards east; 2) the Transpolar Drift shifted axis counterclockwise producing more cyclonic motion in the 1990s, 3) the ice extent and thickness have decreased. These changes are associated with two idealized dominant wind-driven ocean circulation regimes: anticyclonic and cyclonic. Climatological studies (e.g., Proshutinsky and Johnson, 1997) provide a foundation for understanding the significance of these ocean surface conditions. These studies indicate that the Arctic ocean surface layer motion is consistent with the Arctic atmosphere surface layer motion, alternating between cyclonic and anticyclonic circulation regimes. Each regime persists from 4 to 8 years, resulting in a period of 8–16 years. The cyclonic pattern dominated during 1989–1996. Since 1997 the dominant regime has fluctuated, with an anticyclonic pattern being slightly more prevalent (Fig. 5.1).

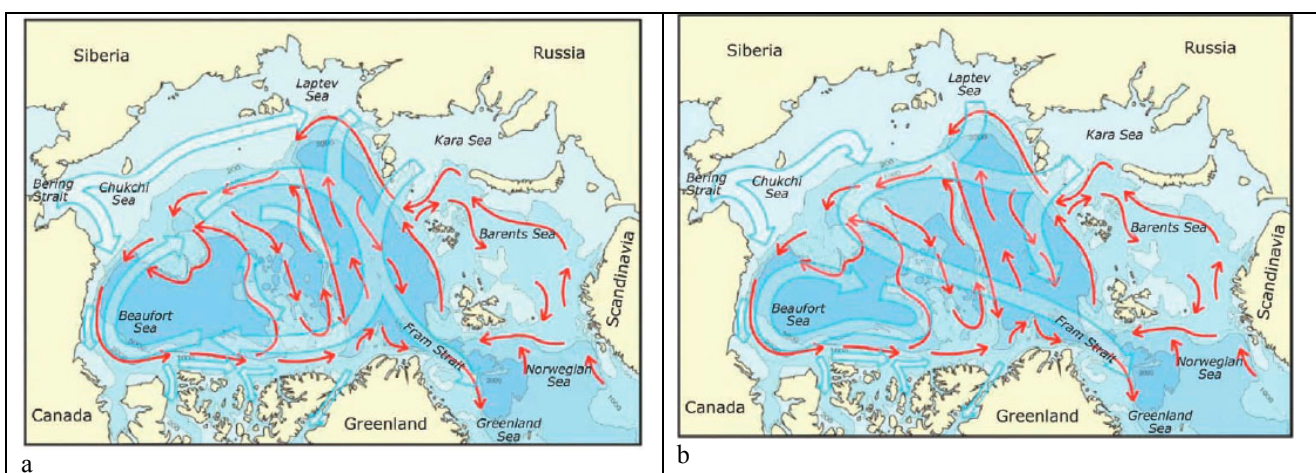


Figure 5.1 Idealized patterns of the dominant circulation regimes of the Arctic Ocean. Two circulation regimes of surface waters (anticyclonic-a; cyclonic-b) are shown in wide blue arrows. In the cyclonic regime the clockwise circulation pattern in the Beaufort Sea region (the Beaufort Gyre) weakens, and the flow across the basin, from the Siberian and Russian coasts to Fram Strait (the Transpolar Drift), shifts poleward. The cyclonic pattern dominated during 1989–1996; the anticyclonic pattern has prevailed since 1997. The Atlantic water circulates cyclonically (red arrows) at approximately 200–800 m deep, independent of the circulation regime of the surface layer. (Adapted from Proshutinsky et al., 2005).

The most recent studies by Shimada *et al.* (2006) and Maslowski *et al.* (2006) indicate that the significant reduction of sea ice in the Canadian Basin observed in 2002–2005 may be attributable in part to an increase of heat flux from the Pacific water layer to the bottom of the sea ice, resulting in sea ice melt. Warming of the Pacific water is associated with an increase of heat flux via Bering Strait. In this region, preliminary observations from a mooring site, established and maintained since 1990, suggest that annual mean water temperatures have been about 1°C warmer since 2002, compared to 1990–2001 (Woodgate *et al.*, 2006). Since 2001, there has also been an increase in the annual mean water transport. Changes in the Pacific water circulation may also influence heat release from the Pacific water to the upper ocean layers. The Atlantic water circulates in the Arctic Ocean at approximately 200–800 m deep. This water penetrates to the Arctic via Fram Strait and St. Anna Trough (Barents Sea). Under extensive surface cooling, it sinks to intermediate depths and forms the warm Atlantic Layer, with water temperatures greater than

0°C. This layer is covered by low-density surface waters and is thus prevented from undergoing heat exchange with the atmosphere. Studies by Maslowski (2000) suggest that the amount of Atlantic Water in the Arctic Basin is linked to the Arctic Oscillation, as shown in Fig. 5.2. The most widely accepted circulation scheme of Atlantic water (Rudels *et al.*, 1994) postulates that it circulates counterclockwise, forming several loops in the Arctic basins.

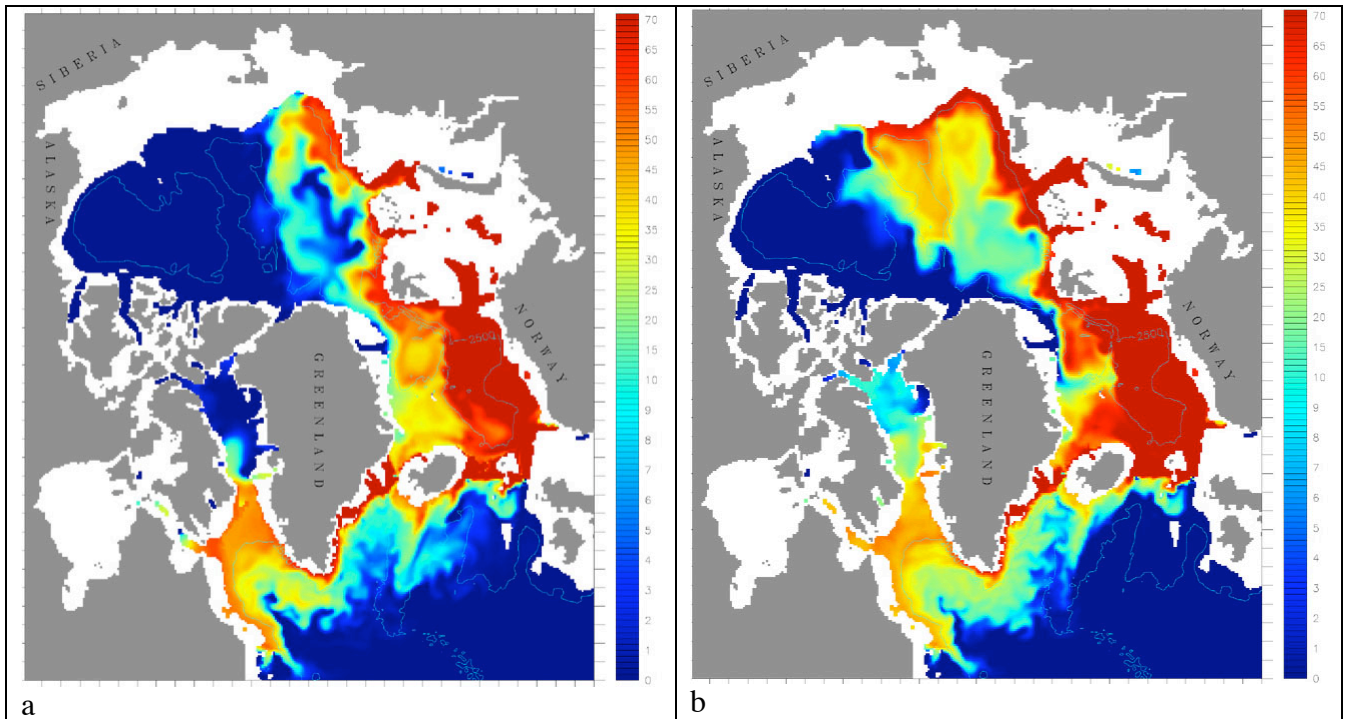


Figure 5.2. Concentration of Atlantic Water tracer (%) averaged over depth of 180-560 m for repeated forcing in 1973 (a) and 1993 (b). 1973 had a low AO while 1993 had a high AO. (Courtesy: W. Maslowski).

5.2 Sea level

From 1954 to 1989 there has been a positive sea level trend along the Arctic coastlines as shown in Fig. 5.3 and 5.4. The rate of sea level rise was estimated as 0.185 cm/year (Proshutinsky *et al.*, 2004). Adding 1990–2004 data increases the estimated rate to 0.191 cm/year. The sea level time series correlates relatively well with the AO index (the correlation coefficient is 0.83). Consistent with the influences of AO-driven processes, the sea level dropped significantly after 1990 and increased after the circulation regime changed from cyclonic to anticyclonic in 1997. In contrast, from 2000 to 2004 the sea level rise rate has increased, in spite of a steady decrease in the AO index. At this point, because of the large interannual variability, it is difficult to evaluate the significance of this change.

The conclusions of the study of Arctic sea level change by (Proshutinsky *et al.*, 2004) are the following:

1. Relative sea level monthly data from the 71 tide gauges in the Barents, Kara, Laptev, East Siberian, and Chukchi Seas have been analyzed in order to estimate the rate of sea level change and major factors responsible for this process in the Arctic Ocean.
2. The Arctic Ocean sea level time series have well pronounced decadal variability which

corresponds to the variability of the North Atlantic Oscillation index. Because of the strength of this variability and the relatively short sea level time series, our assessments of sea level trends remain somewhat uncertain. In spite of this limitation, we have employed statistical methods together with numerical models and estimated the contributions of various factors to the observed sea level change. By subtracting the influence of these factors from the observed regional rate of sea level rise we have been able to estimate the rate of sea level rise due to increase of the global ocean sea mass that is presumably due to the melting of land ice.

3. During the period 1954–1989 the average rate of relative sea level rise over the seas of the Russian Arctic has been 0.185 cm yr^{-1} . This is within range of the rate that has previously been inferred using tide gauge data for the global ocean as a whole [IPCC, 2001]. It is also essentially the same as the rate for the Global Ocean recently inferred by Peltier [2002].
4. In the Arctic, the contribution to the observed rate of sea level rise from the steric effect is 0.064 cm yr^{-1} . This is smaller than the rate of ocean thermal expansion estimated for the global ocean by IPCC [2001]. In the Arctic Ocean, changes in salinity are more important for sea level variability than changes in temperature, and the combination of freshening of the Arctic seas with warming and salinization of the Atlantic layer therefore leads to the rise of sea level along coastlines and the fall of sea level in the central parts of the Arctic Basin.

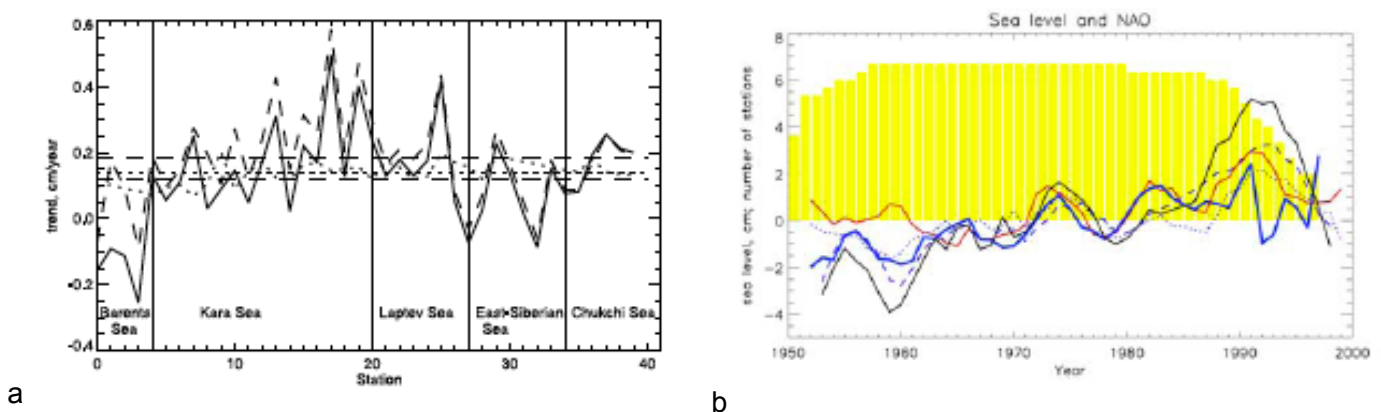


Figure 5.3 (a) Sea level trends for 1954–1989 in different regions of the Arctic. Solid line shows trends from observations. Dashed line shows observed trends corrected for GIA (Glacial Isostatic Adjustment), and dotted line depicts variability of trends associated with the inverted barometer effect, river runoff, and steric effects. Thin horizontal dashed and dotted lines show mean trends for all seas. **(b)** Mean sea level time series for different seas. Dotted lines denote number of coastal stations used for averaging. Mean time series for all seas (thick blue line, 5-year running mean). Mean number of stations used in each sea is shown by yellow bars. Red thick line shows 5-year running mean North Atlantic Oscillation index. Thin dashed line shows sea level variability from 3-D model, and dotted blue line shows variability of sea level due to inverted barometer effect. Solid black line shows sea level from 3-D model corrected for the inverted barometer effect. (Proshutinsky et al., 2004).

5. The contribution of the inverse barometer effect to the Arctic Ocean sea level rise is 0.056 cm yr^{-1} . This is the highest rate of sea level rise among any of the estimates of this factor presented by IPCC [2001] for various regions.
6. The estimated rate of sea level rise due to the effect of wind is 0.018 cm yr^{-1} , but it varies

significantly from region to region. In the Arctic, this effect is due to the gradual decrease of the sea level atmospheric pressure over the Arctic Ocean and therefore to the more strongly cyclonic atmospheric circulation.

7. The contributions of river runoff, evaporation and precipitation to sea level change in the Arctic Ocean are very small and their cumulative effect is negligible. On the other hand, the P-E estimates over the Arctic Ocean are less accurate than the other investigated factors.
8. The residual term of the sea level rise balance assessment, 0.048 cm yr^{-1} , may be due to the increasing of the Arctic Ocean and global ocean mass associated with melting of ice caps and small glaciers and with adjustments of the Greenland and Antarctica ice sheets to the observed climate change.

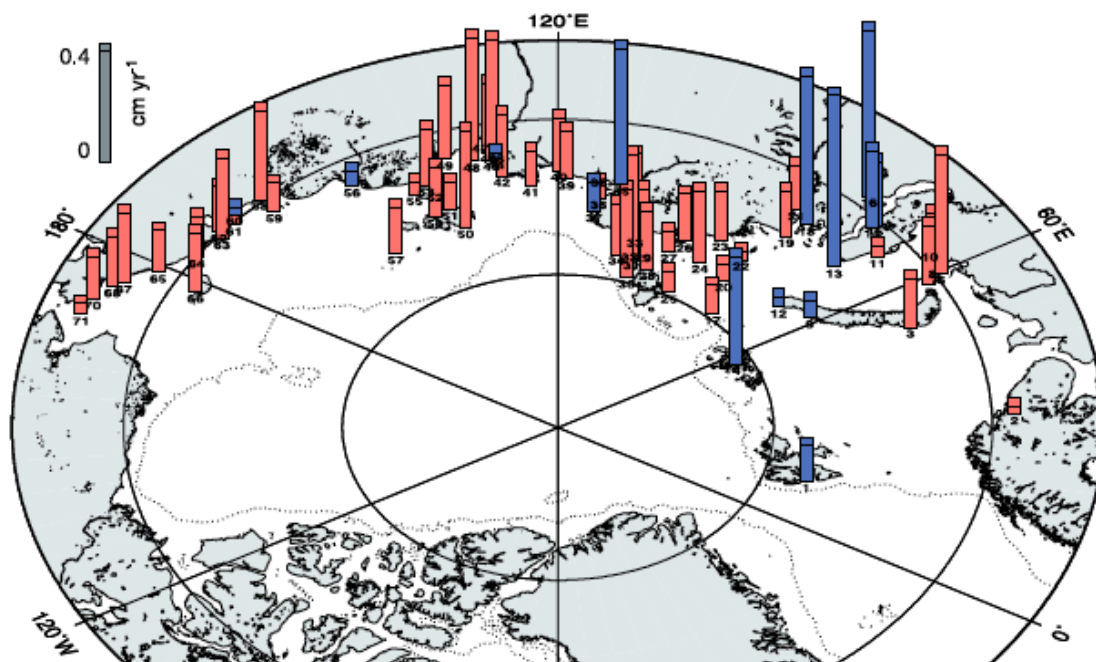


Figure 5.3. Observed sea level trends (cm yr^{-1}) without corrections (red is positive trend, and blue is negative trend). (Proshutinsky et al., 2004).

The long-term sea level change, superimposed on short-term variability due to storm and tides, is of major importance for all offshore and coastal construction planned for several decades into the future.

5.3 Waves in the open ocean

The wave conditions and other met-ocean parameters in open waters of the Arctic Seas have been reviewed by Proshutinsky and Weingarten (1998) in a report provided as part of the INSROP project (<http://www.ims.uaf.edu/insrop-2>). The main results from the wave studies are summarized in this section.

Waves in the Arctic seas are affected by both wind regime and ice conditions. While storm waves are very dangerous for small ships, they can also make the navigation of large ships difficult.

Maximum waves are observed in the arctic seas in autumn. Strong waves and winds can generate a very dangerous phenomenon icing of ships and coastal constructions. Maximum wind waves are observed in the Barents Sea in winter; the wind wave heights in the open part of the Barents Sea may reach 10 - 11 m. These waves are generated by stable westerly or southwesterly winds with velocities of 20 - 25 m/s and duration of 16 - 18 hours. This happens, on average, once or twice every five years. Wave heights of 7 - 8 m are developed by stable (16 - 18 hours) north and northwesterly storms. In the beginning of April, the intensity of waves in the Barents Sea notably decreases. The frequency of waves with heights of 5 m or more is 4 - 5% at this time, increasing to more than 15% in winter. In April--June, waves with heights of 3 - 9 m occur, on average, once in five years. The calmest sea surface is observed in summer when the occurrence of waves with heights of more than 5 m is only 12%. In September, the intensity of waves increases. In November, in the Barents Sea, a wave regime similar to that in winter is established. Maximum wind waves are observed in the open sea (7 - 9 m). In the vicinity of Murmansk, wind waves with heights of 7.5 m have been observed. In winter, well-developed swells are observed in the southern parts of the Barents Sea. The monthly probability of the wind waves with height above 5 meters is shown in Fig. 5.4.

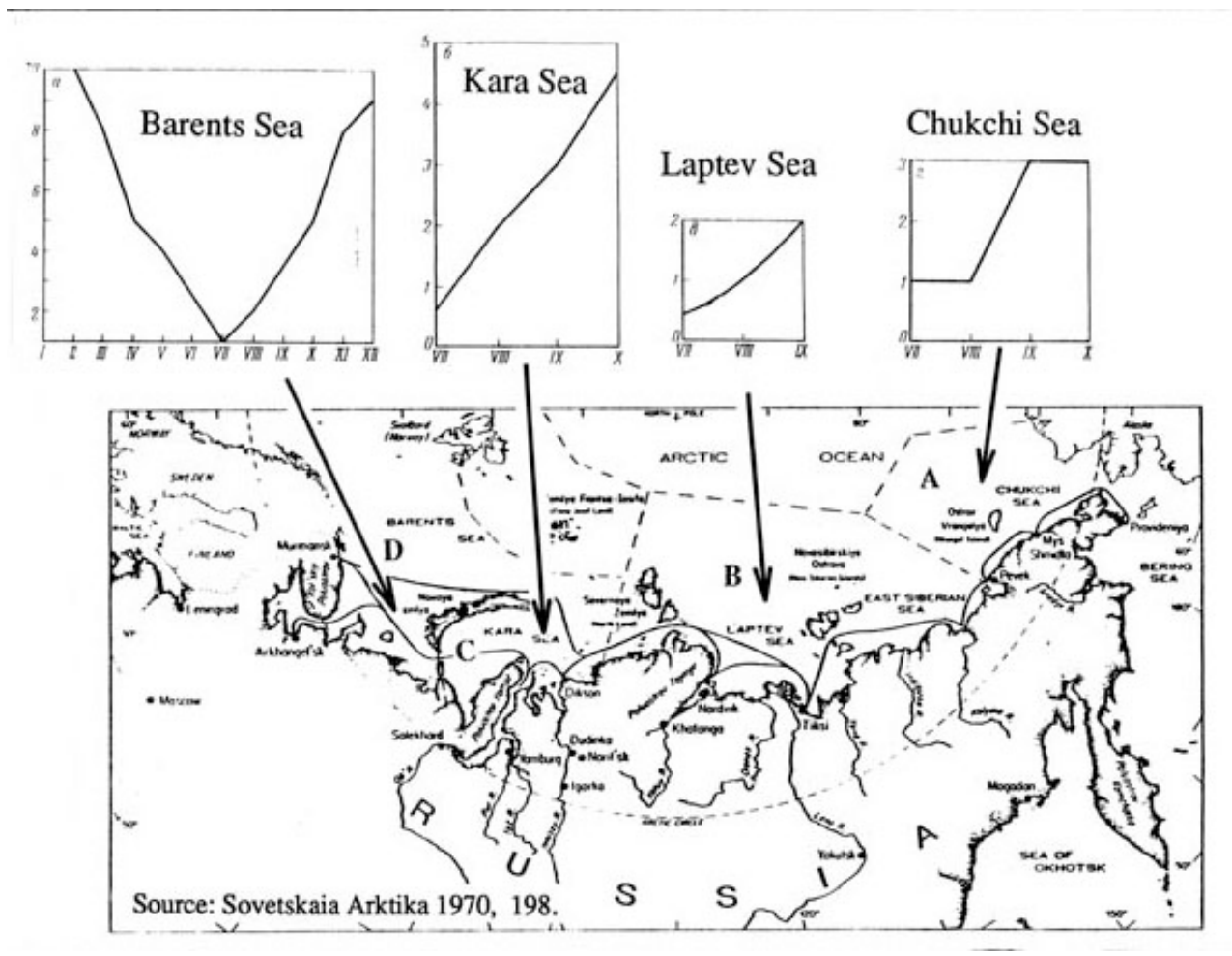


Figure 5.4. Probability of occurrence of wind waves with wave height above 5 meters for the ice-free months in different parts of the Russian Arctic.

In the Kara Sea, in years with small amounts of ice, the fetch lengths range from 100 to 150 km in the beginning of July to 750 - 850 km in September. In July - August, the frequency of waves with

heights of three or more meters is 8 -10%. In September--October it is 12 - 15%. Strong wind waves are observed mostly in the southwestern and northwestern parts of the Kara Sea. In the southwest the sea ice conditions usually do not influence the development of maximum wind waves, and waves can reach 8 m with wavelengths of 150 - 160 m and a period of 10 seconds. Strong wind waves are observed here, with winds coming from all directions. In summer, wind waves are more often generated by northeasterly winds. In the central Kara Sea, where depths and fetch lengths are small, wave development is not significant. Occasionally, more severe waves can penetrate from north and be dangerous for small ships navigating along the Siberian coast. Wind waves with height of 1.5 - 2.5 m occur most frequently in the Kara Sea.

In the Laptev Sea, wind waves with a height up to 1.5 m have a maximum probability of occurrence. Most of the wind waves are developed in the vicinity of the shores and in the central Laptev Sea. In July - August, easterly winds generate maximum wave heights, reaching up to 5 m. In the southeastern Laptev Sea, the maximum height is not above 4 m. In autumn, wind wave heights can reach up to 6 m. Because of the shallow depths and large areas with ice cover, wind waves are relatively modest in the East Siberian Sea. From July to September, the ice edge moves northward and the frequency of strong waves increases, reaching its maximum in September. In August a relatively large area of ice-free water can occur, allowing generation of waves with heights up to 4 m by northwesterly winds. Easterly winds generate waves with heights of less than 2.5 m. In September, when the western part of the East Siberian Sea is mainly ice free the maximum wave height can reach 5 m.

In the Chukchi Sea weak wind waves are most common in July and August. High-pressure conditions and a large area of ice-covered sea inhibit the formation of significant waves. In September and October, wind waves can reach 7 m, while at the end of October the wave heights decrease due to growing ice cover. In the southern part of the Chukchi Sea, the ice cover appears later, and strong wind waves may be generated even in November. In the southeastern part of the Chukchi Sea, waves up to 4.5 m in height can be observed by winds from all directions. With north and northwesterly winds (velocity of about 20 m/s) wave heights can reach 6.5 m in the Bering Strait. Along the coastal shipping route of the Chukchi Sea wave height may reach 6 m during northerly winds.

5.4 Wave in sea ice

When waves propagate into an ice cover, attenuation of the wave amplitude and alteration of the wave dispersion properties occurs. As a wave penetrates into a uniform, large ice sheet, the wave energy is transmitted and shared between the ocean and ice, resulting in what is known as a flexural-gravity wave. For long period waves or for thin ice, waves have lengths, and phase and group velocities similar to those of open water. As the ice thickens for a given wave period, the wavelength, phase, and group velocities will increase over those for the open water case. These changes increase with decreasing wave period. Similarly, wave amplitude decreases with increasing ice thickness and decreasing wave periods, with very long waves retaining amplitudes in ice similar to those of open water. The observation of refraction and attenuation of gravity waves propagation into the ice has been studied in the Arctic by use of SAR (e.g. Shuchman et al., 1994).

Long ocean waves with wavelengths of 150-300 m, generated by storms, travel long distances faster and with less attenuation than the shorter waves. These long waves penetrate across the Marginal Ice Zones in the Barents Sea and Greenland Sea and far into the ice-covered Arctic Basin through openings such as the Fram Strait. The waves propagate as flexural-gravity waves at the interface between the floating sea ice and the underlying water column. Irregularities, such as icebergs, ridges, polynyas and leads, in the ice cover causes scattering of energy favoring the transmission of the long period waves (compared to floe size and dimension of irregularities) compared to the short period waves. Accordingly, the ice cover acts as a low pass filter, removing

the shortest periods near the ice edge and gradually attenuating longer waves as they travel into the ice pack with increasing floe size. Short gravity waves with periods less than 7s, are attenuated within a few hundred meters inside the ice edge while long waves, defined as swell, can propagate several 100 km into the ice pack impacting floe size distributions and the extent of the MIZ.

Studies in the Greenland Sea shows that the attenuation is exponential, with attenuation rate which increase as the square of frequency (e.g. Wadhams, 1986; Wadhams et al., 1988). During passage of intense cyclones strong waves events (more than 1 m in amplitude) have been observed several hundreds of kilometres away from the ice edge in the Sea of Okhotsk (Marko, 2003). Intense wave events have also been observed in more than 500 km into the Antarctic MIZ. Theoretical explanations have been suggested, but not verified. Another important and unknown characteristic of the wave propagation is the group velocity within the sea ice, and the changes of group velocity in ice-covered regions as compared to open water and regions of different ice thicknesses.

Previous work has demonstrated the sensitivity to ice thickness expressed through the selected constitutive laws and their resulting dispersion relations. Therefore, during the last 10 year these has been a significant interest of solving the inverse problem (e.g. Nagurny, 1994, Sagen, 1998; Sandven et al, 2006). This is also a topic within the ongoing IPY project DAMOCLES where several wave buoys will be deployed in the interior Arctic to investigate the validity of the inversion algorithm presented by Nagurny et al, 1994. Nagurny's inversion is based on a very simple wave model based on a continuous visco-elastic thin plate approximation. The wave model is not valid in the MIZ, during summer time in the Arctic, and presumable to simple also during winter time. It is therefore imperative to develop inversions using the more recent and advanced models (e.g. Williams and Squire, 2004, 2007)

The understanding of propagation of long waves within the MIZ and the interior Arctic is of significant relevance both for development and testing of realistic wave models for the MIZ, and for design and planning of resource extraction and navigation activities in such region. The direct impact of wave imposed motion of the sea ice on off-shore installations will have implications on the design of such. Changing wave conditions will change the sea ice conditions significantly and therefore also the operationally in an area. Another effect is that the wave interaction with sea ice produce a lot of acoustic noise which again will impact the underwater acoustic conditions in a broad banded frequency domain. This again will influence the design and performance of acoustic communication systems.

5.4.1 Swell observation techniques

Swell interaction with more or less broken up sea ice is easily observed from the deck of a ship positioned within the MIZ. During periods with moderate to significant swell the ice field can be observed to move up and down making a tremendous sound from the slush ice between the larger ice floes. Visual observations like this are made relatively near the ice edge. Further into the ice pack with larger ice floes the wave amplitude is reduced towards a few millimetres so that we cannot visually observe it. However, the wave action can result in squeaking sounds, indicating internal ice stress/stress release within the floe, or more dramatic events such as break-up of the ice floe.

Hydrophones

Hydrophones deployed in seawater underneath the ice cover are used to record acoustical data generated by swell propagation into the ice pack. Swell propagation has by several investigators been shown to be the major acoustic noise generator in the MIZ (e.g. Johannessen et al, 2003). Swell interaction with the ice cover is the major source of ambient noise in the MIZ. Recent

investigations in the MIZ have shown that swell and ice concentration correlates well with low frequency noise (25-50 Hz) and mid frequency noise (100-1000 Hz) (Sagen, 1998).

Tilt-meters and accelerometers.

Further into the ice pack or during calm wave conditions much less acoustic energy is produced due to swell, and correspondingly it is difficult to pick up the swell under these conditions using hydrophones. Under these conditions it is better to use more sensitive instruments, such as tilt-meters and accelerometer, to measure tiny vibrations in the ice plate. The tilt-meter measures the tilt of the ice floe due to the motion of the swell underneath the ice, while an accelerometer measure the acceleration.

High resolution SAR images

High resolution satellite SAR images of the MIZ can provide information about wavelength and wave propagation direction as shown in Fig. 5.5.

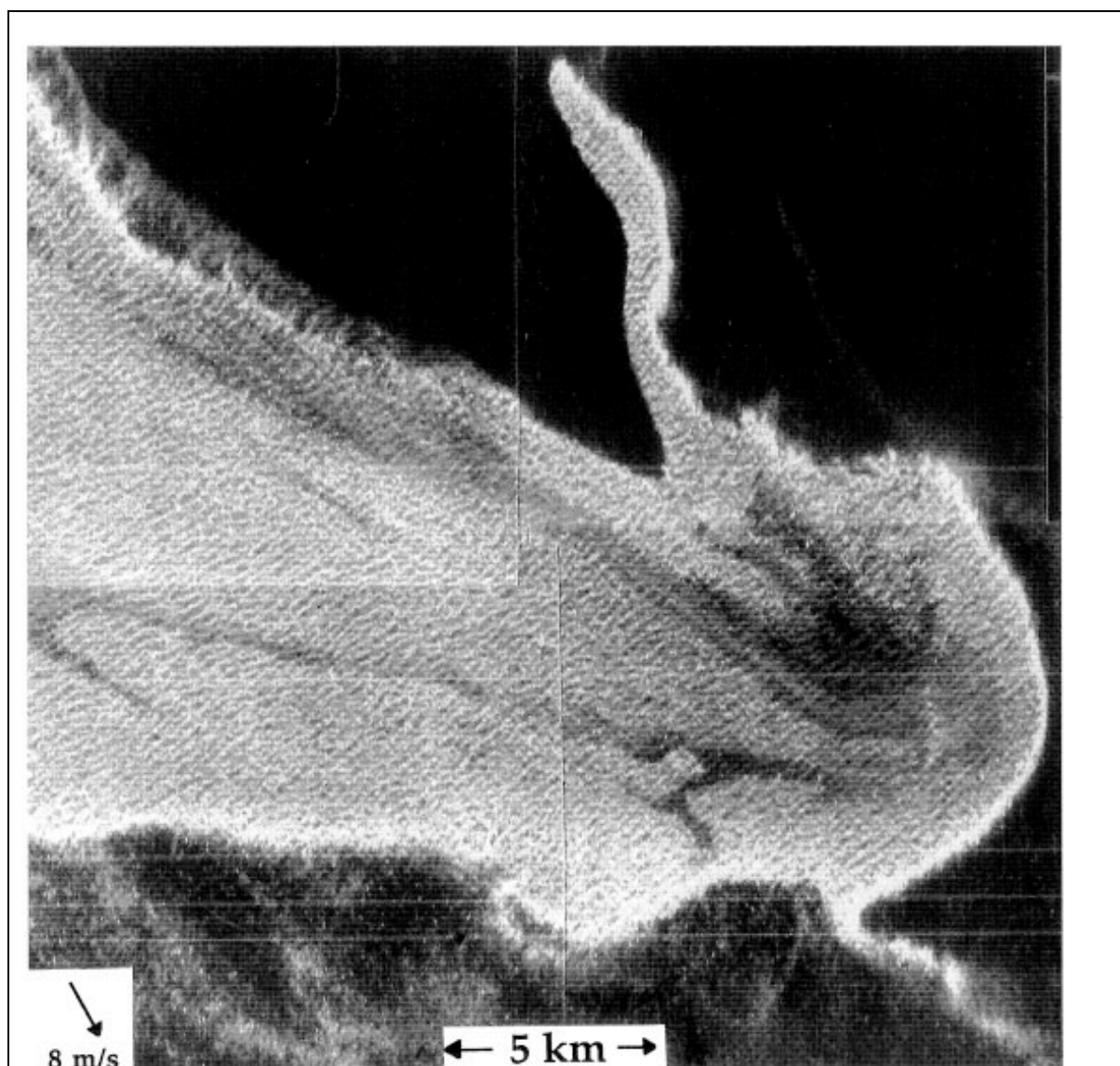


Figure 5.5. Ocean swell waves observed outside and in side the ice edge zone in the Greenland Sea MIZ in April 1987, during MIZEX 87 using Synthetic Aperture Radar (SAR) images with pixels

size of 7.5 m. Approximately 12.5 km across the area. Waves propagate in a northwesterly direction with a wave length of 200 m. Significant wave height was estimated to be 0.7-1.5 m and dominant wave period varied from 12.1s to 13.5 s. (Johannessen et al 2003).

The SAR image in Fig. 5.5 shows a fairly homogenous and regular wave field propagating through a compact ice edge into the ice pack and furthermore into a region influenced by an eddy field, from the open ocean. The compact ice zone consisted primarily of broken up multi year ice.

This example demonstrates that high-resolution SAR images can be used to obtain estimates of the wavelength and wave direction (complex imaging process introduces errors) within the ice pack. Currently, our SAR database at NERSC contains wide-swath images with a resolution of 150 m. To study swell propagation higher resolution is needed. Currently we can obtain 20 m resolution images, but future SAR satellites will provide higher resolution images.

5.4.2 Wave modelling in the MIZ

Significant efforts have been done in modelling of wave propagation in ice-covered regions, including the MIZ. Much of the work involves heavy mathematical methods from complex variable theory such as the Wiener-Hopf method and residue calculus, Green's functions, integral equations and variational calculus.

The ice conditions in the MIZ vary from open water and grease ice to very compact and broken up FY or MY ice causing changes in material properties and thereby the constitutive laws. The dispersion relation which depends on the constitutive laws, gives the connection between wavenumber (π/λ) and wave period, T. There is no general constitutive law covering all ice conditions found in the MIZ, and correspondingly the dispersion relation changes within a MIZ. By measuring the wave periods and wave lengths the dispersion relation provides a tool to verify the wave models and the selected constitutive laws. This requires well planned and co-ordinated experiments. Few experiments have been performed, main problem is to obtain relevant data of ice thickness and elastic properties of the sea ice.

Waves from open ocean propagating into an ice covered region.

Flexible ice sheet models are used in regions with high concentration of ice as in a compact MIZ or in the interior Arctic during winter time (Fox and Squire, 1991, 1994). In frazil ice and pancake ice Wadhams and Holt (1991) successfully used a mass loading model, which is a flexible ice sheet model with no rigidity (Squire, 1993). In the diffuse ice edge a scattering model including solitary floe theory can be used (Wadhams, 1986). General assumptions of these models are small amplitude ocean wave propagating from ocean into a floating semi-infinite ice sheet, so that the principle of superposition of monochromatic solutions can be used. Furthermore, the ice plate is assumed to be thin compared to the wavelength (thin plate approximation).

In the solution by Fox and Squire (1994) a thin elastic plate is used and the solutions are found by representing the velocity potential by modes for open water and for ice covered regions using appropriate boundary conditions. This model is simple and instructive and is used as an example below. The solutions are then matched numerically using the remaining boundary conditions. In the solution by Balmforth and Craster (1999) an analytical solution was found using the Wiener-Hopf technique (e.g. Carrier et al., 1983) based on the similar assumptions about small amplitudes and thin elastic plate.

Wave propagation in a heterogeneous ice covered region

The introduction of irregularities in the ice plate causing significant scattering of the wave field which again increases the complexity of the mathematical problem. Until the last years theoretical models have been built upon a uniform thin plate in which an abrupt transition such as a change of ice thickness or an open crack occurs, where in each case the boundary has been modelled as the free edge of one plate abutting an other plate. The different problems have been solved by solving for different boundary conditions using the Wiener Hopf technique, Greens functions or integral equations. The most recent and advanced mathematical model has been developed by Williams and Squire (2004) solved by using Greens functions and numerical calculations. Their model include a statistical description of the heterogeneity. This model has lately been extended so that the under side of the ice is no longer flat at the same height as the sea surface, as in all the other previous models, but allows for draft (Williams and Squire, 2007). The numerical experiments clearly demonstrate the importance of having the draft included in the model.

5.4.3 Concluding remarks on waves in ice

Recent advances within wave modelling, building on a 20 year long work in the wave modelling group at the University of Otago, New Zealand, is now emerging towards wave propagation models which can be used in the marginal ice zone with a reasonable degree of realism. Although significant work within the field of wave propagation in ice covered regions in the Arctic and Antarctic several unsolved problems exist both within the observation of the waves and within the modelling of the waves. First of all there is a great lack of validation of the wave models. This is because the wave models requires a detailed description of the ice field, such as distribution of ridges and leads, elastic properties of the sea ice and the ice thickness distribution along a defined track. In addition one requires obtaining simultaneously wave recordings (period, wavelength and direction) at several locations along the track and also outside the ice edge. Therefore, a dedicated and well-coordinated wave experiment is required. Such experiments will also increase the knowledge about the elastic properties of different types of sea ice.

5.5 Freshwater from rivers and glaciers

Freshwater from rivers and glaciers play an important role in the dynamics of the Arctic Ocean including sea ice freezing and melting. The river runoff into the Arctic Ocean has increased by about 7 % between 1936 and 1999 (Peterson et al., 2002). In the last two - three decades the increase has been more significant, as shown by Shiklomanov et al. (2000) and Peterson et al. (2006). Recent climate model predictions suggest that precipitation and river runoff will continue to increase in this century (ACIA, 2004). Data on river discharge are available from the database R-ArcticNet which contains data for 48 downstream river gages (www.R-Arcticnet.sr.unh.edu). Estimates of the river inflow have been computed using a hydrological analogy approach in combination with linear and multiple correlation (Shiklomanov *et al.*, 2000). For regions where no analogous site was available, additional meteorological information and water balance simulations were used (Rawlins *et al.*, 2003). The best estimates were obtained for the Asian and European seas, as well as for the Bering Strait and Beaufort Sea, because only relatively small areas there are unmonitored and data are more available.

The river discharge to the ocean for the period 2000–2004 is compared with that for 1980– 1999 for different drainage basins in Table 5.1 (Peterson et al., 2006). The last 5 years were characterized by an increase of total discharge to the Arctic Ocean, mainly due to a contribution from Asian rivers. The mean 2000–2004 discharge from Asia was 110 km³ (5%) higher than for the previous 20 years. The mean discharge to the ocean from North America and Europe for 2000–

2004 was practically unchanged relative to 1980–1999. Adjacent territories such as Bering Strait, Hudson Bay, and Hudson Strait drainage basins had insignificantly higher discharges in 2000–2004 compared with the previous 20 years.

Table 1: Characteristics of the annual inflow to the Arctic Ocean for 1980–2004. (From R-ArcticNet database, www.R-Arcticnet.sr.uoh.edu)

Basin	Mean discharge, 2000–2004	Mean discharge, 1980–1999	Change in mean discharge	Maximum annual inflow, 1980–2004		Minimum annual inflow, 1980–2004	
	km ³ /year	km ³ /year		km ³	year	km ³	year
Bering Strait*	311	301	3.3	362	1990	259	1999
Hudson Bay and Strait	920	905	1.7	1020	1992	770	1981
North America	1170	1170	0	1350	1996	990	1995
North America with Hudson Bay and Strait	2090	2080	0.5	2310	1996	1810	1981
Europe	708	708	0	790	1993	590	1980
Asia	2560	2450	4.5	2780	2002	2150	1982
Arctic Ocean Basin	4440	4330	2.5	4770	1997	3870	1982
Arctic Basin, Hudson Bay and Strait Basins	5670	5530	2.5	6040	1997	5070	1982

* including Norton Sound, Yukon River, and Anadyrsky Bay basins.

Most of the rivers show an increasing trend in annual river discharge over the observational periods. The mean discharge over 2000–2004 for the large Eurasian rivers was 3–9% higher than the discharge over 1936–2004. Thus, the contemporary data further confirm the presence of a significant increasing trend in the freshwater discharge to the Arctic Ocean from Eurasia (Fig. 5.6).

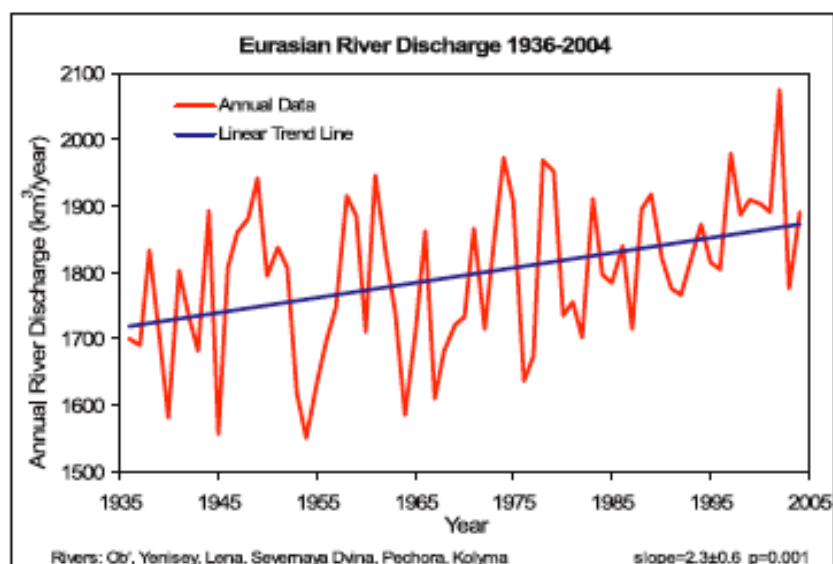


Figure 5.6 Total annual discharge to the Arctic Ocean from the six largest rivers in the Eurasian pan-Arctic for 1936–2004. The least-squares linear increase was 2.3 km³ per year. (Updated from Peterson et al., 2002.)

The contribution of glaciers to the freshwater inflow to the Arctic and world oceans has been increasing as a result of climate warming and will affect many aspects of the Arctic climate system. This comes primarily from glaciers in the Canadian, Russian, and Svalbard archipelagos and from individual ice caps around the Greenland Ice Sheet (GRIS) (Dyurgerov and Meier, 2000, 2005). The Greenland Ice Sheet has been the subject of increased attention in recent years as shown in (Fig. 5.7). Melting of the Greenland ice sheet will add fresh water to the North Atlantic Ocean which have been theorized to weaken or even destruct the Atlantic MOC (Stouffer et a. 2006). Secondly, the Greenland ice sheet stores a freshwater amount equivalent to an increase of the global sea level of 7 meters, implying that even partial melting will influence the global sea level in dramatic ways.

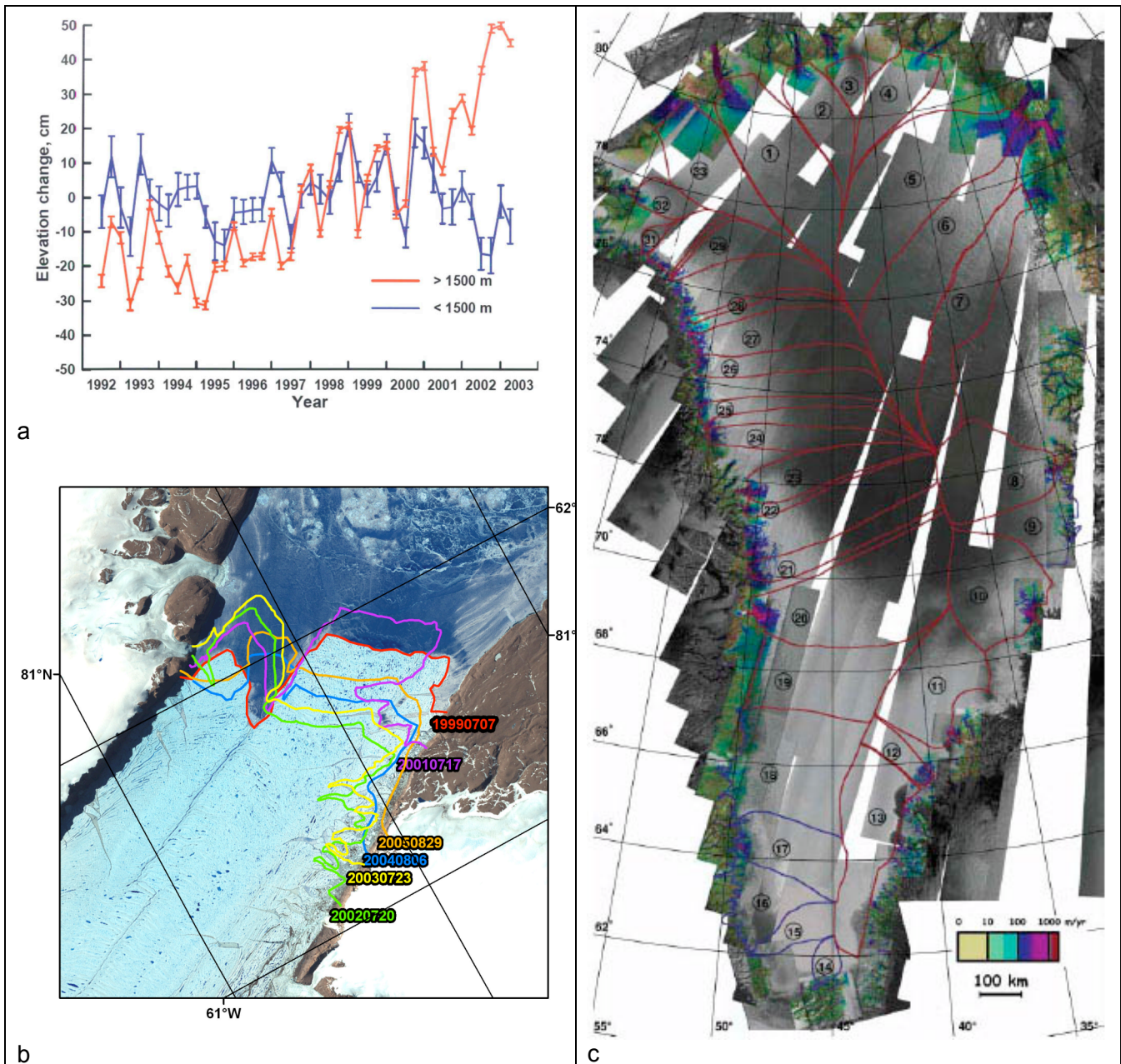


Figure 5.7 (a) Surface elevation of Greenland ice sheet from radar altimeter data (Johannessen et al., 2005), (b) change in ice front from the Paternmann glacier in north Greenland based on analysis

of satellite images between 1999 and 2005 provided by NERSC, (c) mass loss of Greenland outlet glaciers estimated from SAR interferometry (Rignot and Kanagaratnam, 2006). The colour code indicate the areas and magnitude of the mass loss around the edges of the Greenland ice sheet.

Recent observation-based studies of the surface elevation of the Greenland ice sheet diverge; reporting that the interior of the Greenland ice sheet has increased during 1992-2003 (Johannessen et al., 2005), that there is a net positive mass balance for the whole ice sheet for the same period (Zwally et al., 2006), and that there has been a dramatic glacier acceleration between 1996-2005 (Rignot and Kanagaratnam, 2006). It is likely that freshwater inflow to the Arctic Ocean from glaciers will continue to rise as a result of climate warming. Although many small glaciers will disappear, the large glaciers in Canadian, Russian, the Svalbard archipelagos, and the Greenland ice sheet will add to the hydrological cycle as cold glaciers warm and begin producing more runoff.

Peterson et al. (2006) have reported many changes in the freshwater cycle of high-latitude lands and oceans in the past few years. A synthesis of these changes in freshwater sources and in ocean freshwater storage illustrates the complementary and synoptic temporal pattern and magnitude of these changes over the past 50 years (Fig. 5.8).

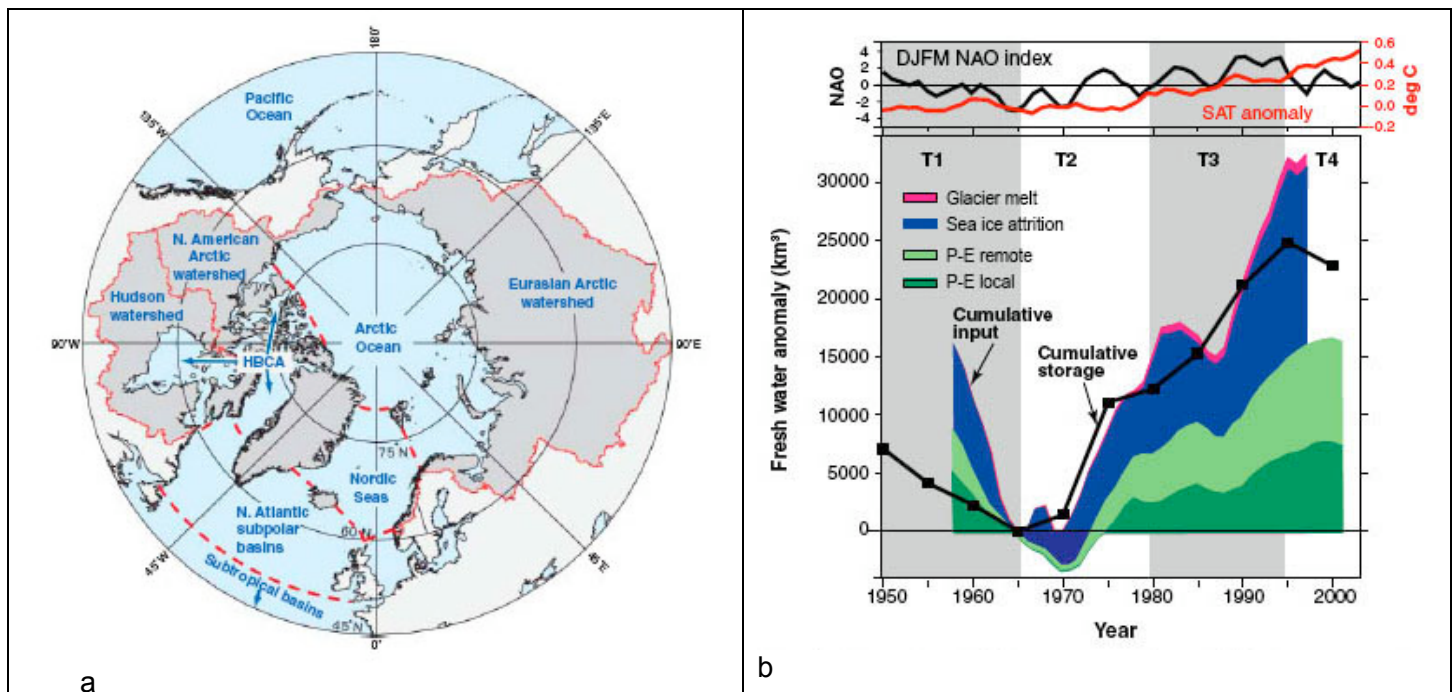


Figure 5.8 (a) Map of the watershed and ocean domains used for estimates of freshwater anomalies by Peterson et al., (2006). Solid red lines delineate watershed boundaries used for calculations of river discharge anomalies. Dashed lines separate regions of the ocean surface used for calculations of P-E anomalies and define the boundaries used for freshwater storage analysis in the Nordic Seas and the North Atlantic Subpolar Basins; (b) Comparison of FW source anomalies and FW storage anomalies relative to 1965 (units are km³). Black curve is cumulative NSSB ocean FW storage. Colored areas represent cumulative FW contributions from P-E local (Subpolar plus Nordic Seas, dark green), P-E remote (Arctic Ocean, HBCA, and river discharge, light green), sea ice attrition (blue), and glacier melt (red). Source contributions are stacked to show total FW source input.

Increasing river discharge anomalies and excess net precipitation on the ocean contributed about 20,000 cubic kilometers of fresh water to the Arctic and high-latitude North Atlantic oceans from

lows in the 1960s to highs in the 1990s. Sea ice attrition provided another 15,000 cubic kilometers, and glacial melt added about 2000 cubic kilometers. The sum of anomalous inputs from these freshwater sources matched the amount and rate at which fresh water accumulated in the North Atlantic during much of the period from 1965 through 1995. The changes in freshwater inputs and ocean storage occurred in conjunction with the amplifying North Atlantic Oscillation and rising air temperatures. Fresh water may now be accumulating in the Arctic Ocean and will likely be exported southward if and when the North Atlantic Oscillation enters into a new high phase. The freshwater changes are summarized in Table 5-2.

Table 5-2. Anomalies for major freshwater sources to the Arctic Ocean, HBCA, Nordic Seas, and Atlantic Subpolar Basins (Peterson et al., 2006). Anomalies for river discharge and P-E are relative to a 1936–1955 baseline. Anomalies for small glaciers and ice caps include melt from the pan-Arctic watershed, Arctic and subarctic islands, and ice caps around but not connected to the Greenland Ice Sheet. Anomalies for sea ice focus specifically on melting of stocks in the Arctic Ocean. Anomalies for small glaciers and ice caps, the Greenland Ice Sheet, and sea ice are relative to a water balance of zero (no net change in volume). In all cases, positive values indicate excess FW inputs to the ocean. Dashed entries indicate no estimates. R-ArcticNET v3.0 is a river discharge archive, and ERA-40 is a reanalysis of atmospheric observations.

Freshwater sources	References	Years covered in references	Avg. anomaly \pm SE for 1990s (km ³ year ⁻¹)	% relative to 1936–1955 baseline
Rivers flowing into the Arctic Ocean	Peterson <i>et al.</i> (4) R-ArcticNET v3.0 (55) Wu <i>et al.</i> (14)	1936–1999 2000–2003 1900–2050	163 \pm 34	+5.3
Rivers flowing into Hudson Bay	Déry <i>et al.</i> (56)	1964–2000	-59 \pm 16	-8.0
Small glaciers, ice caps	Dyurgerov and Carter (5)	1961–2001	38 \pm 13	—
Greenland Ice Sheet	Box <i>et al.</i> (6)	1991–2000	81 \pm 38	—
P-E, Arctic Ocean	ERA-40 (57)	1958–2001	124 \pm 72	+7.6
P-E, HBCA	ERA-40 (57)	1958–2001	81 \pm 33	+15.6
P-E, Nordic Seas	ERA-40 (57)	1958–2001	67 \pm 28	+17.8
P-E, Subpolar Basin	ERA-40 (57)	1958–2001	336 \pm 73	+16.8
Sea ice	Rothrock <i>et al.</i> (7)*	1987–1997	817 \pm 339	—
TOTAL			1649	

*Rothrock *et al.* (7) reported observed changes in sea ice thickness annually from 1987–1997 and also modeled changes over a wider time frame (1951–1999). Thickness has been converted to freshwater volume following Wadhams and Munk (58).

The results of the freshwater studies by Peterson et al. (2006) shows that changes in freshwater inputs and ocean storage occurred in conjunction with the amplifying North Atlantic Oscillation and rising air temperatures. Fresh water may now be accumulating in the Arctic Ocean and will likely be exported southward if and when the North Atlantic Oscillation enters into a new high phase. Increased freshwater accumulation will have impact on sea ice freezing and consequently on the location and variability of the MIZ.

6. Oil spill in ice-covered seas

Pollution in the Arctic has become of increasing concern in recent years. In particular oil pollution in the marginal ice zone as a result of production and transport of oil in Arctic regions. The Exxon Valdez oil spill accident in Alaska in 1989 has been one of the most severe oil pollution accidents with effects on the environment even after two decades (www.pws-osri.org). Prevention and combat of oil spills in ice-covered seas (Fig. 6.1, 6.2, 6.3, 6.4) is a major issue related to exploitation and transport of oil in the Arctic. In this chapter the behaviour of oil in ice and possibilities to recover oil spill in ice areas are reviewed. The main sources of information has been extracted from DeCola et al (2006), Dickins (2004, 2005) and The Prince William Sound Oil Spill Recovery Institute (www.pws-osri.org).

6.1 Behaviour of oil spills in ice conditions

When oil is spilled on water, several weathering processes may take place. In ice conditions, weathering processes are different than those exhibited in warmer waters. For example, spilled oil may not spread as far in the presence of ice floes or irregularities in the ice surface because the ice may create natural barricades to oil movement (Evers *et al.* 2004). However, oil can move hundreds of kilometres from the spill site if it is trapped under or within a piece of ice. Trapped oil may not be released until complete melting takes place-

Factors influencing the behaviour of oil in ice conditions fall into several categories, described in Table 6-1. The nature of the ice tends to dominate other factors in impacting the behaviour of oil after a spill (Evers *et al.* 2004). Ice coverage below 30% is not believed to significantly impact oil behaviour (Dickins and Buist 1999), although it has been observed to impact oil spill recovery activities (Robertson and DeCola 2001). Typically, 30% ice coverage or greater will significantly impact the behaviour of spilled oil (NRC 2003). In turn, the oil itself can impact ice formation by acting as an insulator (to slow ice formation) or speeding ice formation by reducing wave activity. In general, the presence of oil is considered to slow early ice development. If gas is involved, as in a well blowout, the impact of the gas is most likely to cause ice fractures or heaving (Fingas and Hollebhone 2003). Snow may become relevant to spill response if oil is released to, or moves to, the surface of pack or fast ice, or if it is released on land via a pipeline.

Table 6-1: Factors influencing the movement of oil in ice conditions (DeCola *et al.*, 2006)

Category	Relevant factors
Nature of the ice	Type of ice (landfast, pack, or broken; first year, multi-year), presence of structural anomalies (polynas, brine channels, keels), texture on top and bottom, rate of freezing or thawing, movement
Propoerties of the spilled oil	Viscosity, boiling point, emulsification, volatility (ignitability), asphaltene and wax content
Location of the spilled oil	On top of ice (oil well blowout, tank spill, above pipeline spill, valve leak, vessel spill), or below ice (subsea drilling blowout, subsea pipeline leak, underwater valve malfunction)
Distribution of the spilled oil	Thickness of oil, whether it is pooled or sprayed, whether it has landed on ice and become integrated in the ice due to freeze-thaw cycle and/or snow fall
Weather and water	Wind, sea state, temperature, precipitation

Weathering of oil spilled on open water is impacted by multiple factors, including the type of oil, temperature of the oil and the water, wind, current, tides, and weather (Fig. 6.2). The main weathering processes are summarized in Table 6-2. The presence of sea ice and cold ambient temperatures will slow the weathering process. If the oil is frozen or trapped in the ice, the weathering process may halt completely until the oil is thawed and exposed to air and water, allowing the weathering process to resume (Fig. 6.3).



Figure 6.1. Oil in slush ice off the Canadian East Coast in 1986 (Dickins ,2004).

Table 6-2: Weathering processes impacted by sea ice (adapted from Evers et al. 2004)

Process	Open water	Ice or Extreme Cold
Spreading and dispersion	A thick layer of oil grows thinner and covers a larger area of water (depending on the oil).	Ice acts as physical barrier (drift ice) or retardant (grease ice); oil does not spread or disperse as far, and ends up in a thicker layer.
Drift	Oil moves with wind/current	Oil will drift separately from the ice at less than 30% ice coverage, and with the ice at 60-70% (or greater) coverage. Unpredictable in dynamic drift ice conditions.
Evaporation	Relatively fast (thin oil films)	Slower where oil spills are thickened
Emulsification	Higher in areas with breaking waves. Rate of emulsification, total water uptake, and stability of emulsion depend on type of oil.	Total water uptake and rate of uptake may be reduced due to dampening of wave activity by presence of ice.

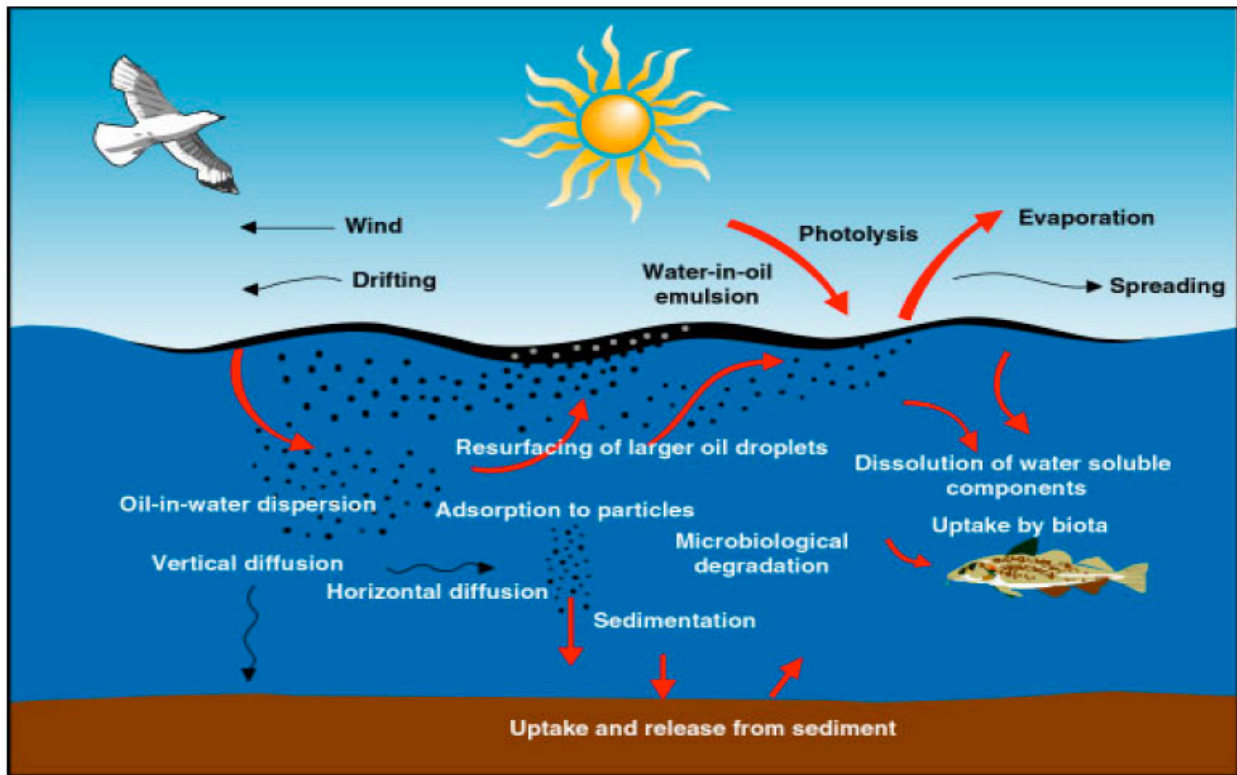


Figure 6.2 Weathering processes of oil spills in open water (Courtesy SINTEF).

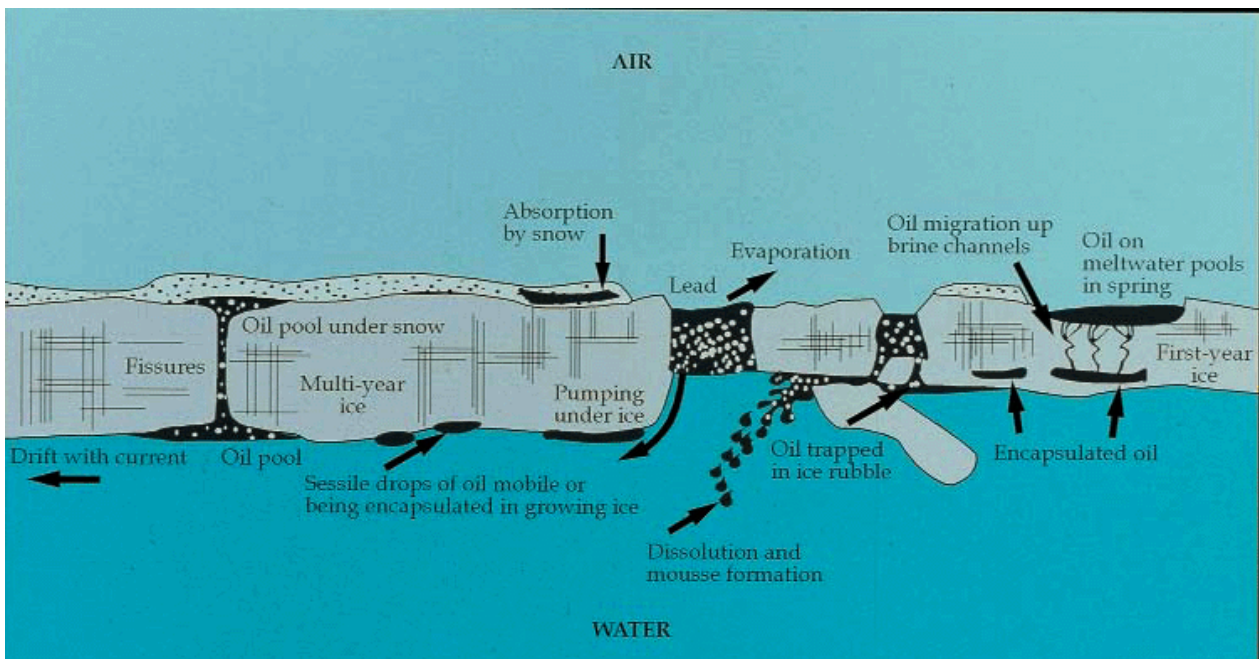


Figure 6.3. Weathering processes of oil spills in sea ice areas (Courtesy Dickins Ass.)

Oil viscosity will still increase in the presence of marine ice, but not as fast as in temperate open water because water uptake and evaporation will be slowed (Evers *et al.* 2004). Evaporation, natural dispersion, and emulsification all impact the volume and surface area of the oil slick; each of these processes may be impacted by cold temperatures and sea ice. Evaporation rate is

determined in part by the type of oil: generally, those components with boiling points below 200° C evaporate within 24 hours of a spill. Evaporation rates will be slowed by cold weather (Singsaas 2005). Just over 27% of the components in Sakhalin crude oil fall into this category. If the type of oil and the presence of waves lead to emulsification, the volume of the oil-water mixture will increase the size of the slick and other weathering processes will slow (NRC 2003).

The presence of ice can impact oil behaviour by trapping the oil, controlling the rate of spread, and making it difficult to track. Observations from actual spills, laboratory experiments, and field studies provide some insight into the ways oil can interact with different ice formations. The oil and ice interaction is heavily influenced by whether the oil is released above or below the ice, as summarized in Table 6-3.

Oil released to open water amid dynamic drift ice will spread at the rate it would normally spread in the open water, areas, but spreading will be impeded by grease or frazil ice between the floes and the ice itself. Due to the density difference between oil and water, spilled oil will likely rise to the surface of a slushy oil and ice mix (Fingas and Hollebone 2003). The slick can also move underneath ice floes/pancakes, or be tossed on top of them in wave action causing bumping and moving of the floes (Wilson and Mackay, 1987). There is no clear answer as to whether oil will move at the same rate as drift ice, or faster or slower (Evers *et al.* 2004), although some studies suggest that oil will move at the same rate and in the same direction as ice (Dickins and Buist 1999).

The actual behaviour of oil spilled to grease or brash ice has been widely variable. Oil has been trapped at the edges of ice pancakes, frozen in place, caught within the structure of the grease ice, observed moving under the ice and dispersing as leads open, and carried underneath brash ice (Fingas and Hollebone 2003). Thus, it is extremely difficult to predict the movement of oil in this dynamic context.

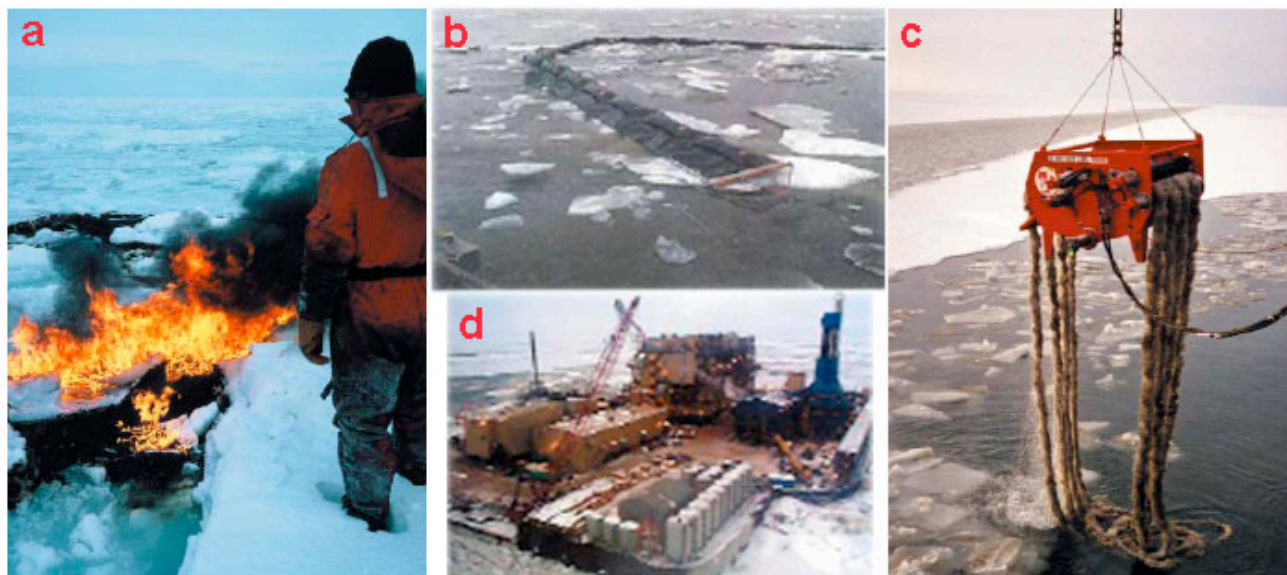


Figure 6.4 (a) Burning crude oil in slush-filled lead off Nova Scotia, Canada, 1986. Photo: SL Ross and DF Dickins, 1987; (b) Conventional containment boom deployed in broken ice during field trials off Prudhoe Bay, Alaska, Spring 2000. Photo: Alaska Clean Seas, 2000; (c) Foxtail rope-mop skimmer in ice. Photo: Alaska Clean Seas; (d) Northstar offshore oil production facility, North Slope Alaska. Photo: D. Dickins

Oil released under fast or pack ice will not spread as evenly as it might on the water surface. The rough underside of the ice will cause the oil to pool in some places, unless the current is strong enough to keep the oil moving (AMAP, 1998). Late-winter ice tends to be rougher in texture and therefore able to hold more oil pooling under its uneven surface. It is estimated that 1.5 million liters/km² of oil could be stored under late winter fast ice along the Alaska North Slope (Dickins and Buist 1999).

Oil trapped under ice may freeze and remain there as it cannot evaporate. The oil will move with the ice until the spring melt and may ultimately be released some distance from the spill site. This process has been referred to as “encapsulation” or an “oil-ice sandwich” (Evers *et al.* 2004, NRC 2003a). A review of field tests and laboratory experiments finds that oil can be partially encapsulated within four hours and fully encapsulated as fast as 24 hours after contact with the ice (Fingas and Hollebone 2003). Oil trapped under multi-year ice could remain in the marine environment for many years and may not be released until it slowly migrates to the surface. Some scientists estimate oil could be trapped under multi-year ice for up to a decade (NRC 2003).

Oil spilled on the surface of an ice sheet tends to pool in ice depressions, and may be trapped under snow cover. However, oil spilled on top of the ice surface will be exposed to the air and subject to evaporation (Owens *et al.* 2005).

Polynyas and leads can change oil behaviour as well. Areas of open water such as polynyas or leads will allow oil to spread more rapidly than it would on the ice surface or below the ice, causing the oil to pool in these areas (Wilson and Mackay, 1987). The weathering process will resume once the oil is exposed to open water, air, and wind in the polynyas and leads, unless it is encapsulated by the ice. Water moving in or out of a lead can cause a “pumping” action, which moves oil out from under ice and into the lead. Pumping of oil into leads can be a dominant oil transport mechanism in the early hours of the spill (Reed *et al.* 1999).

Ultimately, any oil that moves during initial spreading or while frozen in ice could end up on the shoreline. Here the hydrocarbons can mix with the sediment, form emulsions, or cover beaches, depending on the quantity of oil and state of weathering. Oil released under, or moving to, fast ice could reach the shoreline but be invisible to observers until break-up (AMAP, 1998).

Oil spilled on snow, or which migrates through an ice sheet to a snow-covered surface, has not been fully studied and is difficult to track visually because it is obscured. One assumption is that oil in snow will eventually evaporate to the same extent as oil on open water, but it will require more time to do so. Limited testing has been conducted, and current models to estimate the evaporative rate in snow are inadequate (Owens *et al.* 2005).

Bacteria and some fungi will slowly degrade petroleum hydrocarbons spilled in the marine environment; however, degradation is slower in cold water areas than in temperate regions because the oil tends to be more viscous and not evaporate as quickly, making it less accessible to bacteria. Studies conducted on Alaska beaches that were oiled during the *Exxon Valdez* oil spill show that twelve years after the spill, oil was still present in the beach substrata and in a toxic, unweathered liquid form that remained biologically available (Peterson *et al.*, 2003; Short *et al.* 2004). The behaviour of oil in different types of ice is summarized in Table 6-3. Oil behaviour in ice is heavily influenced by the season in which it is spilled. Oil spilled on fast or pack ice during fall freeze-up will likely migrate downwards as the ice develops and remain encapsulated, moving with the ice pack until the spring melt. If oil is spilled in dynamic drift ice during fall freeze-up, it will become part of the ice floes as grease ice solidifies into pancake ice, and continues to build into solid ice formations. A rapid freeze can cause this to happen quickly, making oil recovery operations futile (Wilson and Mackay, 1987).

Table 6-3 Behaviour of oil spilled to different types of ice environments (NRC 2003a)

If oil is spilled	Sub-location	Fate during freeze-up	Fate after thaw
On ice	< 30 % ice cover	As in open water	Melt to open water
	> 30 % ice cover	Mostly trapped in between ice floes	Melt to open water
	In leads	Frozen into ice	Melt to open water
	Frazil/grease/brash ice	Frozen into ice	Melt to open water
Under ice	First year ice	Encapsulated	Rise via brine channels
	Multiyear ice	Encapsulated	Rise or remain in ice
Into ice		Encapsulated	Melt to open water
Onto ice	On ice	Pool & remain on surface	Melt to open water
	Under snow	Absorb into snow	Melt to open water

When the spring melt starts, oil tends to move upwards through the ice and ends up pooling on top of it where weathering processes will take place and the remaining oil will eventually be released to the water wherever the sheet of ice ends up (AMAP, 1998).

As first year ice begins to melt, brine channels open up in the areas where sea salt was concentrated by its exclusion from the ice formation. These opening channels can allow oil trapped in the ice, or under it, to rise to the surface (NRC, 2003). This oil purging process will accelerate as spring temperatures rise above freezing. Thus, oil will increasingly appear on the surface of the ice and develop into thick pools of weathered oil. Fine droplets of oil, such as the spray released from an oil well blowout, may take more time to reach the surface than a thicker slick (Dickins and Buist 1999).

6.2 Predicting the fate of oil in ice

Predicting the fate of oil spilled in ice-infested waters requires new and improved algorithms to take into account the seasonal variation, weathering, and other factors, described above, that affect the behaviour of oil spilled on, in, or under ice. Standard models used to predict the fate of oil spilled in temperate marine waters are inadequate for modelling the fate of oil in dynamic sea ice conditions. This section describes some of the models available, as well as their limitations.

Numerous mathematical calculations have been developed to predict the behaviour of oil in ice conditions. Modelling of oil behaviour in ice began in the 1970s and continues to serve as the basis for much of the current theoretical models. Models tend to describe the behaviour of spilled oil in two categories: (1) on ice and (2) under ice. The first semi-empirical models used three phases to explain the spread of oil on ice (gravity-inertia, gravity-viscosity, and interfacial tension-viscosity) were developed. Later efforts throughout the 1970s and 1980s explored the spread of oil theoretically, in the laboratory and by small field experiments. The sophistication of these models improved as additional physical parameters were added to the modelling algorithms such as the volume of spilled oil, time since spill, ice roughness, oil density and oil viscosity. Modelling experts continue to dispute the relative importance of various model inputs (Fingas and Hollebone 2003). Snow is excluded as a factor in most models. A state-of-art oil weathering model, provided by SINTEF, is illustrated in Fig. 6.5.

The spreading of oil under ice has been studied in laboratory and field experiments. One model examined the space created by under-ice roughness by creating a mould of the underside of ice floes (Fingas and Hollebone 2003). While the flow of oil under ice will be influenced by buoyancy, viscosity, and surface tension, most models predict that the spread of oil under ice is dominated by the subsurface shape of the ice unless strong water currents are present moving oil out of areas in which it might otherwise collect. In the case of a subsurface oil well blowout, a strong current can move oil and gas horizontally in the water column before reaching the ice (Fingas and Hollebone

2003).

Some efforts have been made to quantify the movement of oil in dynamic drift ice or amid smaller chunks of ice such as grease or brash ice; these conditions introduce more variables and are inherently more challenging to predict. One model was developed to modify the original equation developed by Fay and Hoult (in Fingas and Hollebone 2003), but it needs additional testing for validation. Sayed *et al.* (1995) concluded that oil with low viscosity will spread farther in brash ice than more viscous oils. Yapa and Weerasuriya (1997) developed a theoretical model to be used for oil behaviour under drift ice by modifying earlier work on oil under ice to account for seepage into cracks, but this represents only a first step; significant work remains in this area.

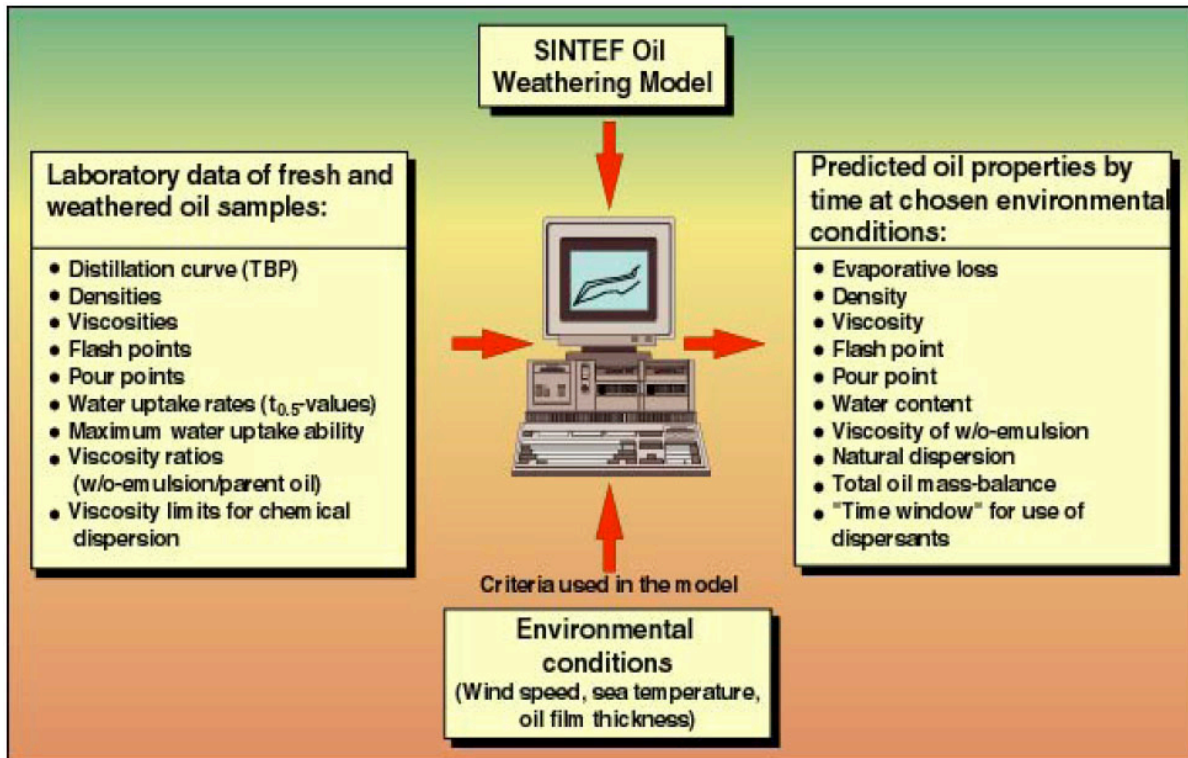


Figure 6.5 The main components of the SINTEF oil weathering model (Courtesy I. Singaas).

Upon reviewing theoretical models of oil behaviour in ice conditions, Fingas and Hollebone (2003) conclude that the existing models are inadequate because most are tested only against laboratory or very small scale field experiments, and are unable to adequately replicate the complexity or uniqueness of different ice-ridden marine environments. Some of the early models are now antiquated due to the development of improved measuring methods. Reed *et al.* (1999) concluded the ice leads play a dominant role in impacting oil behaviour but are not incorporated in most models. It is especially challenging to develop accurate modelling algorithms to predict the behaviour of oil over time, because the characteristics of the oil are constantly changing.

Predicting the fate of oil in the specific circumstances surrounding any incident, especially in an ice environment, is beyond the capacity of existing models. In order to improve oil spill modelling capabilities in sea ice, models must be validated against data from arctic oil spills or large-scale field trials. Because of the high variability of oil behaviour in sea ice conditions, models developed for one region of the arctic may require some adjustment before being applied to other cold-weather regions. Currently, data is available for only a limited range of oil and ice types (Singaas

and Reed 2006). Very little data is available regarding the fate and behaviour of Russian crude oils and crude oil products in ice-infested waters (Singsaas, 2005).

6.3 Oil spill recovery in ice conditions

Compared to temperate, open water conditions, the ability to clean up oil spills in the presence of sea ice is extremely limited and conditional. Dynamic ice conditions present the most significant challenges to on-water spill response. There is very little commercially available equipment appropriate for use offshore in ice-infested waters. Actual experience responding to oil spills in the offshore arctic environment is extremely limited.

Sea ice and other cold climate conditions impose significant limitations on existing spill response technologies and systems. Several factors impact the response gap for spill response in sea ice – technological limits, cold climate efficiency losses, and safety limitations. Mechanical recovery and in-situ burning are the two spill response methods considered applicable in ice-infested waters using existing technologies. Several published studies have considered the potential applicability of each technology in dynamic sea ice and drawn connections between the percentage of ice cover and the potential effectiveness of in-situ burning or mechanical recovery methods. An example using ice boom is shown in Fig. 6.6

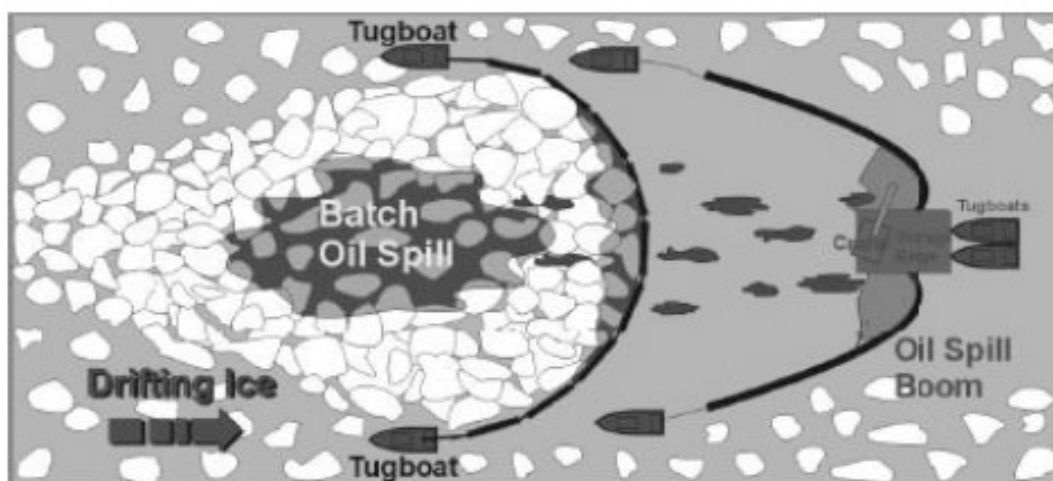


Figure 6.6 Potential use of ice boom to improve mechanical recovery in sea ice (Abdelnour and Comfort, 2001)

Real-world experience deploying mechanical recovery equipment in ice-infested waters reveals that some systems may reach their operating limits well below the ice concentrations proposed in Figure 6.7 and other published studies. For example, the limit to mechanical recovery with containment booms and skimmers in ice-infested waters is estimated to be about 20%. However, the 2000 offshore response exercises in the Alaska Beaufort Sea demonstrated that the actual operating limits were closer to 10%, and that during fall freeze-up, ice conditions as low as 1% constituted the operating limit for a barge-based mechanical recovery system using conventional boom and skimmers. In addition to ice coverage, the characteristics of the ice regime are an important determinant of response efficiency. The 2000 offshore exercises demonstrated that fall ice conditions (freeze-up) can be more challenging than spring break up (Robertson and DeCola 2001, NRC 2003). Therefore, 10% ice coverage in fall may pose different limits than 10% coverage in spring. These complexities make it difficult to develop meaningful guidelines for when certain technologies may or may not function. As Singsaas and Reed (2006) note, "Few of these methods have actually been tested in ice-infested waters, so there are large uncertainties

associated with the listed technologies.” Singaas and Reed (2006) also point out that the recovery capacities (amount of oil removed per unit time) of the response systems listed in the diagram (Fig. 6.7) vary widely.

Response method	Open water	Ice coverage									
		10 %	20 %	30 %	40 %	50 %	60 %	70 %	80 %	90 %	100 %
Mechanical recovery:											
- Traditional configuration (boom and skimmer)	—	—	—							
- Use of skimmer from icebreaker			—	—	—	—	—	—	—	
- Newly developed concepts (Vibrating unit; MORICE)				—	—	—	—			
In-situ burning:											
- Use of fireproof booms	—	—								
- In-situ burning in dense ice							—	—	—
Dispersants:											
- Fixed-wing aircraft	—									
- Helicopter	—	—								
- Boat spraying arms	—	—								
- Boat “spraying gun”	—	—								

Figure 6.7 The operational limits of oil spill response systems in ice-infested waters. It is important to recognise that these tables describe “expected” effectiveness only; there is little real-world data available to correlate these figures.

Figure 6.7 suggests that the operating limits for in-situ burning are reached when ice conditions are in the 30% to 70% range. Above 60-70% ice coverage, in-situ burning is considered to have more promise due to the natural containment afforded by ice in combination with the reduced weathering of oil when ice is present. However, there is little real-world data to support these assumptions regarding the use of in-situ burning at high concentrations of broken ice. The upper limit for dispersant use is also presumed to be 30% to 50% ice coverage. Again, these estimates are drawn primarily from small-scale trials with little correlation to actual spill responses.

The *Field Guide to Arctic Spill Response* describes a number of environmental and operational factors that combine to make arctic oil spill response operations especially challenging. Many of these same factors serve to intensify the potential environmental and wildlife impacts from oil spills in cold climates. It is essential that oil and gas operations be designed and regulated in a manner that addresses these unique response challenges and potentially devastating impacts (Owens et al. 1998):

- High intensity of habitat use during summer season
- Extreme seasonal ecological sensitivity variations
- Unique shore types
- Unique oceanographic and shoreline seasonal changes
- Seasonal ice conditions
- Slower weathering and longer persistence of spilled oil
- Remote logistical support

- *Need to improvise response using available means until support equipment arrives*
- *Safety in cold, remote areas*
- *Low visibility due to fog and snow*
- *Frequency of storms and adverse weather*
- *Cold temperature effects on the efficiency of equipment and personnel*
- *Limited boat operations in ice-infested waters during transition periods, winter dynamic ice conditions*
- *On-ice operations in winter*
- *Seasonal daylight variability*
- *Need for aircraft support for response logistics, surveillance, and tracking*

Because of these significant challenges and the high stakes of oil spills in cold climates, a robust oil spill planning and response infrastructure is needed to support oil development. Industry and government must participate in detailed environmental sensitivity assessments, coastal classifications, computer modelling, and regular training for response team members to ensure that an organized and timely response is possible. Spill response planning requires coordination among spill response organizations, industry, and government agencies (Glover and Dickins 1999).

A mature response system, including major equipment caches and a commitment to research and development, is especially important to respond to the challenges associated with spill response in ice-infested waters (Glover and Dickins 1999). Equipment maintenance and personnel training are equally important, as equipment that is not maintained or operated by skilled technicians is ineffective and potentially dangerous (Steen *et al.* 2003). However, even in regions with well-developed oil spill response programs, large equipment caches, and trained responders on-site, there may be times when environmental conditions preclude any a spill response at all.

The report "Advancing Oil Spill Response in Ice-Covered Waters" (OSRI and ARC, 2004) details a 2003 project identifying programs and research and development projects that will improve the ability of responders to deal with accidental oil spills in fresh or salt-water marine environments where there is ice (Dickins, 2004). The multi-phased project concluded with a two-day workshop held in November 2003 in Anchorage. This report, published in cooperation with the Arctic Research Commission, summarizes and prioritizes the projects reviewed both before the workshop and at the workshop. More information about oil spill and recovery in Arctic waters can be found on www.pws-osri.org and <http://www.dfdickins.com/news.html>.

7. Modelling of primary production and spreading of passive tracers

High-resolution coupled ice-physical-biological models can be used to investigate the effect of sea ice-melting, wind-stress, eddy formation, and biological factors on the plankton production along the ice-edge. Passive tracers (CFCs, time tracers, radionuclides), including surface films and other pollutants, can also be predicted.

7.1 Background and status of knowledge

The Barents Sea is a wide marginal shelf sea and comprises about 30% of the circum-Arctic shelves. It supports one of the richest fisheries of the World Ocean. The MIZ of the Barents Sea comprises a transition between the ice covered waters to the north and the open waters to the South, forming a seasonal, high productivity region, together with the Southern Barents Sea, south of the Polar Front. Stratification is supported in the MIZ by melting sea ice, supply of polar water from the north, low salinity coastal water from the south, and by warming due to solar radiation. During spring and summer stratification is caused by ice melting, supporting a distinct phytoplankton bloom near the ice edge. The timing and maintenance of stratification, associated nutrient supply and primary and heterotrophic productivity, strongly affects the amount of total annual biological production (Ratkova and Wassmann, 2002; Reigstad et al., 2002).

It is a key challenge to improve our understanding of the inherent process of the ice edge region in order to monitor and predict the impacts on the marine life and its biodiversity in an era of global warming, both nationally as a Norwegian governmental responsibility and internationally as the region impacts food supply on global scales. Modelling of the ecosystem in combination with its forcing, the ocean and ice processes, is one way of investigating the important processes of dynamics and ecosystem response. The present tools, whose sub-modules may be optimized for other oceanic regimes, still need improvement, because of the special conditions of the MIZ.

7.1.1 Regional scale and climate related processes

The major constraint on the ice extent is the inflow of Atlantic water which is in turn determined by variations of the large scale wind systems upstream. As the fraction of open water directly influences insolation, the integrated primary production is typically 50% larger in a warm year than a cold year (Wassmann et al., 2006 and Fig. 7.1).

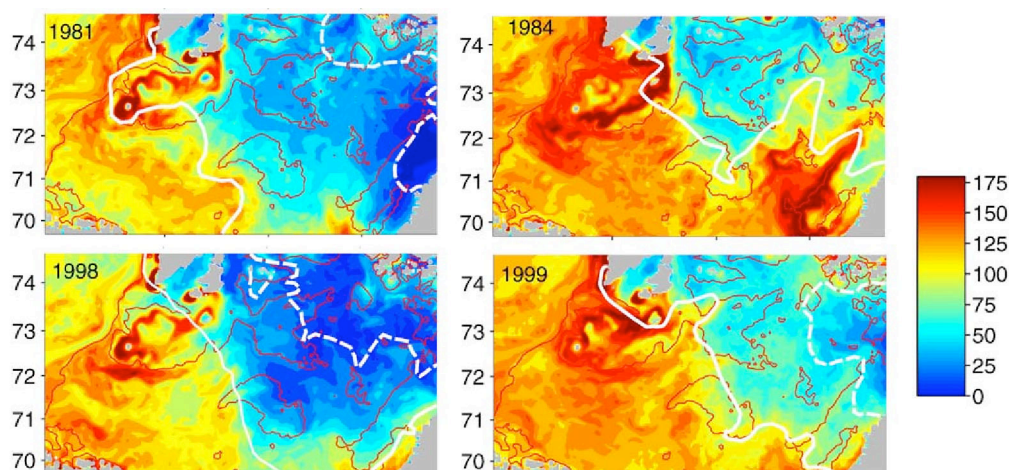


Figure 7.1. Simulated integrated primary production [$\text{gC}/\text{y}/\text{m}^2$] for various years. From top to bottom the temperature of the environment decreases, demonstrating the strong dependency of primary production on temperature (Adapted from Wassmann et al., 2006).

The region is also characterized by regular passes of atmospheric lows during the summer. Such events are usually followed by distinct increases in primary production, due to upwelling and entrainment of nutrient from below the euphotic zone (Wassmann et al., 2006).

Near the ice edge the spring bloom starts much earlier than in the Atlantic domain due to the strong stratification. The pycnocline is typically too steep to be eroded by wind events.

7.1.2 Variability along the ice edge

The ice melt supporting the stratification is unevenly distributed both in time and space, both along the ice edge and within the ice pack. Typically, the ice protrudes over warm water – thus melting subsequently – during local pulses lasting 5 days or so (Budgell, 2005; Wassmann et al., 2006). This local advancing and retreating of the ice edge together with its post-winter location leads to marked variations in the timing of the spring bloom and the duration of primary production and export for a given location. By acting on the ice, the wind indirectly contributes to the ice edge bloom, together with meandering and tidal ocean currents and heat fluxes. Another mechanism is upwelling and downwelling on nutrient supply along an ice edge due to differential wind stress on the ocean surface, as has been the subject of a number of studies (e.g. Røed and O'Brien, 1983; Niebauer, 1985). The coupling of the physical regime to nutrient biogeochemical supply and productivity has recently been investigated in detail by Tamelander and Heiskanen, (2004); Sundfjord et al., (submitted 2006); Kivimäe et al., (in prep).

7.1.3 Mesoscale eddies

The ice edge region is rich in mesoscale (1-10 km) variability (Sandven et al., 1999), mainly triggered by the wind. The modelling of these phenomena is a great challenge, due to the strong coupling between atmosphere and ocean, among other things. Nevertheless, Wassmann et al., (2006) showed how the mesoscale nature of the plankton stocks emerged in a model simulation when refining the grid size from 20 to 4 km. The apparent patchiness shown in such simulations and in observations (Sakshaug et al., 1995) has surprisingly not been subject to further investigations, although it has been extensively studied in many other oceanic regimes. In a mesoscale dynamic environment, including frontal features with vertical velocities of order 10m/day, the time scales of the physical and the biological processes become comparable.

The stress on the ocean surface, by the wind or indirectly by the ice, can also structure the mesoscale eddy field in the ocean. The differential roughness over open ocean, floating ice rubble and compact ice, together with differences in vertical momentum transport in the atmosphere due to the structure of the boundary layer, all lead to gradients in the stress acting on the ocean surface. This leads to divergent cross-ice edge flows, leading to up- or downwelling. In turn, pressure gradients are set up across the ice-edge, with geostrophic jets along the ice edge. These jets are prone to instabilities and eddies are shed. In a typical scenario with the wind having a component along the ice-edge with the ice to the right, looking down-wind, the Ekman flow tends to compress and compact the ice edge, thus reducing the effect of differential momentum transfer (Fig. 7.2).

With the opposite wind direction, the area with high roughness is expanded and there is a positive feed-back, leading to much larger alteration of the mixed layer depth and hence the eddies, with a correspondingly more substantial primary production due to nutrient pumping both from below and from the under-ice region.

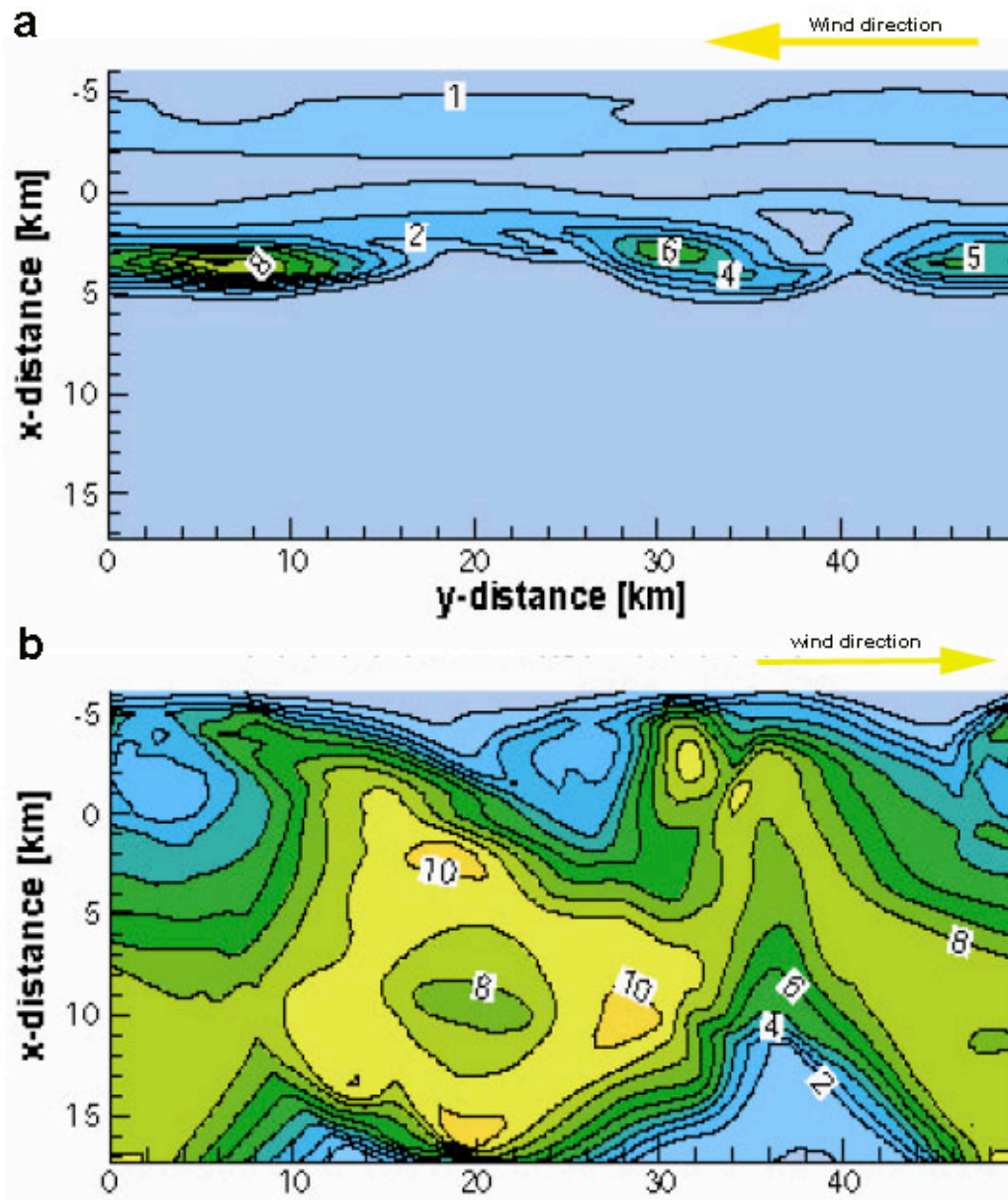


Figure 7.2. Primary production along an ice edge, subject to different wind forcing scenarios. (a): The wind blows toward the left, pressing the ice (located in the upper half of the panel) toward its right looking down-wind. The stress on the ocean is reduced, leading to a weak ice edge jet, breaking up into smaller eddies, transporting some nutrient into the open sea, leading to patches of growth. (b): Turning the wind, drags the ice outwards, expanding the area with high roughness, increasing the stress. Strong currents evolve, rapidly breaking entirely into eddies. Growth is very large due to the up-welling of nutrient from the ice covered part and light availability due to the diverging and finally melted away ice.

7.1.4 Links between climate and processes on shorter time scales

The links between weather and climate are not straightforward and it is not obvious how the important high-frequency variability affecting the biological systems will be affected by climate change. Due to lack of good, coupled regional ocean-ice-atmosphere models, the standard approach is to apply stand-alone ocean-ice models. However, their results are very sensitive to the forcing data and schemes (Budgell, 2005; Harms et al., 2005; Wassmann et al., 2006). The forcing data usually stem from interpolated reanalysis fields from NCEP or ERA40, subject to various ad hoc corrections of obvious biases, e.g. too little cloudiness(/fog) over the MIZ. The differences are further translated into e.g. the radiation budgets (Budgell, 2005; Harms *et al.*, 2005; Schrum *et al.*, 2005), and thus heating, stratification and ultimately the algal bloom itself.

7.1.5 Coupling of atmosphere and ocean

The large horizontal temperature difference associated with the moving sea ice edge presents a fundamental modeling challenge, namely that all subcomponents (air, water, ice) need to be modeled as a fully coupled system. The induced circulations in the atmosphere and ocean amplify the turbulent exchange significantly. Moreover, the so-called breeze flow extends for tens of kilometers involving large volumes of air-water into joint vertical circulation. The modifications of the turbulent exchange lead to changes of the transport properties of the boundary layers of the atmosphere and the ocean, ultimately influencing the conditions for biological productivity at the ice edge.

Also in the open ocean itself quantitative assessment of turbulent exchange meets large difficulties as the vertical diffusion schemes in models are inaccurate in simulations of the entrainment and the stably stratified turbulence, although recent progress has been made by including the effects of wind waves and breaking in ocean turbulence closure models (Burchard, 2002; Umlauf and Burchard, 2005; Jenkins 1994; Cushman-Roisin and Jenkins, 2006).

Common approaches based on reanalysis of atmospheric data and turbulent mixing (e.g. Budgell, 2005) generally reveal intrinsic inconsistencies between mean wind and temperature/density profiles, hence reducing their credibility. A proper approach should correctly account for patchiness of turbulence in stratified fluids and reproduce the amplification of the turbulent mixing in the MIZ. The failure of conventional methods to represent biophysical and dynamical coupling with turbulent mixing in stably stratified and heterogeneous fluids is a major bottleneck in our understanding of air-sea interaction and the biological productivity.

7.2 Modelling

Biophysical systems involve a huge set of variables and governing parameters. 3D numerical modeling can be an elusive approach in identifying important dynamics and sensitive parameters of such systems. Since there is no unique biogeochemical model (e.g. Flynn, 2005), there exist many models which emphasize various sub-processes, depending on the scope of the actual investigation.

The NERSC coupled biogeochemical-ocean circulation model consists of a version of MICOM (Bleck, 1992), coupled to an biogeochemical model by Broström and Drange (2000). This model focuses on the carbon cycle, predicting total CO₂ and alkalinity of the sea water, but also involving a nitrogen-based ecosystem model, predicting nitrate, ammonia, phyto- and zooplankton and detritus. The model has been used on the small scale (meso-scale) to investigate the effect of eddies and up-welling along an ice edge (Fig. 7.2). The model has also been set up on a global lay-out to investigate interannual variability in CO₂ uptake, subject to daily forcing.

Also at NERSC, the physical ocean model Hybrid Coordinate Ocean Model (HYCOM) (Bleck,

2002) has been coupled to the primary productivity model NORWECOM (Aksnes *et al.*, 1995). This model includes the nutrients nitrate, silicate, and phosphate and has two phytoplankton groups (diatoms and flagellates). An individual based model (IBM) for the copepod *Calanus finmarchicus* has also been coupled to HYCOM. Both NORWECOM and the IBM were developed at the Institute of Marine Research. Currently, the model system is used to investigate the influence of eddies and the front between the Norwegian Coastal Current and the Norwegian Atlantic Current on the primary production and timing of the spring bloom in this area. The position of this front affects the stratification of the water and therefore also the conditions for a bloom (Rey, 2004). The results from NORWECOM are also used as food availability in the IBM. The IBM is used to study shelf recruitment of *C. finmarchicus*. The shelf population of *C. finmarchicus* is important for the survival of herring larvae (Holst *et al.*, 2004).

The SINMOD model has been developed at SINTEF over a 20 year period and is well adapted to studies of the North Atlantic and of the Barents Sea in particular (Slagstad and McClimans 2005, Wassman *et al.* 2006, Ellingsen *et al.* 2007). The physical part of the model is based on the 3D primitive equations that are solved on an Arakawa C- grid. A recent evaluation for the Barents Sea is found in Slagstad and McClimans (2005). The current version of the ecosystem module includes 13 state-variables (Wassmann *et al.*, 2006).

In addition to the biogeochemical variables one can add various other tracers, such as CFCs (chlorofluorocarbons), time tracers, radionuclides etc., i.e. quantities that are relatively independent of the biogeochemical system, or whose forcing functions are well known. In this category can also be mentioned oil spills.

7.3 Research needs

A key issue is to model the biogeochemical processes in the Barents Sea ice edge region at a sufficiently high resolution (i.e. 1 km or better). Only at this resolution one can be able to quantify the effect of episodic air-sea-ice interactive processes and mesoscale dynamics on the vertical exchange, nutrient supply and light climate for primary production.

To achieve this, we need

- To improve spatial patterns and spectral composition and interrelations of the forcing components and the description of ice/ocean/atmosphere interaction.
- To identify the characteristics of spatial variability, timing and sequence of primary, secondary and export production during a spring bloom event, as well as remineralization depths etc.
- To validate and recommend a regional scale biophysical model including ice edge processes and the parameterizations of mesoscale processes therein, based on comparison of several models.

8. Conclusions and recommendations

The Arctic MIZ regions, and in particular the Barents Sea, are important areas for exploitation of marine resources. Presently drilling for oil and gas is carried out year-round, and a dramatic increase in the transport of Russian oil and gas through the Barents Sea is foreseen. As human activity in the area is increasing, there is rising concern for its impact on the vulnerable Barents Sea ecosystem. Also, potential conflicts between different activities (fisheries, petroleum, transport, tourism) have become more obvious. Scientifically, the region is characterized by complex and dynamic interactions of physical, chemical and biological ocean, sea ice and atmospheric boundary layer processes at a wide range of scales. Limitations in the observing and modelling systems are present, and knowledge gaps exist. It is therefore timely to undertake a

stepwise approach toward building a Barents Sea monitoring system. The deep Nordic and the shallow (average 230 m) Barents Seas are closely connected through the Norwegian Atlantic Current and the Norwegian Coastal Current (NCC). These currents act as the highway for transporting heat, salt/freshwater and upstream pelagic, chemical and biological material into the Barents Sea (Sakshaug et al., 1991; Slagstad et al., 2000, Dommasnes et al., 2000). Large seasonal, inter-annual and decadal variations are characteristic for the transport of Atlantic Water and coastal water into the Barents Sea (Loeng et al., 1997; Hamre, 2000; Ingvaldsen et al., 2004; Skardhamar and Svendsen, 2005; Budgell, 2005). The patterns of variations are to some extent related to the North Atlantic Oscillation (NAO) and its implications for the ocean climate, including extremely cold conditions in the eastern part of the Nordic Seas and Barents Sea (weak Atlantic transport) in the mid 1960s (Stein et al., 1998; Furevik et al., 2002; ICES, 2005) to extremely warm conditions in the eastern part of the Nordic Seas and Barents Sea (large Atlantic transport) in the early 1990s. These fluctuations in the Barents Sea environment and climate have an impact on the extent and concentration of sea ice, and make the ecosystems highly variable on a wide range of spatial and temporal scales. The ecological responses (Hamre, 2000) associated with marine climate swings can be summarized for the layman as “warm anomalies are good, cold anomalies are bad,” primarily because warm anomalies imply reduced ice cover, enhanced plankton transport and production (improved food supply) and more rapid growth. However, this does not hold for the whole Barents Sea system. In the northern Barents Sea, much of the marine megafauna is sea ice dependent, and reductions in sea ice translate into reductions in habitat for these arctic endemics. A challenging but fruitful approach to advancing our understanding of the marine environment is to integrate heterogeneous observations with a suitable set of properly validated models capable of assimilating observations.

A major challenge is to build up operational monitoring and forecasting systems for the Arctic regions in general and for the MIZ in particular.

This can be achieved through the integration and refinement of existing observation and modeling systems, including data assimilation, data analysis, model validation and information and dissemination system development as well as use of novel data collection (Fig. 8.1 a). When completed a dissemination system to support and improve marine research and knowledge-based ecosystem assessment, prediction and management will be operational for wealth creation and sustainable using web server technology (Fig. 8.1 b).

In order to build up operational monitoring and forecasting systems, it is necessary to:

- improve model predictions through comparative testing and validation of several existing, fine-resolution, coupled ocean-sea ice-ecosystem models, and through assimilation of observations;
- improve predictive models of the ecosystem and contaminant transport by advancing the understanding of key physical processes (e.g., turbulence, upwelling, frontal meandering, eddy formation) that impact chemical and biological processes;
- produce monitoring information from available and new observation networks, exploiting new field programs that will collect more data and make data rapidly (up to near real time) available, and operational models addressing time scales of hours to years, suitable for scientific users and management issues, including contribution of basic ecological knowledge for targeted species;
- disseminate daily updated information of value-added products and data to the Barents Sea marine user community by implementing and operating a web-based Information system
- apply the web-based Information system for public outreach, teaching and training to

increase the insight and understanding of the Arctic environment.

The main information products from observation and modelling systems are: ocean circulation; water mass, sea ice properties and distribution; transport pathways; algae blooms, plankton production and distribution; fish larvae transport, growth and distribution; transport and spreading of contaminants. This information, in turn, will be used and made available for studies of effects on ecosystems such as fish recruitment; contaminant transport, distribution, accumulation of contaminants, subsequent exposure on plankton and fish larvae; impact of physical and lower trophic ecosystem changes on higher trophic levels.

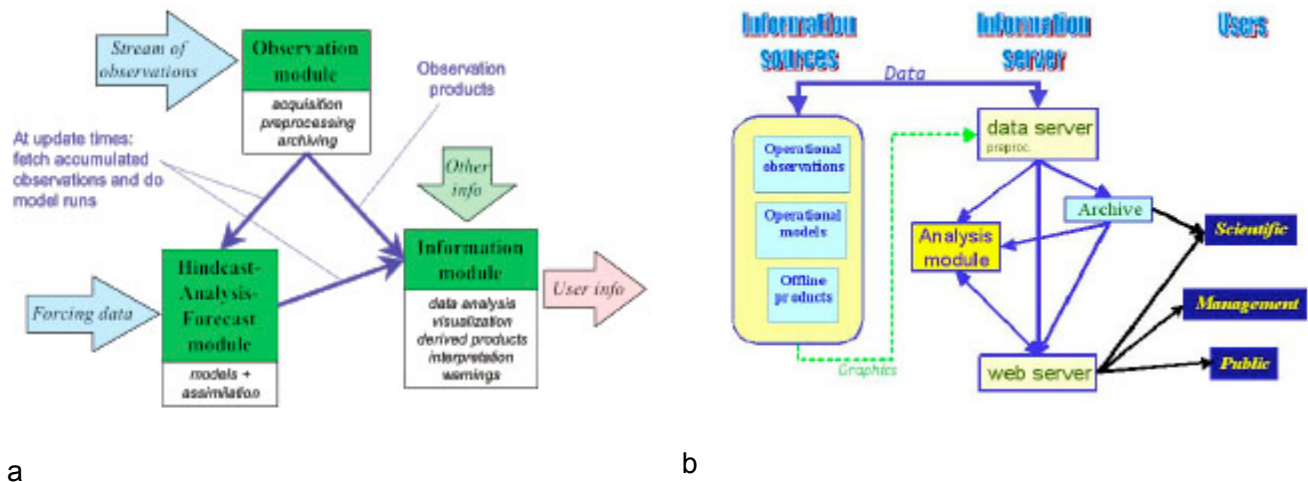


Figure 8.1 (a) Schematic illustration of the monitoring system concept for MONBASE (Monitoring the Barents Sea Environment), a system proposed by Johannessen et al., (2006); (b) Schematic illustration of the Pilot Ocean Monitoring System (POMS) developed and running under the MONCOZE project (Hackett et al., 2006; <http://moncoze.met.no>).

Operational services on met-ice-ocean conditions in the Arctic Ocean and the MIZ areas are extremely important for safe and cost-effective industrial and transport activities as well as for protection of the vulnerable environment. In order to improve the operational services, it is necessary to develop forecasting systems using numerical models and data assimilation techniques. Furthermore, availability of marine observations and development of dissemination services are essential for improvement of services. The marine observations that form the basis for operational services is basically the same as those needed for climate research. It is therefore relevant that these two topics are considered simultaneously when planning an Arctic marine monitoring and forecasting systems. A pre-requisite for building up monitoring and forecasting systems for the MIZ areas is to improve the observing systems both from in situ measurements and from satellite systems.

In order to build operational oceanography services for the Arctic regions, the Arctic GOOS is being established as a regional alliance of organizations and institutions involved in monitoring and forecasting of the Arctic seas (Sandven et al., 2005). The most important role of Arctic GOOS will be to produce and disseminate information to users. For the MIZ, one of the main tasks will be to develop improved sea-ice dynamical model. Sea ice modelling will be part of an integrated system using in situ and satellite data, several numerical models and data assimilation, as shown in Figure 8.2.

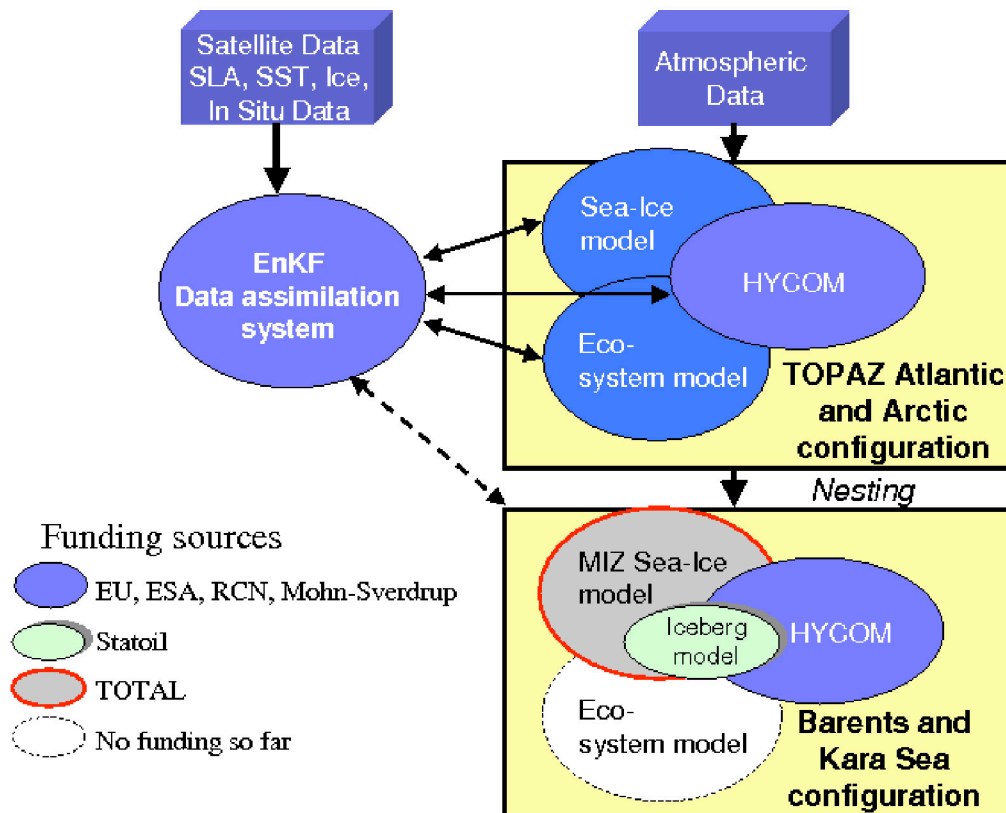


Figure 8.2 NERSC data assimilative and nested modeling system under development with funding from EU, ESA, Norwegian Research Council and industry.

In the next few years there will be enhance research activities in the Arctic seas as part of the International Polar Year 2007 – 2009. There will be many field expeditions with new data collection, more intensive satellite monitoring, and increased modeling efforts in order to increase our understanding of the Arctic environment. Information about the International Polar Year can be found on <http://www.ipy.org>.

Acknowledgement

The review study resulting in this report has primarily been supported by Total E&P Norge. In addition to the authors, several other scientists at NERSC and partner institutions have provided material used in the report. Institutes and scientists mentioned in the reference list are all acknowledge for the text and illustrations used in the report.

References

- Abdelnour, R., Johnstone, T., Howard, D., & Nisbett, V. (1986). Laboratory testing of an oil-skimming bow in broken ice. Environmental Studies Revolving Funds Report, No. 013. Ottawa, Canada. 60 pp.
- Abramov, V. and G. K. Zubakin. Russian iceberg observations 1970-1989, OKN IDAP report, December 1992, 37 pp.
- Abramov, V. Atlas of Arctic Icebergs. Backbone Publishing Company, 1996, 70 pp.
- ACIA (2004). Impacts of a warming Arctic: Arctic Climate Impact Assessment, November, 2004 (<http://amap.no/acia/>).
- Aksnes, D.L., Ulvestad, K.B., Balino, B.M., Berntsen, J., Egee, J.K. and Svendsen, E., 1995. Ecological Modeling in Coastal Waters - Towards Predictive Physical-Chemical-Biological Simulation-Models. *Ophelia*, 41: 5-36.
- Alekseev, G. V., O. M. Johannessen, A. A. Korablev and A. Y. Proshutinsky. Arctic Ocean and sea ice, In *Arctic Environment Variability in the Context of Global Change* (eds. L. P. Bobylev, K. Ya Kondratyev and O. M. Johannessen), Springer Praxis Publishing, Chichester, UK, 2004, 471 pp.
- Arashkevich, E., Wassmann, P., Pasternak, A. and Riser, C.W., 2002. Seasonal and spatial changes in biomass, structure, and development progress of the zooplankton community in the Barents Sea. *Journal of Marine Systems*, 38(1-2): 125-145.
- Arctic Monitoring and Assessment Programme (AMAP), <http://amap.no>
- Atlas Arktiki [Atlas of the Arctic], 1985. Moscow, 204 p., (in Russian).
- Balmforth and Craster (1999). Ocean waves and ice sheets. *J. Fluid Mech.* (1999) vol.395, pp. 89-124.
- Bertino, L., Lisæter, K. A., Counillon, F., Kegouche, I., Winther, N., Parouty, S., 2005. The TOPAZ monitoring and prediction system for the Atlantic. In: H. Dahlin, N. C. Flemming, P. M., Pettersson, S. (Eds.), *European Operational Oceanography: Present and Future*, 4th EuroGOOS Conference, June 2005, Brest, France. Office for publication of the EC, Luxembourg, pp. 456–459.
- Bleck, R., Smith, L., 1990. A wind-driven isopycnic coordinate model of the north and equatorial atlantic ocean. 1. model development and supporting experiments. *J. Phys. Oceanogr.* 95, 3273–3285.
- Bleck, R., 2002. An oceanic general circulation model framed in hybrid isopycnic-Cartesian coordinates. *Ocean Modelling*, 4(1): 55-88.
- Bryden, H. L. and Imawaki, S. (2001) Ocean heat transport. In: *Ocean Circulation and Climate*, Siedler et al. (Eds.) Academic Press, pp. 455–474
- Budgell, W. P., 2005. Numerical simulation of ice-ocean variability in the Barents Sea region: Towards dynamical downscaling. *Ocean Dynamics*, DOI 10.1007/s10236-005-0008-3.
- Burchard, H., 2002. *Applied Turbulence Modelling in Marine Waters*. Springer, Berlin. Vol. 100 of Lecture Notes in Earth Sciences.
- Burchard H., Bolding K., Kuhn W., Meister A., Neumann T., and Umlauf L., 2006. Description of a flexible and extendable physical-biogeochemical model system for the water column, *Journal of Marine Systems*
- Carrier, Krook, Pearson (1983) *Functions of a complex variable*. Hod books, Ithaca, New York.
- Cushman-Roisin, B., and A.D. Jenkins, 2006. On a non-local parameterisation for shear turbulence and the uniqueness of its solutions. *Boundary-Layer Meteorology* 118, 69-82
- DeCola, E., Tim Robertson, Sierra Fletcher, Susan Harvey (2006): *Offshore Oil Spill Response in Dynamic Ice Conditions: A Report to WWF on Considerations for the Sakhalin II Project*. Alaska, Nuka Research, WWF, April 2006, 74 pp.
- Dickins, D.F. (2005). *Oil spill behaviour and oil spill response in ice conditions: a review. Volume II: Technical and Operational Review of Offshore Oil-in-Ice Response Strategies*. Background Paper Number 4.2, Sakhalin Energy Investment Company, Ltd.

- Dickins Associates Ltd. (2004). Advancing Oil Spill Response in ice-covered waters, 18 pp. Prince William Sound Oil Spill Recovery Institute, Cordova, Alaska, USA (www.pws-osri.org)
- Dementev, A.A., 1985. Meteorologicheskie i Aerologicheskie Usloviya Novozemeelskoy Bory [Meteorological and Aerological Conditions of the Novaya Zemlia Catabatic Winds], Problemy Arktiki i Antarktiki, Vol. 61, pp. 65-70, (in Russian).
- Deser, C., J. E. Walsh and M. S. Timlin (2000) Arctic Sea Ice Variability in the Context of Recent Atmospheric Circulation Trends, *Journal of Climate*, DOI: 10.1175/1520-0442(2000)
- Dickins, D. & Buist, I. (1999). Countermeasures for ice-covered waters. *Pure Applied Chemistry* Vol. 71, No. 1. pp. 173-191.
- Dommasnes, D., et al.,(2000), An ecopath model for the Norwegian Sea and Barents Sea, *Can. Journal of Fish. Aquat. Sci.*, 57, 1-5.
- Divine, D. V., and C. Dick (2006), Historical variability of sea ice edge position in the Nordic Seas, *J. Geophys. Res.*, 111, C01001, doi:10.1029/2004JC002851.
- Dyrugerov, M.B. and M.F. Meier (2000) Twentieth century climate change: Evidence from small glaciers, *PNAS*, 97(4), 1406-1411.
- Dyrugerov, M.B., and M.F. Meier (2005) Glaciers and the changing earth system: A 2004 snapshot. Boulder, Colorado, University of Colorado Institute of Arctic and Alpine Research Occasional Paper 58, 117 pp.
- Ellingsen, I.H., Dalpadado, P., Slagstad, D. and Loeng, H.,. Impact of present and future climatic conditions on the physical and biological environment of the Barents Sea. Climatic Change. in prep
- Evers, Karl-Ulrich et al. (2004). State of the art report on oil weathering and on the effectiveness of response alternatives. ARCOP project (<http://www.arcop.fi>).
- Fingas, M.F. and Hollebone, B.P. (2003). Review of the behaviour of oil in freezing environments. *Marine Pollution Bulletin* 47. Pp. 333-340.
- Flynn, K. J., 2005. Castles built on sand: dysfunctionality in plankton models and the inadequacy of dialogue between biologists and modelers. *J. Plakton Res.*, 12,: 1205-1210.
- Fox, C. and V. A. Squire (1994). On the oblique reflexion and transmission of ocean waves at shore fast sea ice. *Phil. Trans.R. Soc. Lond. A*(1994) 347, 185-218.
- Fox, C. and V. A Squire (1991). Strain in Shore Fast Ice Due to Incoming Ocean Waves and Swell, *J. Geophys. Res.* Vol.96, (C3), 4531-4547.
- Furevik, T., M. Bentsen, H. Drange, J.A.Johannessen and A. Korablev, (2002), Spatial and temporal variability of the sea surface salinity in the Nordic Seas, *Journal of Geophysical Research-Ocean* , Vol. 107, No. C12.
- Gascard, J.-C., Kergomard, C., Jeannin, P.-F., Fily, M., 1988. Diagnostic study of the fram strait marginal ice zone during summer from 1983 and 1984 marginal ice zone experiment lagrangian observations. *J. Geophys. Res.* 93 (C4), 3613–3641.
- Glover, N. & Dickins, D. (1999). Oil spill response preparedness in the Alaska Beaufort Sea. Reprint of material presented in 1996 Symposium on Oil Spill Prevention and Response and 1999 International Oil Spill Conference.
- Gray, J. M. N. T., Morland, L. W., 1994. A two-dimensional model for the dynamics of sea ice. *Phil. Trans. R. Soc. Lond. Ser. A* 347, 219–290. H`akkinen, S., 1986. Coupled ice-ocean dynamics in the marginal ice zones: Up/down-welling and eddy generation. *J. Geophys. Res.* 91, 819–832.
- Haas, C., and H. Eicken (2001) Interannual variability of summer sea ice thickness in the Siberian and Central Arctic under different atmospheric circulation regimes, *J. Geophys. Res.*, 106(C3), 4449-4462.
- Haas, C. (2004) Late-summer sea ice thickness variability in the Arctic Transpolar Drift 1991–2001 derived from ground-based electromagnetic sounding. *Geophys. Res. Lett.*, 31, L09402, doi: 10.1029/2003GL019394. Hansen, J. (2006) Global temperature trends: 2005 summation. <http://data.giss.nasa.gov/gistemp/2005/>
- Hackett, B., J. Albretsen, L.P. Røed, J.A. Johannessen and E. Svendsen, (2006), The MONCOZE Pilot Ocean Monitoring System (POMS); A Tool for Marine Environmental Monitoring, *Proceedings of 4th EuroGOOS Conference, 6-9 June 2005, Brest, France.*
- Hakkinen, S., 1986. Coupled ice-ocean dynamics in the marginal ice zones: Up/down-welling and eddy

- generation. *J. Geophys. Res.* 91, 819–832.
- Hamre, J. (2000), Effects of climate and stocks interactions on the yield of North-East Arctic cod. Results from multispecies model run, *ICES CM 2000*.
- Harms, I. H., Schrum, C., Hatten, K., 2005. Numerical sensitivity studies on the variability of climate-relevant processes in the Barents Sea *J. Geophys. Res.*, 110 (C6): Art. No. C06002.
- Hibler, III, W. D., 1980. Modeling a variable thickness ice cover. *Mon. Wea. Rev.* 108, 1943–1973.
- Hibler III, W. D., 1979. A dynamic thermodynamic sea ice model. *J. Geophys. Res.* 84, 815–846.
- Hilmer, M. and P. Lemke (2000) On the decrease of Arctic sea ice volume, *Geophysical Research Letters*, 27, pp. 3751–3754.
- Holloway, G. and T. Sou, 2002. Has arctic sea ice rapidly thinned? *J. Clim.*, 15, 1691–1698.
- Holst, J.C., Røttingen, I. and Melle, W., 2004. The herring. In: H.R. Skjoldal (Editor), *The Norwegian Sea Ecosystem*. Tapir Academic Press, Trondheim, pp. 559.
- Hopkins, M., 1996. On the mesoscale interaction of lead ice and floes. *J. Geophys. Res.* 101 (C8), 18315–18326.
- Huang, Z. J., Savage, S. B., 1998. Particle-in-cell and finite difference approaches for the study of marginal ice zone problems. *Cold Reg. Sci. Tech.* 28, 1–28.
- Hunke, E. C., Dukowicz, J. K., 1997. An elastic-viscous-plastic model for sea ice dynamics. *J. Phys. Oceanogr.* 27, 1849–1867.
- Hurrell, J. W., 1995: Decadal trends in the North Atlantic oscillation regional temperatures and precipitation. *Science*, 269, 676–679..
- ICARP II: Working Group 6 – Arctic Shelf Seas, Draft Science Plan (Eds. Kassens et al.) 2005 (www.icarp.dk)
- ICES (2005), Report of the Working Group on Oceanic Hydrography (WGOH), 11-14 April 2005, Narrangansett, USA. *ICES CM 2005/C:06*. 144 pp.
- Ingvaldsen, R.B., L. Asplin, and H. Loeng (2004), Velocity field of the western entrance to the Barents Sea, *J. Geophys. Res.*, 109, C03021, doi:10.1029/2003JC00181.
- IPCC (2001) Climate change: the scientific basis. Intergovernmental Panel on Climate Change. www.ipcc.ch
- Jenkins, A.D., 1994. A stationary potential-flow approximation for a breaking-wave crest. *Journal of Fluid Mechanics*, 280: 335–347.
- Johannessen, J. A., Johannessen, O. M., Svendsen, E., Shuchman, R., Manley, T., Campbell, W. J., Josberger, E. G., Sandven, S., Gascard, J. C., Olaussen, T., Davidson, K., Van Leer, J., 1987. Mesoscale eddies in the Fram Strait marginal ice zone during the 1983 and 1984 marginzl ice zone experiments. *J. Geophys. Res.* 92 (C7), 6754–6772.
- Johannessen, O. M., S. Sandven, W. P. Budgell, J. A. Johannessen and R. Shuchman. Observation and Simulation of Ice Tongues and Vortex-Pairs in the Marginal Ice Zone. Nansen Centennial Volume, American Geophysical Union Monograph 85, pp. 109 - 136, 1994.
- Johannessen, O. M., H. Sagen, S. Sandven, and K. Stark (2003). Ambient noise caused by Ice-Edge Eddies in the Greenland and Barents Seas. *IEEE Journal of oceanic engineering*, Vol 28, No. 2, April 2003
- Johannessen, O.M., L. Bengtsson, M.W. Miles, S.I. Kuzmina, V.A. Semenov, G.V. Alekseev, A.P. Niagurny, V.F. Zakharov, L.P. Bobylev, L.H. Pettersson, K. Hasselmann, and H.P. Cattle (2004) Arctic climate change: Observed and modeled temperature and sea ice variability. *Tellus*, 56A, 328–341
- Johannessen, O.M., K. Khvorostovsky, M.W. Miles, and L.P. Bobylev (2005) Recent ice-sheet growth in the interior of Greenland, *Science*, 310, 1013–1016.
- Johannessen, J.A., B. Hackett, E. Svendsen, H. Søliland, L.P. Røed, N. Winther, L. Pettersen, J. Albretsen and M. Skogen, (2006). Monitoring the Norwegian Coastal Zone Environment – the MONCOZE approach. In *European Operational Oceanography: Present and Future*, Proceedings of 4th International Conference on EuroGOOS, 6-9 June 2005, Brest, France, Eds. H. Dahlin, N. C. Flemming, P. Marchand and S. E. Pettersson, 811–817
- Karl, T., 1998: Regional trends and variations of temperature and precipitation. *The Regional Impacts of Climate Change: An Assessment of Vulnerability*, R. T. Watson, M. C. Zinyowera, R. H. Moss,

- and D. J. Dokken, Eds., Intergovernmental Panel on Climate Change, Cambridge University Press, 412–425.
- Kivimäe C., Bellerby R.G.J., Sundfjord A. and Omar A.M., Variability of new production and CO₂ air-sea exchange in the north-western Barents Sea in relation to sea ice cover. *In preparation for submission to Journal of Marine Research*.
- Kwok, R., G.F. Cunninham, H.J. Zwally, and D. Yi (2006) ICESat over Arctic sea ice: Interpretation of altimetric and reflectivity profiles. *J. Geophys. Res.*, *111*, C06006, doi: 10.1029/2005JC003175
- Large, W. C., McWilliams, J. C., Doney, S. C., 1994. Oceanic vertical mixing: A review and a model with a nonlocal boundary layer parametrization. *Rev. Geophys.* *32* (4), 363–403.
- Laxon, S., N. Peacock, and D. Smith (2003) High interannual variability of sea ice thickness in the Arctic Region. *Nature*, *425*, 947–950.
- Lepparanta, M., 2005. The Drift of Sea Ice. Springer-Praxis.
- Loeng, H., V. Ozhigin, B. Ådlandsvik (1997), Water fluxes through the Barents Sea, *ICES J. Mar. Sci.*, *54*, 310-317.
- Løset, S., 1993. Some aspects of floating ice related sea surface operations in the Barents Sea. Ph.D. thesis, University of Trondheim, Norway.
- Lu, Q.-M., Larsen, J., Tryde, P., 1989. On the role of ice interaction due to floe collisions in marginal ice zone dynamics. *J. Geophys. Res.* *94* (C10), 14525–14537.
- Marko (2003). Observations and analyses of an intense wave-in-ice event in the Sea of Okhotsk. *J. Geophys. Res.*, Vol. 108, NO.C9, doi: 10.1029/2001JC001214
- Maslowski, W., B. Newton, P. Schlosser, A.J. Semtner, and D.G. Martinson: Modeling Recent Climate Variability in the Arctic Ocean, *Geophys. Res. Lett.*, *V. 27*(22), pp. 3743-3746, 2000.
- Maslowski, W., J.L. Clement, W. Walzowski, J.S. Dixon, J. Jakacki, and T.P. McNamara (2006) Oceanic forcing of Arctic sea ice at gateways and margins of Pacific and Atlantic water inflow. *Eos, Trans. AGU*, *87*(36), Ocean Sci. Meet. Suppl., Abstract OS32P-05.
- Melling, H., D.A. Riedel, and Z. Gedalof (2005) Trends in the draft and extent of seasonal pack ice, Canadian Beaufort Sea. *Geophys. Res. Lett.*, *32*, L24501, doi: 10.1029/2005GL024483.
- Mellor, M., 1986. The mechanical behaviour of sea-ice. In: *Geophysics of Sea Ice*. Plenum Press, New York, pp. 165–281.
- Nagurnyi, A.P., V.G. Korostelev and V.V. Ivanov (1994) Multiyear variability of sea ice thickness in the arctic basin measured by elastic-gravity waves on the ice surface, *Meteorol. Hydrol.*, *3*, pp. 72-78 (in Russian).
- National Research Council (NRC). (2003). *Oil in the sea III: inputs, fates, and effects*. The National Academies Press. Washington, DC.
- Niebauer, H.J. and Alexander, V., 1985. Oceanographic frontal structure and biological production at an ice edge. *Continental Shelf Research*, *4*: 367-388.
- OSRI and ARC (2004), Prince William Sound Oil Spill Recovery Institute and U.S. Arctic Research Commission. Advancing oil spill response in ice covered waters.
- Overland, J. E., C. H. Pease, R. W. Preisendorfer, and A. L. Comisky, 1986: Prediction of vessel icing, *J. of Climate and Applied Meteorology*, *25*, 1793-1806.
- Overland, J. E.; Spillane, M. C.; Percival, D. B.; Wang, Muyin; Mofjeld, H. O., (2004). Seasonal and Regional Variation of Pan-Arctic Surface Air Temperature over the Instrumental Record, *Journal of Climate*, vol. 17, Issue 17, pp.3263-3282
- Ovsienko, S., 1976. Numerical modelling of the drift of ice. *Izvestiya, Atmospheric and Oceanic Physics* *12* (11), 1201–1206.
- Owens, E.H., L.B. Solsberg, M.R. West and M. McGrath. 1998. Field guide for oil spill response in Arctic waters. Prepared for Emergency Prevention, Preparedness, and Response Working Group, Arctic Council.
- Owens, E. et al. (2005). The behaviour and documentation of oil spilled on snow- and ice-covered shorelines. *Proceedings from the International Oil Spill Conference*. Miami, Florida. May 15-19.
- Peltier, W. R. (2002), Global glacial isostatic adjustment: Paleogeodetic and space-geodetic tests of the ICE-4G (VM2) model, *J. Quat. Sci.*, *17*, 491–510.

- Peterson, C. H., S. D. Rice, J. W. Short, D. Esler, J. L. Bodkin, B. E. Ballachey, and D. B. Irons (2003) Long-Term Ecosystem Response to the Exxon Valdez Oil Spill, *Science*, Vol. 302, 2082-2086.
- Peterson, B. J., R. M. Holmes, J. McClelland, C. J. Vörösmarty, R. B. Lammers, A. I. Shiklomanov, I. A. Shiklomanov, and S. Rahmsdorf (2002) Increasing river discharge to the Arctic Ocean. *Science* 298 (13. December 2002), 2171-2173.
- Peterson, B. J., J. McClelland, R. Curry, R. M. Holmes, J. E. Walsh and K. Aagaard. Trajectory Shifts in the Arctic and Subarctic Freshwater Cycle. *Science*, Vol. 313, 25 August, 2006.
- Pfirman, S., W.F. Haxby, R. Colony, and I. Rigor (2004) Variability in Arctic sea ice drift. *Geophys. Res. Lett.*, 31, L16402, doi: 10.1029/2004GL020063.
- Polyakov, I., G.V. Alekseev, R.V. Bekryaev, U. Bhatt, R. Colony, M.A. Johnson, V.P. Karklin, D. Walsh, and A.V. Yulin (2003) Long-term ice variability in Arctic marginal seas. *J. Climate*, 16(12), 2078–2085.
- Polyakov, I.V., et al. (2005) One more step toward a warmer Arctic. *Geophys. Res. Lett.*, 32, L17605. doi: 10.1029/2005GL023740.
- Prinsenber, S. J., I. K. Peterson, S. Narayanan, and J. U. Umoh, 1997: Interaction between atmosphere, ice cover, and ocean off Labrador and Newfoundland from 1962–1992. *Can. J. Aquat. Sci.*, 54, 30–39..
- Proshutinsky, A.Y., and M.A. Johnson (1997) Two circulation regimes of the winddriven Arctic Ocean. *J. Geophys. Res.*, 102(C6), 12,493–12,514. Przybylak, R. (2002) *Variability of Air Temperature and Atmospheric Precipitation in the Arctic*. Dordrecht, The Netherlands, Kluwer, 330 pp.
- Proshutinsky, T, and T. Weingarten. INSROP Phase 2 project: Natural Conditions and Ice Navigation, 1998 (<http://www.ims.uaf.edu/insrop-2>)
- Proshutinsky A., I.M. Ashik, E.N. Dvorkin, S. Häkkinen, R.A. Krishfield, and W.R. Peltier (2004) Secular sea level change in the Russian sector of the Arctic Ocean. *J. Geophys. Res.*, 109, C03042, doi: 10.1029/2003JC002007.
- Proshutinsky, A., J. Yang, R. Krishfield, R. Gerdes, M. Karcher, F. Kauker, C. Koeberle, S. Hakkinen, W. Hibler, D. Holland, M. Maqueda, G. Holloway, E. Hunke, W. Maslowski, M. Steele, and J. Zhang (2005) Arctic Ocean Study: Synthesis of model results and observations. *Eos, Trans. AGU*, 86(40), 368, 10.1029/2005EO400003.
- Ratkova, T.N. and Wassmann, P., 2002. Seasonal variation and spatial distribution of phyto- and protozooplankton in the central Barents Sea. *Journal of Marine Systems*, 38(1-2): 47-75.
- Rawlins, M.A., R.B. Lammers, S. Froking, B. Fekete, and C.J. Vörösmarty (2003) Simulating pan-Arctic runoff with a macro-scale terrestrial water balance model. *Hydrol. Proc.*, 17, 2521–2539.
- Reed, Mark et al. (1999). Oil spill modelling towards the close of the 20th century: overview of the state of the art. *Spill Science and Technology Bulletin*. Volume 5, Number 1.
- Reigstad, M., Wassmann, P., Riser, C.W., Oygarden, S. and Rey, F., 2002. Variations in hydrography, nutrients and chlorophyll a in the marginal ice-zone and the central Barents Sea. *Journal of Marine Systems*, 38(1-2): 9-29.
- Rey, F., 2004. Phytoplankton: the grass of the sea. In: H.R. Skjoldal (Editor), *The Norwegian Sea Ecosystem*. Tapir Academic Press, Trondheim, pp. 559.
- Rheem, C. K., Yamaguchi, H., Hiroharu, K., 1997. Distributed mass/discrete floe model for pack ice rheology computation. *J. Mar. Sys.* 2, 101–121.
- Rhines, P. B. (2006). Sub-Arctic oceans and global climate. *Weather*, Royal Meteorological Society, Vol. 61, No. 4, April 2006, pp 109 – 118, doi: 10.1256/wea.223.05
- Rignot, E.J., D. Braaten, S.P. Gogineni, W.B. Krabill, and J.R. McConnell (2004) Rapid ice discharge from southeast Greenland glaciers, *Geophysical Research Letters*, 31(L10401), doi:10.1029/2004GL019474.
- Rignot, E. and P. Kanagaratnam (2006) Changes in the Velocity Structure of the Greenland Ice Sheet, *Science*, 311(5763), 986-990.
- Rigor, I., and J.M. Wallace (2004) Variations in the age of Arctic sea-ice and summer sea-ice extent. *Geophys. Res. Lett.*, 31, L09401, doi: 10.1029/2004GL019492

- Robertson, T. and DeCola, E. (2001). Joint agency evaluation of the spring and fall 2000 North Slope broken ice exercises. Prepared for Alaska Department of Environmental Conservation, U.S. Department of the Interior Minerals Management Service, North Slope Borough, U.S. Coast Guard, and Alaska Department of Natural Resources. Anchorage, Alaska.
- Romanov, I.P. (1995) *Atlas of Ice and Snow of the Arctic Basin and Siberian Shelf Seas*, edited by A. Tunik, Backbone Publishing, Elmwood Park, USA, 277 pp
- Rothrock, D.A., Y.Yu and G.A. Maykut, 1999. Thinning of the Arctic sea-ice cover. *Geophys. Res. Lett.* **26**(23), 3469-72
- Rudels, B., E.P. Jones, L.G. Anderson, and G. Kattner (1994) On the intermediate depth waters of the Arctic Ocean. In *The Polar Oceans and Their Role in Shaping the Global Environment: The Nansen Centennial Volume*, O.M. Johannessen, R.D. Muench, and J.E. Overland (eds.), Washington, D.C., American Geophysical Union, 33–46.
- Røed, L.P. and O'Brien, J.J., 1983. A coupled ice-ocean model of upwelling in the marginal ice zone. *Journal of Geophysical Research*, **88**: 2863-2872.
- Sagen, H. Ambient noise in the Marginal Ice Zone (1998). Dr. Scient thesis, NERSC and University of Bergen, Norway.
- Sakshaug, E., A. Bjørge, B. Gulliksen, H. Loeng, F. Mehlum, (1991), Økosystem Barentshavet (book in Norwegian), *Universitetsforlaget AS*, Trondheim, Norway, ISBN 82-00-03963-3.
- Sakshaug, E., F. Rey & D. Slagstad, 1995. Wind forcing of marine primary production in the Northern atmospheric low-pressure belt. In: Skjoldal, H. R., C. E. C. Hopkins, K. E. Erikstad & H. P. Leinaas (Eds.), *Ecology of fjords and Coastal Waters*. Elsevier, Amsterdam: 15-25.
- Sandven S., Johannessen O.M., Miles M.W., Pettersson L.H., Kloster K., (1999). Barents Sea seasonal ice zone features and processes from ERS 1 synthetic aperture radar: Seasonal Ice Zone Experiment 1992. *Journal of Geophysical Research*, **104**, (C7), 15843-15857
- Sandven, S., O. M. Johannessen, E. Fahrbach, E. Buch, H. Cattle, L. Toudal Pedersen and T. Vihma. The Arctic Ocean and the Need for an Arctic GOOS. EuroGOOS Publication No. 22, March 2005, 50 pp.
- Sandven, S. et al (2006). Sea ice thickness observation system. SITHOS final science report. NERSC technical Report no 270. (<http://sithos.nersc.no/SITHOS/>)
- Sayed, Mohamed et al. (1995). Spreading of crude petroleum in brash ice: effects of oil's physical properties and water current. *International Journal of Offshore and Polar Engineering*. Volume 5, Number 2. June.
- Schrum, C., Harms, I. H., Hatten, K Modelling air-sea exchange in the Barents Sea by using a coupled regional ice-ocean model. Evaluation of modelling strategies. 2005. *Meteorol. Zeitschr.* **14**, 801-808
- Schweiger, A.J. (2004) Changes in seasonal cloud cover over the Arctic seas from satellite and surface observations, *Geophysical Research Letters*, Vol. **31**, L2207, doi:10.1029/2004GL020067, 2004.
- Serreze, M.C., F. Carsey, R.G. Barry, and J.C. Rogers (1997) Icelandic low cyclone activity: Climatological features, linkages with the NAO and relationships with recent changes in the northern hemisphere circulation. *J. Climate*, **10**, 453–464.
- Shen, H. H., Hibler III, W. D., Leppäranta, M., 1986. On applying granular flow theory to a deforming broken ice field. *Act. Mech* **63**, 143–160.
- Shen, H. H., Hibler III, W. D., Leppäranta, M., 1987. The role of floe collisions in sea ice rheology. *J. Geophys. Res.* **92** (C7), 7085–7096.
- Shiklomanov, I., A. I. Shiklomanov, R. B. Lammers, B. J. Peterson, and C. J. Vörösmarty (2000) In *The Freshwater Budget of the Arctic Ocean* (Ed. E. L. Lewis), Kluwer Academic, Dordrecht, Netherlands, 2000, pp. 281-296.
- Shimada, K., T. Kamoshida, M. Itoh, S. Nishino, E. Carmack, F. McLaughlin, S. Zimmermann, and A. Proshutinsky (2006) Influence of Pacific summer water on the recent anomalous reduction of ice cover in the Arctic Ocean. *Eos, Trans. AGU*, **87**(36), Ocean Sci. Meet. Suppl., Abstract OS33N-01.
- Short, J.W., Lindebert, M.R., Harris, P.M., Maselko, J.M., J.J. & Rice, S.D. (2004). Estimate of oil persisting

- on the beaches of Prince William Sound 12 years after the Exxon Valdez oil spill. *Environmental Science and Technology*. Jan 1: 38(1): 19-25.
- Shuchman, R.A., C. Rufenach, and O.M. Johannessen. "Extraction of Marginal Ice Zone Thickness Using Gravity Wave Imagery," *Journal of Geophysical Research*, Vol. 99, No. C1, pp. 901-918, 15 January 1994.
- Shuchman, R., R. Onstott, O. M. Johannessen, S. Sandven. Processes at the ice edge – The Arctic. Chapter 18, pp. 373-396 in *Synthetic Aperture Radar. Marine User's Manual* (Eds. Jackson, C. R. and J. R. Apel), National Oceanic and Atmospheric Administration, September 2004, 464 pp.
- Singsaas, I. (2005). Weathering of oils in open sea and ice-infested waters. ARCOP Workshop, St. Petersburg, Russia. 19-20 October. (<http://www.arcop.fi>).
- Singsaas, I. and Reed M. (2006). Oil spill response in ice-infested waters—need for future developments. *Interspill 2006*. London, UK.
- Skardhamar, J. and H. Svendsen, (2005), Circulation and shelf-ocean interaction off North Norway, *Continental Shelf Research*, 25, 1541-1560.
- Slagstad, D., K. Tande, W. Melle, B. Ellertsen, and F. Carlott, (2000), Regional dynamics of Calanus in the Norwegian Sea in response to ocean climate in 1997, ICES C.M.
- Slagstad, D. and McClimans, T.A., 2005. Modeling the ecosystem dynamics of the Barents sea including the marginal ice zone: I. Physical and chemical oceanography. *Journal of Marine Systems*, 58(1-2): 1-18.
- Spring, W. Ice Data Acquisition Summary Report, MOBIL Research and Development Corporation, Dallas, Texas, February 1994, 140 pp.
- Squire, V. A. A comparison of the mass-loading and elastic plate models of an ice field (1993), *Cold Regions Science and Technology*, 21, 219-229.
- Steen, A., deBettencourt, M., Pond, R., Julian, M., Salt, D. & Liebert, T. (2003). Global challenges to preparedness and response regimes. *Proceedings of the 2003 International Oil Spill Conference*.
- Stein, M., J. Lloret, and H-J. Ratz, (1998), North Atlantic Oscillation (NAO) Index – environmental variability effects on marine fisheries?, *Sci. Coun. Res. Doc. NAFO*, No98/20.
- Stouffer, R.J., J. Yin, J.M. Gregory, K.W. Dixon, M.J. Spelman, W. Hurlin, A.J. Weaver, M. Eby, G.M. Flato, H. Hasumi, A. Hu, J.H. Jungclaus, I.V. Kamenkovich, A. Levermann, M. Montoya, S. Murakami, S. Nawrath, A. Oka, W.R. Peltier, D.Y. Robitaille, A. Sokolov, G. Vettoretti, and S.L. Weber (2006) Investigating the causes of the response of the thermohaline circulation to past and future climate changes, *Journal of Climate* (submitted 2007).
- Stroeve, J.C., M.C. Serreze, F. Fetterer, T. Arbetter, W. Meier, J. Maslanik, and K. Knowles (2005) Tracking the Arctic's shrinking ice cover: Another extreme September minimum in 2004. *Geophys. Res. Lett.*, 32(4), L04501, doi: 10.1029/2004GL021810.
- Sundfjord A., Fer. I., Kasajima Y. and Svendsen H., Observations of turbulent mixing and hydrography on the Marginal Ice Zone of the Barents Sea., *submitted to Journal of Geophysical Research*
- Tamelander, T and Heiskanen, A-S , 2004.: Effects of spring bloom phytoplankton dynamics and hydrography on the composition of settling material in the coastal northern Baltic Sea. *Journal of Marine Systems*, 52, 217-234
- Thingstad, T. F. and F. Rassoulzadegan 1999. Conceptual models for the biogeochemical role of the photic zone microbial food web, with particular reference to the mediterranean sea." *Progress in Oceanography* 44, 271-286.
- Thompson, D.W.J., and M. Wallace (1998) The Arctic Oscillation signature in the wintertime geopotential height and temperature fields. *Geophys. Res. Lett.*, 25(9), 1297–1300.
- Thompson, D. W. J., J. M. Wallace, and G. Hegerl, 2000: Annular modes in the extratropical circulation. Part II: Trends, *J. Climate*, 13, 1018-1036.
- Thorndike, A. S., Rothrock, D. A., Maykut, G. A., Colony, R., 1975. The thickness distribution of sea ice. *J. Geophys. Res.* 80 (33), 4501–4513.
- Umlauf, L. & H. Burchard, 2005. Second-order turbulence closure models for geophysical boundary layers. A review of recent work. *Continental Shelf Res.*, 25, 795-827.

- Untersteiner, N. (1993) "SHEBA, a research program on the Surface Heat Budget of the Arctic Ocean", National Science Foundation Arctic Systems Science Report no. 3. 1993.
- Wadhams, P., 1978. Wave decay in the marginal ice zone measured from a submarine. *Deep-Sea Res.* 25, 23–40.
- Wadhams, P. "The seasonal ice zone" in *The geophysics of sea ice* (1986). Edited by N. Untersteiner, NATO ASI Ser. B. 146, 825-991.
- Wadhams, P., Squire, V. A., Ewing, J. A., Pascal, R. W., 1986. The effect of the marginal ice zone on the directional wave spectrum of the ocean. *J. Phys. Oceanogr.* 16, 358–376.
- Wadhams, P., V.A. Squire, D.J. Goodman, A.M.Cowan, S.C. Moore (1988). The attenuation Rates of ocean Waves in the Marginal Ice Zone. *J. Geophys. Res.* Vol.93, No. C6, 6799-6818.
- Wadhams, P., B. Holt. Waves in Frazil and Pancake Ice and Their Detection in Seasat Synthetic Aperture Radar Imagery (1991). *J.Geophys.Res.* **96**, (C5), 8835-8852.
- Wassmann, P., Slagstad, D., Riser, C.W. and Reigstad, M (2006). Modelling the ecosystem dynamics of the Barents Sea including the marginal ice zone: II. Carbon flux and interannual variability. *Journal of Marine Systems*, 59(1-2): 1-24.
- Walsh, J. E., and C. M. Johnson, 1979: An analysis of arctic sea ice fluctuations, 1953–77. *J. Phys. Oceanogr.*, 9, 580–591..
- Walsh, J. E., W. L. Chapman and T. L. Shy, 1996: Recent decrease of sea level pressure in the central Arctic. *J. Climate*, 9, 480-486.
- Warren, S. G., I. G. Rigor, N. Untersteiner, V. F. Radionov, N. N. Bryazgin and Y. I. Alexandrov. Snow depth on Arctic Sea Ice. *Jour. Climate*, Vol. 12, pp. 1814 – 11829, 1999
- Williams, T. D. and Squire, V. A. Oblique scattering of plane flexural-gravity waves by heterogeneities in sea-ice. *Proceedings of the Royal Society of London, Series A*, 460(2052), 3469-3497 DOI: 10.1098/rspa.2004.1363 (2004).
- Williams, T. D. and Squire (2007), V. A. The effect of submergence on scattering across a transition between two floating flexible plates. *Journal of Fluid Mechanics*, under review.
- Wilson, D. & MacKay, D. (1987). The behaviour of oil in freezing situations. Environment Canada. Available from U.S. Department of Interior Marine Minerals Service.
- WMO SEA-ICE NOMENCLATURE (2005) WMO Report No.259, http://www.aari.nw.ru/gdsidb/XML/sea_ice_nomenclature.html
- Woodgate R.A., K. Aagaard, T.J. Weingartner (2006) Interannual changes in the Bering Strait fluxes of volume, heat and freshwater between 1991 and 2004, *Geophys. Res. Lett.*, 33, L15609, doi: 10.1029/2006GL026931.
- Yapa, P. & Weerasuriya, S. (1997). Spreading of oil spilled under broken floating ice. *Journal of Hydraulic Engineering*. August.
- Yu, Y., G.A. Maykut, and D.A. Rothrock (2004) Changes in the thickness distribution of Arctic sea ice between 1958–1970 and 1993–1997. *J. Geophys. Res.*, 109, C08004, doi: 10.1029/2003JC001982.
- Zhang, X., J.E. Walsh, J. Zhang, U.S. Bhatt, and M. Ikeda (2004). Climatology and interannual variability of Arctic cyclone activity. *J. Climate*, 17, 2300– 2317.
- Zubakin, G. K., A. K. Naumov and I. V. Buzin (2004). Estimates of ice and icebergs spreading in the Barents Sea. Paper no. 2004-JSC-381, 8 pp.
- Zwally, H.J., M.B. Giovinetto, J. Li, H.G. Cornejo, M.A. Beckley, A.C. Brenner, J.L. Saba, and D. Yi (2005) Mass changes of the Greenland and Antarctic ice sheets and shelves and contributions to sea-level rise: 1992-2002, *Journal of Glaciology*, **51**(175), 509-527.
- Zwally, H. J, (2006)